Title No. 51-26

An Interpretation of Some Published Researches on the Alkali-Aggregate Reaction*

Part 1—The Chemical Reactions and Mechanism of Expansion

By T. C. POWERS and H. H. STEINOUR†

SYNOPSIS

Research results are interpreted as having the following indications: The relative reactivity of a given form of silica is determined by the number of interrupted silicon-oxygen-silicon linkages, a matter of specific surface and "holes" due to disorderly atomic arrangements. Caustic attack on reactive silica in the presence of excess lime produces a nonswelling lime-alkali-silica complex if chemical equilibrium is reached. In affected concrete some of this complex is produced, but abnormal swelling is due to the formation of an alkali-silica complex which is not in equilibrium with lime. The persistence of the nonequilibrium product appears to be due to the inability of lime to diffuse into the reactive particle where alkali-silica complex has formed. Expansion of concrete is probably due primarily to the swelling of solid alkali-silica complex, but it may also be due to hydraulic pressure generated by osmosis, or by both mechanisms.

INTRODUCTION

The various papers pertaining to the cement-aggregate, or alkali-aggregate, reaction that have now been published represent an impressive body of research. In spite of this, the chemistry and physics of the phenomena have by no means been fully worked out. Various authors have effectively interpreted their data, but it seems that uncertainties and divergences of viewpoint exist that might be reduced if greater efforts at synthesis were not made. The present paper (in two parts) is offered as one such effort. In it we bring some of the principal facts together, and endeavor to interpret them from a single point of view. Hypothetical and speculative elements in this interpretation will be recognized, though more so in the second than in this initial part of the paper. We hope, however, that the hypothetical elements may lead to further experiments by various investigators so that the eventual solution of these matters may thus be brought nearer.

Since historical reviews are available in the literature,[1,2a] we shall now reproduce one here, assuming that the major results of the many laboratory

*Received by the Institute Dec. 28, 1953. Title No. 51-26 is a part of copyrighted JOURNAL OF THE AMERICAN CONCRETE INSTITUTE, V. 26, No. 6, Feb. 1955, *Proceedings* V. 51. Separate prints are available at 50 cents each. **Discussion** (copies in **triplicate**) should reach the Institute not later than June 1, 1955. Address 18263 W. McNichols Rd., Detroit 19, Mich.

†Members American Concrete Institute, Manager, Basic Research, and Manager, Literature Research Section, respectively, Portland Cement Assn., Chicago, Ill.

and field investigations that have been reported since T. E. Stanton's discovery[3] of caustic attack on reactive silica in concrete are familiar to the reader, at least in a general way. Moreover, we shall not attempt to cite all the published work that might have a bearing on our discussion or to evaluate all such researches; our object is to present certain hypotheses by making use of such published data as seem best suited to that purpose. Although the scope of this discussion is thus limited, we have reason to believe that if our principal hypothesis is valid at all, it might apply also to conditions not specifically considered here.

The phenomenon to be explained presents four aspects: (1) the nature of the reactions ultimately responsible for expansion that may occur when the concrete contains silica in a reactive form; (2) the mechanism of the abnormal expansion; (3) the safe amount of alkali; and (4) the control of alkali by finely divided reactive silica. The first two of these four aspects are discussed in this paper. The last two are discussed in the second, final paper.

THE CHEMICAL REACTIONS

The caustics that attack opal or other reactive silicas are known to be sodium and potassium hydroxides, commonly derived from the alkalies in portland cement. The caustics may also come from alkali-bearing zeolitic minerals if these happen to be constituents of the aggregate, the lime from the cement displacing the alkali from the zeolites. Under some circumstances the caustics may be obtained from solutions outside the affected concrete. Ordinarily the caustics are derived from the cement.

The reactive aggregates most often mentioned are those containing opal or acidic minerals in the vitreous state. Microscopical observations reported by various investigators support the conclusion that the caustic attacks the surface and gradually penetrates the reactive particle. This sometimes produces a structural alteration recognizable as a "reaction rim."

When evaporable water in the concrete is scarce and the alkali concentration not too high, the reaction product is a solid. If more water becomes available, the reaction product becomes softer, reaches a jellylike consistency, and may become a colloidal solution (a sol) or even a true solution. Except when the reaction product is obviously fluid, it should be regarded as a gel, whether or not it exhibits a jellylike appearance. When it is dry and friable, all it lacks, we believe, is water to give it the appearance normally associated with the term "gel."

Reactive silica

To reach an understanding of the chemistry of the caustic attack we may start with a consideration of reactive silica. A few years ago P. C. Carman[4] presented a discussion of the properties and behavior of colloidal silica, interpreted, as he said, in the light of modern views on the structure of silica and silicates. We shall therefore draw freely on Carman's paper.

As already mentioned, many investigators have found opal and various

siliceous volcanic rocks to be reactive. Opal is a highly condensed silica gel. Vitreous rocks are glassy, an indication that the melt cooled too rapidly to permit an orderly growth of crystals. By applying Carman's hypothesis concerning silica gel and vitreous silica, we found a plausible explanation of what makes some forms of silica reactive. No attempt is made to deal with the more complex reactive rocks, though the findings concerning pure silica are suggestive of the physicochemical factors that probably influence the reactivity of other rocks.

In all forms of silica the basic structural unit is a silicon ion, Si^{4+}, surrounded by four oxygen ions, $O^{=}$, the arrangement being that of a tetrahedron. A particle of crystalline silica is made up of such tetrahedra, the tetrahedra being linked together through their vertices, each vertex being occupied by an oxygen ion that is common to two tetrahedra. Carman says, "In the various crystalline forms of silica, tetrahedra are linked to form an oriented, three-dimensional network, while, in vitreous silica, tetrahedra are linked to produce a random three-dimensional network. It seems obvious that similar principles should be applied to the constitution of colloidal silica"—in the present case, silica gel.

The structure of silica can be represented on one plane by a schematic diagram such as Fig. 1 (also after Carman). In the diagram, the tetrahedron composed of a silicon ion surrounded by four oxygen ions is represented, arbitrarily, by a square with the four oxygen ions at the corners and the silicon ion in the center. This shows how a continuous structure is built, each oxygen ion being linked to two silicon ions. The three-dimensional counterpart of this structure would form a silica crystal.

In the interior, the valence of each ion is satisfied, four for each silicon and two for each oxygen. These ions therefore do not carry unneutralized charges. However, for the chemical composition of the whole to be SiO_2, the tetrahedra at the surface of the crystal cannot be completed. The oxygen ion at the surface can be bonded to only one silicon ion instead of two as in the interior. Thus it is left with one unsatisfied negative charge. Similarly, each silicon ion at the surface lacks one oxygen ion and it correspondingly bears one unsatisfied positive charge.

If moisture is available, the charges on the surface of the silica bring about surface hydration, as illustrated in Fig. 2. The positive hydrogen ion from the water joins with the negative oxygen ion on the surface of the silica particle and the hydroxyl ion, OH^{-}, from the water joins with the positive silicon ion, thus completing the silicon-oxygen tetrahedron. The result is a surface layer of OH groups. Water held in this manner may be

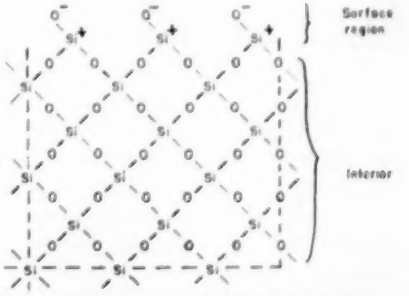

Fig. 1—Unhydrated surface of silica (Diagrammatic)

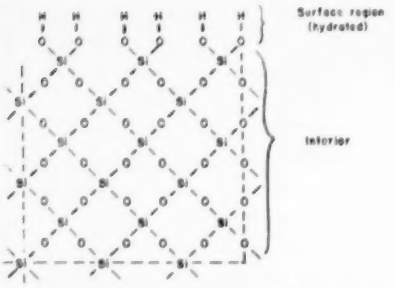

Fig. 2—Hydrated surface (Diagrammatic)

regarded as adsorbed water, since the quantity is proportional to the surface area and not to the total amount of silica.

The hydrogen ion held by an oxygen ion at the silica surface is bound less firmly than is the *OH* group as a whole. Hence, ionization in an aqueous medium frees some of the hydrogen, producing free hydrogen ions. The *surface* of the silica particle therefore is weakly acidic.

This explains why the chemical properties of silica are influenced significantly by the degree of subdivision of the silica or by the imperfections in its crystal structure. If the silica particle is macroscopic (low specific surface), its acidic character is not noticeable because the number of hydrogen ions per mole of SiO_2 is almost vanishingly small, for the hydrogen ions are produced only at the boundaries of the particle. Obviously, if smaller particles are produced by subdivision of a macroscopic particle, the number of adsorbed water molecules and hence the number of free hydrogen ions per mole of silica increases and the "reactivity" increases.

There is a limit to the possible subdivision of a silica particle. This limit is a single silicon-oxygen tetrahedron which with its hydrogen ions obtained from water corresponds to orthosilicic acid, H_4SiO_4, or

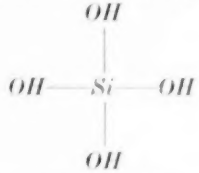

However, in a pure aqueous solution silicic acid does not remain unassociated. By "condensing," or joining together through splitting off water, molecules of orthosilicic acid tend to produce silica particles of colloidal size with only the surface of the particles remaining hydrated. The solution becomes one of colloidal silica, that is, a silica sol.

If the silica concentration in a silica sol exceeds about 1 percent, the silica is able to undergo further condensation by a linking together of colloidal particles to form a continuous structure having some degree of rigidity. Such condensation also involves the splitting off of water and the forming of new silicon-oxygen-silicon linkages. The silica sol becomes silica gel.

The gel, at first a weak, open framework of solid material, becomes more concentrated by drying and shrinking; that is, the structure tends to collapse, forming additional silicon-oxygen-silicon linkages. The gel thereby becomes harder and stronger. This process carried further produces the silica gel known in nature as opal.

Vitreous silicas are similar to a condensed silica gel in one important respect. The silicon-oxygen tetrahedra are linked together to form a three-dimensional network, but the network encloses many holes that would not have been present had an orderly crystallization been possible. Each hole is the site of unsatisfied silicon and oxygen charges. Because of the difference in manner of formation, the surface ions of oxygen and silicon in vitreous silica are probably not initially hydrated, as in silica gel, nor are the holes likely to be immediately accessible to water as are the pores in silica gel.

A dense silica gel or a vitreous silica cannot be peptized (dispersed) by exposing it to water. However, silica can be peptized by strong alkalies. The first step in the reaction with sodium hydroxide is as follows:*

$$\text{--Si--}OH + Na^+ + OH^- = \text{--Si--}O^-Na^+ + H_2O$$

From this we see that the initial action of sodium hydroxide is an acid-base neutralization, for a surface hydrogen ion unites with a free hydroxyl ion to form a free water molecule, leaving a negatively charged surface-oxygen atom satisfied by a sodium ion. This is the end condition when a dilute solution of sodium hydroxide is used. If the sodium hydroxide concentration is higher, the following further reaction takes place, given enough time:

$$\text{--Si--}O\text{--Si--} + 2NaOH = \text{--Si--}O^-Na^+ + Na^+O^-\text{--Si--} + H_2$$

Thus, as high enough concentration, the sodium hydroxide not only removes and neutralizes the surface hydrogen ions, but also severs silicon-oxygen-silicon linkages that hold the whole mass together. The reaction at the broken linkages is similar to that at the surface. By this process, amorphous silica is reduced to colloidal particles (a silica sol); higher hydroxide concentrations produce smaller sol particles. This is the reaction that evidently takes place when caustic alkalies attack opal or vitreous silica in concrete. It is an attack brought about by the aggressive effect of the OH^- ion. The alkali hydroxides are capable of more aggressive action than other hydroxides, primarily because they are more soluble and can produce higher hydroxyl ion concentrations.

This modern interpretation of silica reactivity as given by Carman explains why it is that the various investigators have found different ratios of silica to alkali in the gel deposits and exudations of affected concrete. As the alkali invades a reactive particle, opal for example, the first stages of the attack will break only the most accessible and weakest silicon-oxygen-silicon linkages.† This will weaken and soften the stone with at first not much change in its appearance. As the process continues, the silica gel becomes more and more peptized, the particles of colloidal silica thus produced becoming smaller. The caustic action is accompanied by an invasion of water which produces swelling. Hence, a sample taken at any given time during the course of the

*The reader may note that this expression shows the reaction of a surface silicon atom with its adsorbed (chemisorbed) OH group and the sodium hydroxide in solution. The sodium replaces the hydrogen of the OH group, but remains an ion, held by the negatively charged oxygen atom bound to the silicon atom.

†In a random structure, bonds of the same kind do not necessarily have equal strengths.

attack will contain a ratio of soda to silica that depends on the stage of peptization that has been reached at the time the sample was taken. The higher the ratio of soda to silica, the higher the degree of peptization. It is therefore correct to speak of the product as an alkalic silica as did McConnell, Mielenz, Holland, and Greene[2b] or as an alkali-silica complex as did Vivian[5] rather than a definite alkali silicate.

Occurrence of alkali-silica complex in concrete

The occurrence of an alkali-silica complex in concrete seems at first to be an anomaly. Along with the necessary reactive silica and alkali hydroxides, the concrete contains also an abundant supply of calcium hydroxide, which should keep the liquid phase (in the concrete) saturated with this component. Now, calcium hydroxide reacts with alkali silicates to form relatively insoluble products. How is it, then, that the alkali-silica complexes can form and persist without interference from the calcium hydroxide? We shall discuss this question after first presenting evidence, obtained by Kalousek,[6] regarding the products to be expected under equilibrium conditions.

Kalousek found that when $Ca(OH)_2$, $NaOH$, and $SiO_2 \cdot aq$ and water are intermixed the reaction product is composed of all four constituents. The composition of the product depends on the amount of alkali available, for the proportion of soda in the solid is dependent on the concentration in solution. When the liquid phase is saturated with calcium hydroxide, the equilibrium products are as given in Table 1. At least within the range of alkali concentrations included in Table 1, the product is a white precipitate not at all resembling the jelly-like deposits or exudations often found in affected samples of concrete. The product is predominantly a calcium silicate with a part of the lime replaced by alkali. As the concentration of alkali is lowered, the composition of the product approaches that of hydrated dicalcium silicate. At soda concentrations above 20 g per liter, the product contains about one mole of lime and one-fifth to one-fourth mole of alkali per mole of silica.

Kalousek assumed* that the calcium silicate product formed in hydrated portland cement might be fundamentally like the gels formed in his experiments. If so, alkali would be a constituent of cement gel, and the concentration of the alkali in the free water in the paste would be predictable on the basis of Table 1 from the ratio of alkali to silica in the cement. In connection with preparing this paper a series of analyses was performed, to check the validity of this assumption. We found that cement gel does not take up as much alkali as do the gels formed from the reaction between lime, alkali, and silica under the conditions of Kalousek's experiments (Table 1). The work leading to this conclusion is described in an appendix. The experiments enabled us to determine the approximate, actual distribution of alkali between the solid and liquid phases in portland cement paste. These experiments were made with water-saturated, hardened pastes. They show (for varied alkali contents in cement) the strengths of the alkali solutions that

*Later work has led him to a different conclusion.[7]

TABLE 1—SOME OF KALOUSEK'S DATA ON THE EQUILIBRIUM PRODUCTS OF MIXTURES OF SODA, LIME, SILICA, AND WATER WHEN THE LIQUID PHASE IS SATURATED WITH CALCIUM HYDROXIDE

Composition of solution, g per l			Composition of solid phase in equilibrium with solution, molar ratios			
Na_2O	CaO	SiO_2	Na_2O	CaO*	SiO_2	H_2O
0.20	0.912	0.003	0.003	1.98	1.00	3.2
2.4	0.237	0.003	0.04	1.47	1.00	3.3
5.5	0.100	0.005	0.07	1.32	1.00	3.0
9.2	0.039	0.012	0.14	1.18	1.00	2.9
11.6	0.023	0.014	0.19	1.05	1.00	2.7
22.3	0.016	0.071	0.21	1.00	1.00	2.6
50.9	0.01	0.178	0.22	0.97	1.00	2.7
75.2	0.01	0.220	0.24	1.03	1.00	2.9
100.6	0.01	0.498	0.25	1.04	1.00	2.6

*These are Kalousek's computed values. The values for the other oxides were obtained by analysis.

develop and make possible the attack on reactive aggregate. The results are given in Fig. 3. The concentrations generally lie below 15 g Na_2O per liter, which is a $NaOH$ concentration of about one-half mole per liter. Of course, when the paste is not water-saturated, the strength of caustic solutions may greatly exceed the limits indicated in Fig. 3.

Kalousek's findings *should* apply to the reaction between the caustic solution in the concrete and a reactive mineral in the aggregate such as opal; such a reaction is clearly within the lime-soda-silica-water system that he studied.* The anomaly spoken of earlier is that the product which such a system apparently should produce is not that which has been found in samples of affected concrete.† Instead, at least part of the product of the reaction is made up principally of alkali, silica, and water. Knowing that the reaction can occur within the boundaries of an opal particle, we can conclude that the calcium hydroxide in the solution external to the mineral boundary does not penetrate the particle as far as the alkali does.

When deposits of alkali-silica complex are found in concrete, they are found in particles of reactive aggregate or in adjoining cracks or voids. The alkali that produced these deposits must have come from, or through, adjacent parts of the concrete. Vivian[5 (p. 68)] and others have demonstrated that alkali (also

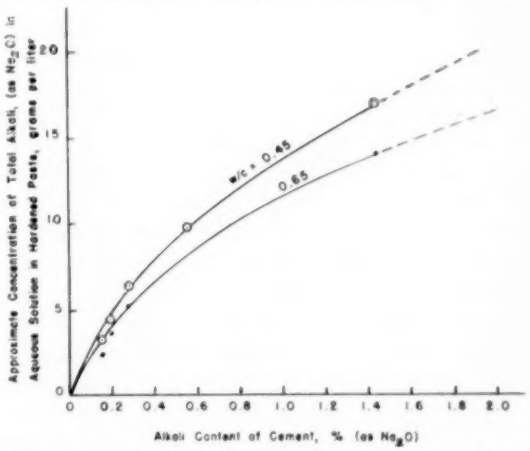

Fig. 3—Concentration of aqueous solutions in hardened cement paste

*Kalousek's experiments involved soda but not potash. Since K_2O seems to act approximately like Na_2O in alkali-aggregate reaction, equivalent stoichiometry is assumed, on a tentative basis.

†Kalousek recognized this anomaly and suggested that Hansen's theory[6] of a semipermeable membrane might explain it.

water) does diffuse from one region to another during the course of the alkali attack. As soon as the alkali in immediate contact with the reactive mineral is used up, diffusion brings more alkali to the border of the mineral particle and carries it on into the particle as the attack proceeds. If lime takes part in the reaction, it also must diffuse into the reactive particle since, in the early stages at least, the silica is immobile.

The solution in cement paste is normally saturated with lime, since solid calcium hydroxide is formed. However, owing to the common ion effect, alkali hydroxide depresses the calcium ion concentration. This is borne out by the data of Table 1, where the solutions of low silicate concentration are primarily solutions of the two hydroxides. From the data on alkali concentrations obtained in our experiments on cement pastes, we know that initially the alkali hydroxide concentration expressed as equivalent Na_2O may be as high as 15 g per liter. The corresponding concentration of CaO would be about 0.02 g per liter. But, in the lime-alkali-silica complex the amount of lime exceeds the amount of alkali at least four to one. If such a product is to be formed as lime and alkali diffuse toward the interior of the reactive particle, the lime must reach the reaction site much faster than the alkali can react. The solubility data just noted suggest that the necessary amount of lime may not reach a reaction site at the necessary rate.

Experimental evidence cited in a paper to follow this one is interpreted to mean that the lime-alkali-silica complex is produced under some circumstances and that therefore lime sometimes does manage to reach a reaction site fast enough. It will be shown that when the alkali content is sufficiently low, opal particles as big as 16-30 mesh may perhaps be converted completely to the lime-alkali-silica complex. It will be shown, though, that at higher alkali concentrations the lime is apparently not able to diffuse over a distance as great as this at the required rate.

Although consideration of relative solubilities and diffusion and reaction rates can account for the formation of the alkali-silica complex in the presence of an excess of calcium oxide, it does not account for the persistence of the alkali-silica complex over a period of years. The alkali-silica complex is not in equilibrium with the lime external to the reactive particle, even though the amount of lime in solution may be low. Unless there is some special hindrance to the passage of the calcium ions, they should gradually convert the alkali-silica complex to the insoluble complexes described by Kalousek.

Such special hindrance does seem to exist, as shown by experiments reported by van der Burgh in 1932,[8] and other experiments reported more recently by Vivian[5 (p. 64)]. Vivian placed a viscous sodium silicate gel in an open tube and then immersed the whole in a saturated calcium hydroxide solution. Gradually a white precipitate formed which it is reasonable to believe must have been one of the kind found by Kalousek in his equilibrium studies. This precipitate occurred entirely in the layer of calcium hydroxide. The line of demarcation between the calcium hydroxide solution and the gel remained unchanged and no precipitate formed below the line at any time

during the experiment, at least so far as was apparent to the eye. The originally viscous alkali gel gradually softened and finally became fluid. This experiment demonstrated that sodium silicate diffused into the upper layer and reacted with the calcium hydroxide, and that the calcium hydroxide did not diffuse appreciably into the alkali-silicate layer.

Van der Burgh's experiments differed considerably from Vivian's, but perhaps were even more striking. Van der Burgh prepared silica gel using sodium silicate and hydrochloric acid. Thus, sodium chloride was a by-product. He placed some of the unwashed gel in water maintained saturated with calcium hydroxide. A white, coherent layer of reaction product formed over the silica gel but after some weeks did not become thicker. Microscopic examination revealed that under this layer, which was about 0.5 mm thick, there was a layer of liquid several millimeters thick. When van der Burgh repeated the experiment with washed gel, he obtained an outer layer of reaction product but no liquid layer underneath. He concluded that after a sufficient thickness of solid reaction layer had formed, this layer could no longer be penetrated by calcium ions, but could be penetrated by the other ions present. Thus, in the case of the unwashed gel, the diffusion of the other ions would bring hydroxyl ions below the layer in exchange for chloride ions. This would produce sodium hydroxide, and, in the absence of calcium ion, a soluble sodium silicate would be formed—hence, the liquid layer. Van der Burgh thought of the solid reaction layer as a calcium silicate, but we judge that the product that formed in contact with the sodium hydroxide must have been a lime-soda-silica complex. It is of interest that van der Burgh estimated the thickness of the solid reaction layer at 0.5 mm, which is about 20 thousandths of an inch.

From both van der Burgh's and Vivian's experiments it appears that a layer of lime-alkali-silica complex can so hinder the passage of calcium ion as to bring it practically to a stop.

It thus seems to be established that the initial attack of the alkali and lime builds up a zone of lime-alkali-silica complex which, when it reaches requisite thickness, hinders the diffusion of calcium ions across the boundary region of the reactive particle but at the same time allows alkali and water to pass. This enables deposits of pure alkali-silica complex to form and remain in concrete for an indefinite period. As will be seen in the following paper, the thickness of the layer of lime-alkali-silica complex is probably not the same under all conditions but is dependent on the concentration of alkali and possibly on other factors.

In the paper to follow this one we shall attempt to show that when lime diffusion is hindered, the alkali-aggregate reaction produces an expansive gel; also that under certain conditions lime diffusion is not so hindered and the reaction produces a nonexpansive gel.

MECHANISM OF EXPANSION

Hansen's osmotic pressure theory

In 1944 W. C. Hansen[9] advanced the theory that the abnormal expansion of concrete resulting from the reactions of caustic soda or caustic potash and reactive aggregate is due to hydraulic pressure (fluid pressure) generated through the process of osmosis. The generation of osmotic pressure as generally understood requires a solution, an external supply of solvent, and (between the two) a semipermeable membrane. In this case, Hansen considered the solution to be aqueous sodium silicate, the solvent to be water, and the membrane to be the hardened cement paste or mortar surrounding particles of reactive silica.

Hansen's explanation is not accepted by all who have studied the phenomenon. Some have observed evidence of severe expansion where, they believed, fluid pressure could not possibly be the cause; in some cases, fractures developed through only the central portions of the reactive aggregate particles, without evidence that fluid had been present. In these cases, an expansive reaction rim still attached to the core of the particle is indicated. L. S. Brown of this laboratory has observed numerous examples of this kind and has for many years emphasized the significance of such observations. As shown in reference 10, p. 586, and Table 5, first group, Vivian found that expansion may develop in specimens stored in an atmosphere dried with calcium chloride.* Such observations have seemed to justify at least a reasonable doubt that fluid pressure is the cause of expansion.

On the other hand, almost all observers have, in some specimens, found pockets or cracks in the concrete filled with alkali-silica complex which could have functioned as the solution part of an osmotic pressure cell. Moreover, Hansen's direct laboratory experiments demonstrated that sodium silicate solutions in conjunction with cement paste or concrete as a semipermeable membrane do produce osmotic pressures. McConnell, Mielenz, Holland, and Greene[2a] confirmed Hansen's experiments and demonstrated pressures of considerable intensity.

With these different observations apparently unreconciled, it seems to some that the problem is still unsolved and that an explanation in terms of an entirely different mechanism should be sought.

We believe that the apparently conflicting evidence is actually in harmony and can be explained in terms of one fundamental cause. It can be shown that abnormal expansion could in all cases be due to the generation of a pressure by a process fundamentally like osmosis even when the concrete is relatively dry and lacks evidence that the expansion was caused by hydraulic pressure.

Extension of osmotic pressure theory

To show how the apparently conflicting evidence just mentioned can be reconciled we must first discuss the process of osmosis. Usually we think

*No expansion with respect to original dimensions was observed; rather, on this basis the specimens contracted. However, relative to the dimensions of the control specimens after drying, the specimens containing reactive particles showed expansion.

that osmotic pressure develops from the tendency of a solvent to enter a solution under conditions where the resulting volume increase of the solution is resisted. Such resistance is manifested by a rise in hydrostatic pressure. Although the phenomenon has been known for about 200 years, no single explanation of it suitable in all respects has been advanced. The explanations that are satisfactory in most respects are based on the theory of molecular bombardment, some authors holding that the bombardment of the solute molecules on the membrane confining the solution is indirectly the cause of the pressure, and others supporting the view that the pressure is due to the bombardment of the solvent molecules. The fundamental difficulties surrounding these theories are described by Glasstone,[11] and others.

Fortunately, it is not necessary to visualize the mechanism of pressure generation to understand the conditions necessary to the generation of pressure. Glasstone says: "In the study of osmotic pressure the essential point to be borne in mind is that for some reason connected with the solute molecules the partial free energy, chemical potential or activity of a solvent molecule is less in a solution than in the pure liquid; . . . " This means that if conditions are such that water in concrete will lose some of its thermodynamic activity or available energy when it moves into a region where alkali-silica complex exists, that movement will occur regardless of the mechanism involved. Just as water seeks its own level under the influence of gravity, thus reducing its energy of position (potential energy), it will tend to move within concrete in whatever way is required to equalize its available energy.

The relative vapor pressure of water is an index to its available, or "free," energy. A body of pure water under a pressure of 1 atmosphere will evaporate in a closed space until a certain vapor pressure is produced, which vapor pressure is characteristic of water at the existing temperature. However, the water in a solution cannot maintain as high vapor pressure as can pure water. The difference in vapor pressure is due to the dissolved substance. The ratio of the vapor pressure maintained by the solution to that maintained by pure water is used by the physical chemist to calculate how much the free energy diminishes when water becomes part of a solution.

Thus, whenever the water at a given point in concrete has a vapor pressure different from that of the water in another part, the water will tend to move from one region to the other in such a way as to reduce the indicated difference in free energy. Vivian[5 (p. 68)] demonstrated that water moved from a region in a test specimen where no alkali-silica complex existed to a region where it did exist. He thereby demonstrated that the water held by an alkali-silica complex is at a lower free energy level than water external to the complex. This means that pure water will enter the complex if such entry is physically possible, and may continue to do so until the complex is reduced to an infinitely dilute solution.

Suppose we have a means of applying pressure to a solution without applying pressure to the solvent, in this case water. We could find a particular pressure that would just prevent more water from entering the solution.

The stronger the solution the greater the pressure required to prevent the entry of additional water. The magnitude of the pressure required to prevent the entry of water is called the osmotic pressure of the aqueous solution. The stronger the solution the lower the vapor pressure of the water it contains and the higher the osmotic pressure.

To apply a pressure to the solution and not to the water, we must be able to keep the solution separate from the water and at the same time keep the solution accessible to the solvent—water. Keeping the solution separate from the water is accomplished by the semipermeable membrane which permits free passage of the water but not of the solute. The membrane is essential not only to permit the selective application of pressure, but also to prevent the solute from diffusing out, for it also tends to move to regions where its free energy will be lower.

Actually, a membrane need not have the properties of a molecular sieve—one that holds some atoms or groups of atoms and lets others pass. Any rigid, permeable layer separating the solution from the solvent will allow some osmotic pressure to develop if the rate of diffusion of the solute through the layer is lower than the rate of diffusion of the solvent. The duration of the osmotic pressure and the fraction of the theoretical pressure that can be developed by such an imperfect membrane depends on the relative rates of diffusion and on the permeability of the layer, that is, the membrane.

In the experiments conducted by Hansen, and by McConnell, Mielenz, Holland, and Greene, a sodium silicate solution was separated from pure water by a wall of concrete or cement paste, the wall forming one side of a closed chamber. If sodium silicate was able to escape from the chamber through the wall of concrete or paste at all, it did so more slowly than pure water could move through the wall. Consequently, it was possible for the experimenters to develop pressures as high as 500 psi as the water moved into the solution.

What we have just described is osmotic pressure and an osmotic-pressure cell in its most familiar form. However, osmotic pressure can develop under conditions quite different from those just described. Let us consider, for example, a solution which is by nature immobile. There are certain solids that can take up water and swell. Certain clay minerals are crystals which can be penetrated by water in a manner that can be regarded as solution. When water is taken in, the crystal expands. The water might be prevented from entering by applying a suitable counteracting pressure to the solid. We may call this osmotic pressure developed without the aid of a semipermeable membrane.*

When the solvent enters such a "solution" the amount of expansion possible is limited by the "solubility." The pressure required to prevent expansion will depend upon the degree to which the solid has become saturated; the higher the degree of saturation the smaller the osmotic pressure.

*The "solute" remains, in this case, attached to the crystal. Such attachment performs the same function as a semipermeable membrane when the dissolved ions or molecules are free to move.

Thus it is that, if the solution is a liquid, osmotic pressure can be generated only with the aid of a semipermeable membrane, the pressure being hydrostatic. But if the solution is a solid, the semipermeable membrane is not essential.

At this point we begin to deal with variants of the usual concepts of solvents and solutions, and we encounter problems in terminology. It is not customary to use the term "osmotic pressure" in connection with solids; osmotic pressure has always been dealt with experimentally and in the textbooks as hydraulic pressure. The force exerted by the swelling of a solid is customarily called swelling pressure. Moreover, the solids most often dealt with in connection with swelling in water are not regarded as being in aqueous solution. Such solids are called gels and the water is supposed to be in the gel and not vice versa. The solid part of the gel plays the role of solvent; the water, the role of solute. But the water in such a system is not called a solute nor is the gel called a solvent. Instead, the water is said to be adsorbed on the surfaces of the small particles of solid material making up the gel, or in some cases it may be regarded as adsorbed in interplanar spaces within the crystals.

A gel-water system is not called a solution for several reasons. For example, a solution is supposed to be a single, homogeneous phase containing two or more components. A gel-water system is not considered to be homogeneous.

These various terms were brought into scientific literature to deal with differences that are mostly of degree. Although adsorbed water cannot be said to be dissolved *in* the solid, it is sometimes thought of as being dissolved *on* the solid. That is to say, we use the term "surface solubility" (Glasstone, *ibid*, p. 656). A finely divided solid on which the water is "surface-dissolved" (adsorbed) is made up of many small units, each of which is an aggregation of many molecules, which molecular aggregations water is unable to disperse. If the water were able to disperse them fully, we would have a true solution and if some of the water tended to stick with some of the atoms of the dispersed solid (now a solute), we would probably speak of hydrated molecules or ions.

The distinctions intended by the different terms are clear when we are dealing with solids that are unmistakably gels on the one hand, and solutions that are unmistakably homogeneous on the other. When dealing with borderline cases, the existence of the two sets of terminology is sometimes confusing.

The differences that give rise to these different nomenclatures are only of minor concern to us here. Whether water is held in a liquid solution, a solid solution, or a "surface solution," an energy potential does exist between that water and free water, provided that the solution is not infinitely dilute or that the gel is not already water-saturated. When equilibrium does not exist, the same kind of change will take place in each case—that is, free water will tend to enter the solution or the gel, thus diminishing the initial free-energy potential.

Hence, to know that water will have a tendency to enter a given region we need only to establish that the water already in that region exhibits less free energy than the water outside; the particular mechanism by which the energy potential is created is a secondary matter. Conversely, when water is observed to move spontaneously from one region to another, we know that for some reason an energy potential exists.

Up to this point we have spoken of swelling as if it were produced by the imbibition of pure water. Actually, the liquid imbibed from cement paste is a solution. The free energy of the solvent (water) is less than that of pure water. The imbibition of water and swelling is due to the fact that the free energy of water in the alkali-silica complex is still lower than that of the water in the surrounding paste.

We need to keep in mind that although the mechanism by which the free energy of water is reduced is immaterial, different substances will show characteristic differences in the amount of water that they can take up while undergoing the same change in free energy. A relatively dry sodium silicate in which the residual water exhibits a vapor pressure equal to one-half that of bulk water at the same temperature would have to take up a large quantity of water and increase its volume several fold in order to raise the free energy of the water in the sample to, say, 98 percent of that of pure water. In contrast, for the same change in free energy, a portland cement gel could take up only a very small amount of water and would increase in volume only a fraction of 1 percent.

As to the volume changes resulting from water imbibition, we know that if water enters a true solution, the volume increase of the solution will usually be some large fraction of the volume of water that enters. If water enters a dry gel, the volume increase of the gel is related in a very complicated manner to the amount of water that enters. This complication comes from the fact that in a dry or semidry state the gel is a porous solid possessing strength and elasticity. The first water that enters does not fill the pores. It becomes adsorbed and brings about energy releases that cause the solid to expand in a manner and to a degree not simply related to the volume of the water entering. The volume increase of the solid is due in part to the effect of water in diminishing the surface tension of the solid colloidal units of the gel. The surface tension of these solid units tends powerfully to compress them. Consequently, when this tension is reduced, the units expand.

The changes in volume due to such surface tension effects are of consequence only when dealing with the changes of microscopic magnitude that occur in cement gel and the like. With such gels the solids that compose them are precipitated in water and the coagulation that solidifies them occurs in water. Consequently, at the time of formation the surfaces of the gel particles are completely saturated. For this reason these gels can imbibe water only if they have first been dried. When they do imbibe water, they are unable to imbibe any more than the amount required to resaturate the surfaces. Such gels usually cannot swell beyond their original dimensions.

(A cement may, of course, undergo continued hydration, an effect not dealt with here.)

The comparatively small volume changes of gels like cement gels are probably not due entirely to the surface tension effects just described. It is likely that some of the volume change is due to displacement of gel particles relative to each other.

The alkali-silica complex differs from cement gels in important respects. An alkali-silica complex can be created in a practically dry state,[10] though in such a state it will not have the characteristic appearance of a gel. Such gels have the power to imbibe water and swell almost, if not quite, without limit; they are classed as *unlimited swelling gels* in contra-distinction to the limited swelling type to which cement gel belongs. The ability to swell without limit is due to the peptizing effect of the alkali hydroxide in the complex, as mentioned in the preceding section.

When an alkali-silica complex imbibes water and swells, the swelling is probably due primarily to the displacement of colloidal units with respect to each other, the volume changes due to changes in surface tension of the solid phase probably being comparatively small. The displacement of particles produced by the alkali attack is apparently a dispersion process whereby the invading water penetrates between the interconnected particles, gradually separating them. The water thus supplements the effect of the alkali in causing the original solid to lose its rigidity—its yield value becomes smaller and smaller. Finally, the gel seems to lose all its rigidity and becomes fluid. Even when the water supply is too restricted to soften the gel very much, the gel can be fluidized by a highly concentrated caustic.[12] We have already seen that this is due to the almost unlimited peptizing ability of the caustic.

Casting back over the ground now covered we see that although the underlying cause is thermodynamically the same in all cases, the amount of water that can enter a gel under stipulated conditions depends on the physical and chemical characteristics of the gel, *i.e.*, whether it is of the limited swelling or unlimited type. The alkali-silica complex can form in the dry state and can swell on imbibition of water, apparently without limit, granted sufficient peptization. The other gel, a lime-alkali-silica complex is evidently, like cement gel, of the limited swelling type.

We can conclude that swelling pressure able to cause concrete to dilate significantly beyond its original dimensions can be produced only by the gel of the unlimited swelling type—the alkali-silica complex. If the alkali-silica complex is fluid, and if it is confined, pressure may be generated as described by Hansen, that is, it may be hydraulic (osmotic). If the complex is solid, that is, still a solid reaction rim, pressure may be generated through the swelling of the rim, even though cracks or cavities are present that would relieve hydraulic pressure. If the reaction rim, though solid, is plastic, semi-hydraulic pressure could develop, the pressure being hydraulic to the degree that it is equal in all directions. The fundamental cause of swelling is the

same in all cases—the entry of water into a region where the effect of a solute or of adsorption reduces its free energy.

The foregoing explanation of the mechanism of producing swelling through cement-aggregate reaction is in agreement with some features of explanations previously advanced. It involves the same mechanism proposed by Hansen: The swelling is due to imbibition of water, as Hansen supposed, but it is not necessarily the result of hydraulic pressure maintained by a semipermeable membrane. McConnell, Mielenz, Holland, and Greene[25] concluded that "osmotic pressure cells commonly are formed at the walls of reactive aggregate sockets." They also concluded that the first-formed gels are viscous and low in water content, and that development of more fluid gel generally takes place only after fracturing has resulted. Vivian, whose explanation is nearly the same as ours, concluded that no semipermeable membrane is involved—that the expansion is due to swelling of solids only. We, on the other hand, believe that Vivian's conclusion was influenced by his observations on small laboratory specimens. When cracks occur in such specimens, soft or fluid gels may exude to the surface without producing further swelling. In mass concrete, however, isolated cracks may fill with alkali-silicate solution, and thereafter the soft gel or solution in such cracks may develop osmotic pressure, the concrete itself functioning as a semipermeable membrane. However, all such swelling is likely to be of less consequence than that which will have occurred earlier, that is, the swelling that produces the cracks that later become osmotic pressure cells. Hence we agree with Vivian that solid swelling is probably the primary cause of damage. This is the position that L. S. Brown of these laboratories has long maintained. Some of his evidence is set forth in a paper which will probably reach publication at about the same time as this one.

SUMMARY

This first part of our paper has dealt with two of the four topics mentioned in the introductory paragraphs, namely, the nature of the reaction that may occur when concrete contains reactive silica, and the mechanism of abnormal expansion when caused by alkali-aggregate reaction. Though only the reactions of "free" or hydrous silica were developed, it is believed that siliceous glasses and silicates such as have been found to be susceptible to alkali attack may react in a somewhat analogous manner. Also, the mechanism of expansion is probably the same or at least similar. The principal conclusions reached are summarized below.

On the chemical reactions

(1) Most reactive rocks are amorphous or contain amorphous constituents. The amorphous constituent may be a condensed gel or it may be vitreous. Both the gel and the vitreous states of silica are characterized by discontinuities in structure. Silicon and oxygen atoms are exposed at all surfaces, and at discontinuities. The exposed atoms do not have their chemical valencies fully satisfied within the solid. This leads to chemisorption of water, and to

surface reaction with caustic alkalies by both silica gel and vitreous silica.

(2) Caustic alkali when sufficiently concentrated breaks silicon-oxygen-silicon linkages and thus extends its range of reaction. The circumstances of the attack may leave the solid still one connected mass, or the action may continue until a sol is produced, or until only a solution remains. The ratio of alkali to silica in the product increases as the attack progresses. The product is an alkali-silica complex of indefinite composition.

(3) The formation and continued existence of the alkali-silica complex in concrete is anomalous because of the presence of ample calcium hydroxide which under equilibrium conditions should form lime-alkali-silica complex. Apparently, the alkali-silica complex is able to form and persist because of inability of the lime to diffuse to the reaction site at a sufficiently high rate. This may be owing to the low solubility of calcium hydroxide in caustic alkali, and also to difficulty experienced by calcium ion in penetrating the layer of lime-alkali-silica complex that apparently first forms around the particle.

On the mechanism of expansion

Expansion is produced when the alkali-silica complex imbibes water. The initial, most damaging expansion probably occurs while the reaction product is still solid, though expansion may occur after the product becomes plastic or fluid, if initially formed cracks have no outlets. The force is that of swelling pressure or osmotic pressure (hydraulic), the two being fundamentally alike.

REFERENCES

1. Jones, F. E., "Reactions Between Aggregates and Cements: I. Alkali-Aggregate Interaction—General," *Research Paper* No. 14, National Building Studies (Great Britain), 1952.

2a. McConnell, D., Mielenz, R. C., Holland, W. Y., and Greene, K. T., "Cement-Aggregate Reaction in Concrete," ACI JOURNAL, Oct. 1947, *Proc.* V. 44, pp. 93-128.

2b. McConnell, D., Mielenz, R. C., Holland, W. Y., and Greene, K. T., Discussion of a paper by Willard H. Parsons and Herbert Insley: "Aggregate Reaction with Cement Alkalies," ACI JOURNAL, Part 2, Dec. 1948, *Proc.* V. 44, pp. 632-1 to 632-6.

3. Stanton, T. E., "Influence of Cement and Aggregate on Concrete Expansion," *Engineering News-Record*, V. 124, 1940, pp. 171-173; "Expansion of Concrete Through Reaction Between Cement and Aggregate," *Proceedings*, ASCE, V. 66, 1940, pp. 1781-1811.

4. Carman, P. C., "Constitution of Colloidal Silica," *Transactions*, Faraday Society, V. 36, 1940, pp. 964-973.

5. Vivian, H. E., "XV. The Reaction Product of Alkalis and Opal," *Bulletin* No. 256, Commonwealth Scientific and Industrial Research Organization, Melbourne, Australia, 1950, pp. 60-78.

6. Kalousek, G. L., "Studies of Portions of the Quaternary System Soda-Lime-Silica-Water at 25° C," *Journal of Research*, National Bureau of Standards, V. 32, 1944, pp. 285-302.

7. Kalousek, G. L., and Adams, M., "Hydration Products Formed in Cement Pastes at 25 to 175 C," ACI JOURNAL, Sept. 1951, *Proc.* V. 48, pp. 77-90.

8. van der Burgh, A. J. P., "The Reaction of Lime on Silicic Acid in Relation to the Hardening of Portland Cement" (In Dutch), *Chem. Weekblad*, V. 29, 1932, pp. 616-618.

9. Hansen, W. C., "Studies Relating to the Mechanism by which the Alkali-Aggregate Reaction Produces Expansion in Concrete," ACI JOURNAL, Jan. 1944, *Proc.* V. 40, pp. 213-27.

10. Vivian, H. E., "Studies in Cement-Aggregate Reaction. VII. The Effect of Storage Conditions on Expansion and Tensile-Strength Changes of Mortar," *Journal*, Council for Scientific and Industrial Research, V. 20, 1947, pp. 585-594.

11. Glasstone, Samuel, *Textbook of Physical Chemistry*, 2nd edition, D. Van Nostrand Co., Inc., New York, N. Y., 1946, p. 651.

12. Vivian, H. E., "XII. The Effect of Amount of Added Alkalis on Mortar Expansion," *Bulletin* No. 256, Commonwealth Scientific and Industrial Research Organization, Melbourne, Australia, 1950, pp. 31-47.

Appendix—Description of Experiments on Strength of Caustic Solutions in Cement Pastes

We have on hand specimens of neat cement paste over two years old. These specimens were cast in glass tubes 10 in. long by 1¼ in. in diameter. At the time of casting the mold was equipped with an axial core about ½ in. in diameter. On the day following casting this core was removed, leaving the specimen as a cylinder of cement paste encased in glass, the wall thickness of the paste cylinder being about ⅜ in. As soon as the core was removed, the hole was filled with tap water and the upper end of the tube was closed with a rubber stopper. During the more than two-year period of curing, water was added when needed to maintain the original level, but none was ever removed.

Ten such specimens were selected representing five different cements having compositions of four ASTM types. For each type of cement, two different water-cement ratios, 0.45 and 0.65, were represented.

The quantity of curing water in each specimen was measured, and the concentrations of sodium and potassium were determined by means of a flame photometer. Data from companion specimens were used to estimate the amount of water fixed by hydration (nonevaporable water) and the amount that remained free (evaporable water) within the boundaries of the paste. Calculations were then made of the total amount of alkali in solution, the calculations being based on the assumption that the concentration of the alkali in the evaporable water in the paste would be the same as the concentration of the alkali in the curing water. In view of the long curing period, and the facility with which alkali can be leached out, this assumed equalization of concentration is believed to be amply justified.

The data obtained are given in Table A-1. These data, from specimens prepared for other purposes, are not as precise as could be desired. For example, the data on evaporable water are, in several cases, estimated on the basis of experimental data from companion samples having a different water-cement ratio. However, the principal indications of the results could not have been different if precise values had been available for all measured quantities, as will be seen presently.

As shown in Table A-1, the total amounts of alkali in solution were calculated from the measured concentrations. The amount of solution in the central well was measured, and the amount of evaporable water was also known or closely estimated by interpolation. The total alkali in aqueous solution was obtained by multiplying the sum of the weight of curing water and the weight of evaporable water in the specimen ($w_c' + w_e$) by the measured concentration, of Na_2O or K_2O (column 6 or 7).

The results expressed as percent of cement weight are tabulated in columns 8 and 9. In Fig. A-1 they are plotted against the original alkali contents of the cements (columns 10 and 11). Fig. A-1 indicates that most of the alkali in the cement is in aqueous solution. The extent to which the plotted curve in Fig. A-1 falls away from the dashed line indicates the limited degree to which alkali was held by the solid phases. At low concentrations of alkali, the amount in aqueous solution appears to be equal to the total alkali within the estimated experimental error. As the total alkali increases, the amount of alkali in aqueous solution becomes progressively less than the total alkali. When the alkali content of the cement is 1 percent, about 75 percent of the alkali is in solution. The nature of the relationship is such as to suggest that some of the alkali is adsorbed by the cement gel, the amount adsorbed increasing with the concentration.

TABLE A-1—DATA ON AMOUNTS OF ALKALI IN AQUEOUS SOLUTION IN HARDENED CEMENT PASTES

1	2	3	4	5	6	7	8	9	10	11	12	13	14
Cement No.	w/c*	w_e/c	w_e'/c	$\frac{w_e + w_e'}{c}$	Observed concentration in curing water, g per g of water		Calculated alkali in aq. soln., g per g of cement		Alkali originally in cement, g per g of cement		Calculated concentration of aq. soln. without leaching		Total as Na_2O, g per l
					Na_2O	K_2O	Na_2O	K_2O	Na_2O	K_2O	Na_2O, g per l	K_2O, g per l	
15754	0.45	0.272	0.19	0.46	0.0035	0.0031	0.0016	0.0014			4.0	3.5	6.3
	0.65	0.404	0.26	0.66	0.0027	0.0022	0.0018	0.0014			3.4	2.6	5.1
Avg.							0.0017	0.0014	0.0017	0.0016			
15761	0.45	0.34	0.20	0.54	0.0143	0.0061	0.0077	0.0033			12.8	6.4	17.0
	0.65	0.54	0.28	0.82	0.0102	0.0043	0.0084	0.0035			10.7	5.1	14.1
Avg.							0.0082	0.0034	0.0113	0.0044			
15756	0.45	0.27	0.20	0.47	0.00090	0.0028	0.00042	0.0013			1.1	3.3	3.3
	0.65	0.47	0.30	0.77	0.00063	0.0020	0.00048	0.0015			0.8	2.5	2.4
Avg.							0.00045	0.0014	0.0005	0.0017			
15758	0.45	0.33	0.24	0.57	0.0044	0.0063	0.0025	0.0036			5.3	6.9	9.9
	0.65	0.53	0.30	0.83	0.0032	0.0044	0.0026	0.0036			4.0	5.3	7.5
Avg.							0.0026	0.0036	0.0030	0.0040			
15763	0.45	0.21	0.24	0.45	0.0009	0.0037	0.00041	0.0017			1.2	5.0	4.5
	0.65	0.41	0.35	0.76	0.0008	0.0030	0.00061	0.0023			1.1	4.3	3.9
Avg.							0.00050	0.0020	0.0005	0.0022			

Key: w/c = water-cement ratio by weight, g per g of cement
w_e/c = evaporable water in the paste, g per g of cement
w_e'/c = curing water in central hole of specimen, g per g of cement
$\frac{w_e + w_e'}{c}$ = total amount of solvent, g per g of cement
c = weight of original cement, g

*Nominal; not corrected for bleeding.

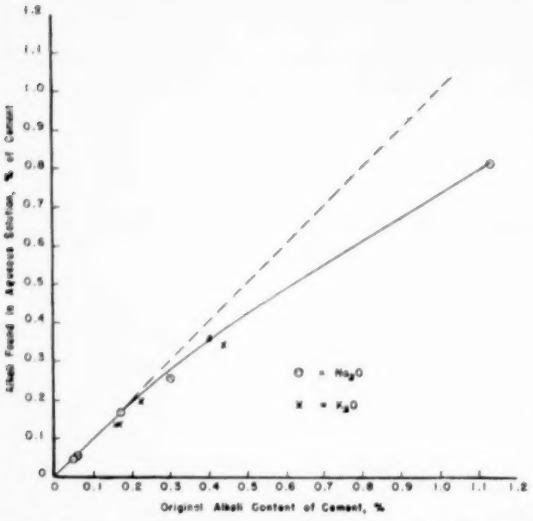

Fig. A-1—Amounts of alkali found in solution in relation to alkali content of cement

The amount of alkali held by the cement gel is much less than that held by the gels formed in the system studied by Kalousek.* By means of the relationships found by Kalousek, we calculated the amount of Na_2O that would have been in solution had the relationships for cement gel been the same as for the lime-alkali-silica complexes. The results are given in Table A-2.

It seems safe to assume that all the alkali in the cement is in solution or will go into solution as alkali is removed by leaching or by chemical reaction. In confirmation of this we have, in earlier experiments, removed all the alkali from specimens of the kind described above simply by removing the glass shells and exposing the pastes to a large volume of limewater initially free from alkali. Within a comparatively short time, both the sodium and potassium contents were reduced to concentrations that could not be detected with the flame photometer. Indeed, this ability to leach out the alkali was to be expected even had Kalousek's data applied (see Table 1).

Columns 12, 13, and 14 of Table A-1 give the alkali concentrations which, calculations indicate, would have prevailed had there been no leaching from the hardened paste into the curing water. In making these calculations, an allowance was made for the increase in the amount of adsorption that would accompany the increase in solution concentration. This allowance for increased adsorption was made by establishing an empirical relationship between the amount of alkali adsorbed and the solution concentration. The amount adsorbed in the tests as made was taken to be the difference between the amount shown in column 8 or 9 and the corresponding amount in column 10 or 11.

TABLE A-2—CALCULATED AND FOUND AMOUNTS OF Na_2O IN AQUEOUS SOLUTION

Cement No.	w/c, by wt.	Calculated Na_2O in aqueous solution, g per g of cement	Amount of Na_2O found, g per g of cement	Ratio of found to calculated
15754	0.45	0.00023	0.0016	7.0
15761	0.45	0.0017	0.0077	4.5
15756	0.45	0.000065	0.00042	6.4
15758	0.45	0.00051	0.0025	4.9
15763	0.45	0.000052	0.00041	7.9

*This conclusion is of interest with respect to questions quite apart from the subject of this paper. It shows, as has now been concluded by Kalousek,[7] that cement gel is not chemically like the gels formed when lime, silica, and alkali are brought together. It is a fact, therefore, that should be taken into consideration in studies of the stoichiometry of cement gel.

Special Purpose Waterfront Structure of Precast Reinforced Concrete*

By WIN E. WILSON†

SYNOPSIS

Describes the design and construction of a special ramp, built for the U. S. Navy, using a precast concrete system. Basically, it consists of precast reinforced concrete bearing piles set on the apexes of equilateral triangles supporting precast girders which in turn support triangular deck slabs. The tops of the piles were fitted with special anchors and bearing plates to receive the connections at each end of the girders.

THE JEHEEMY RAMP

This special purpose structure, a "Jeheemy ramp," is at the U. S. Navy amphibious base on the strand below Coronado, Calif. The origin of the name "Jeheemy" is not known. The Jeheemy is a rubber-tired vehicle used for picking up naval landing craft from the water and transporting them to shore for repair and maintenance. (The original concept of the device probably came from the well-known Ross lumber carrier.) These vehicles come in assorted sizes the largest of which is approximately 60 ft long, weighs about 35 tons, and is capable of lifting an LCM (landing craft) weighing 35 tons. Motive power is provided by tractors. About two-thirds of the total load of the Jeheemy and supported craft is distributed between the two sets of dual rear wheels which have airplane-type tires. This results in a wheel load of 50,000 lb. Fig. 1 shows a Jeheemy in operation.

Fig. 1—Jeheemy in use

*Presented at the ACI Seventh Regional Meeting, Los Angeles, Calif., Oct. 29, 1954. Title No. 51-27 is a part of copyrighted JOURNAL OF THE AMERICAN CONCRETE INSTITUTE, V. 26, No. 6, Feb. 1955, *Proceedings* V. 51. Separate prints are available at 35 cents each. **Discussion** (copies in **triplicate**) should reach the Institute not later than June 1, 1955. Address 18263 W. McNichols Rd., Detroit 19, Mich.

†Partner, Wilson and Wilson, Engineers, Los Angeles, Calif.

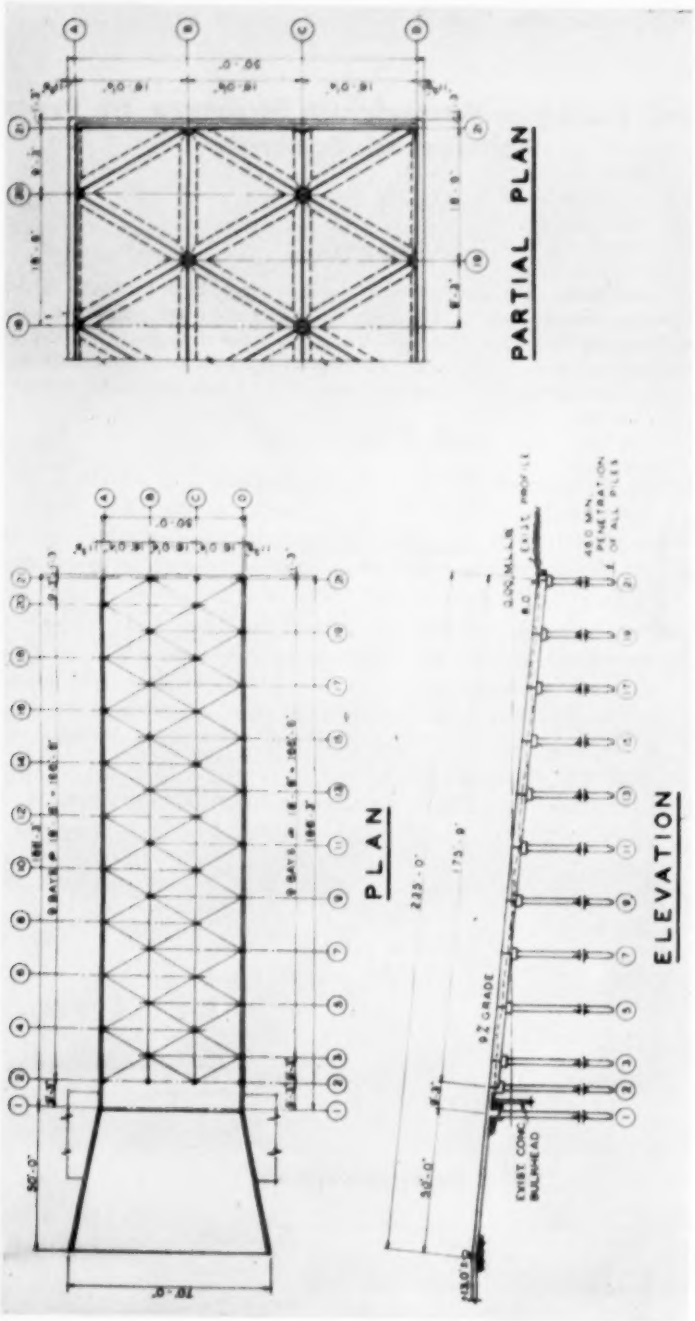

Fig. 2—Plan and elevation of ramp

Soon after the establishment of the base and the development of the Jeheemy, an emergency ramp was constructed in 1943 using precast concrete slabs laid directly on the sloping sand bottom of the bay. Due to the movement of the sand bottom occasioned probably by tidal action and propeller wash, the slabs became displaced and eventually the heavy wheel concentrations caused practically complete disintegration. In 1952 it was decided to study feasible methods of reconstruction of the ramp. After an investigation of the operating conditions a report outlined three possible methods of reconstruction.

The first of these contemplated the construction of a supported deck of reinforced concrete somewhat similar to a seaplane landing ramp. This method contemplated the use of precast piles and conventional cast-in-place reinforced concrete deck. This scheme would have necessitated the construction of a temporary bulkhead surrounding the site and the dewatering of the working area.

The second scheme also called for reinforced concrete, utilizing precast piles, girders, and slabs so detailed as to permit setting under water, thus eliminating the need for the temporary bulkhead and the cost of dewatering.

A third plan was developed which envisioned an overhead bridge crane extending from the shore out over the water with the steel structure supported on either caissons or bearing piles extending above the high water line.

Preliminary designs and cost estimates were made on each of the three schemes with an analysis of the advantages and disadvantages of each. The overhead bridge crane method was not recommended because of high maintenance costs and personnel problems involved in maintaining three crews of operators for the cranes to make the facility available at any hour of the day or night. In addition, the Navy considered that the permanent structure of the type proposed would pose an operational hazard considering that it would be used for training and inexperienced personnel would be operating the landing craft. In addition to these factors the preliminary cost estimate indicated this to be the most expensive of the three plans.

The two schemes employing reinforced concrete were deemed to be more practical. Comparative cost estimates showed only a relatively small saving using the completely precast method. Consequently it was finally recommended that plans for the two schemes be developed and comparative bids taken.

The Department of the Navy, however, selected the precast system without alternates and the working plans were prepared on this basis.

Fig. 2 shows the system selected. Basically it consists of precast reinforced concrete bearing piles set on the apexes of equilateral triangles supporting precast girders which in turn support triangular deck slabs. The tops of the piles were fitted with special anchors and bearing plates to receive the connections at each end of the girders. As seen in Fig. 3, the top of each girder was recessed to receive the deepened stiffening member around the

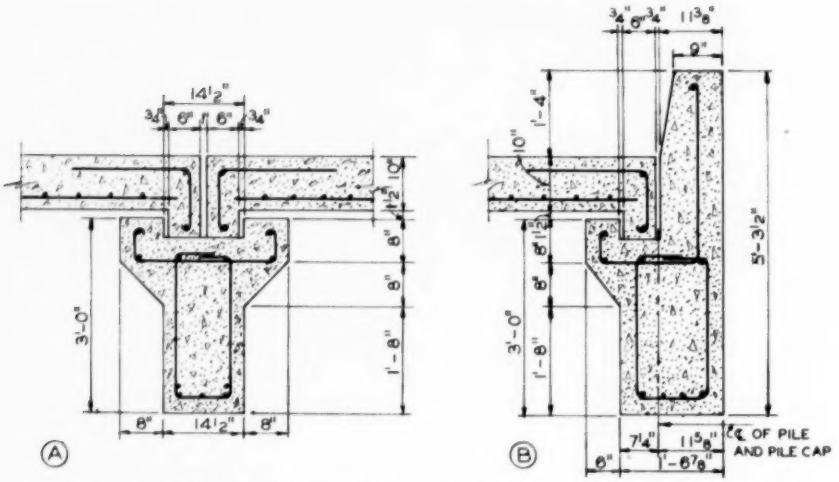

Fig. 3—Details of typical girders. (A) Typical interior girder. (B) Typical edge girder

edge of the slabs. The boundary girders along both sides of the ramp were deeper than the interior girders, thus providing the deck with an elevated curb. Openings were left between the curb ends to facilitate the removal of sand which might be washed onto the deck.

The triangular shape was selected for the slabs to minimize stresses which might have occurred in rectangular panels due to accidental errors in the grades of the pile caps. To provide for uniform bearing between the slabs and the girders in case of misalignment, ½ in. of nonorganic, preformed expansion joint material was placed in the trough of the girders before setting the slabs.

In the design of the structure, the 50,000-lb wheel load was the controlling factor for moment and shear. The slabs were designed as flat plates and no attempt was made to reduce moments by developing continuity of the adjoining elements.

ERECTION PROCEDURE

All of the various component parts entering into the precast work were cast by the contractor on the base a short distance from the job site.

The contractor built a temporary trestle and traveling crane down the center of the ramp for driving the piles and setting the various units. After driving the piles a steel caisson approximately 5 ft in diameter was driven around the pile to a depth sufficient to prevent boiling, and the caisson was dewatered. The top of the pile was then prepared for the cast-in-place concrete pile cap which was approximately 3 ft in diameter. Prior to casting a steel bearing plate was positioned with suitable anchors to prevent lateral displacement of the pile and to receive the ends of the girders. These plates were accurately placed to line and grade with the surface paralleling the

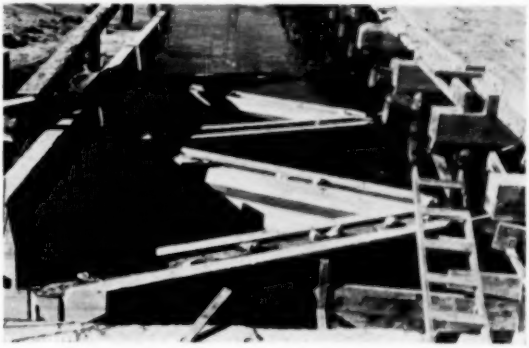

Fig. 4—Precast girders in position at the inboard end of ramp

surface of the ramp. After the cap had set, the caisson was removed and reused. As the water grew deeper toward the outboard end of the ramp the length of caissons was increased by welding sections together. As a matter of interest, it was discovered that at the outboard end the penetration required to effectively seal the bottom inside of the caisson against boiling due to pressures on the outside conformed almost exactly to the average value found on the graph in the article by Byron J. Prugh in the November, 1953, issue of *Civil Engineering*, namely 16 ft corresponding to an unbalanced head of approximately 13 ft.

Upon removal of the caissons the contractor placed the precast girders. Fig. 4 shows a number of these in position at the inboard end. In the deeper water farther off shore it was necessary to use a diver to position and secure the girders.

Fig. 5—Positioning girders using pipe guides over the anchor bolts

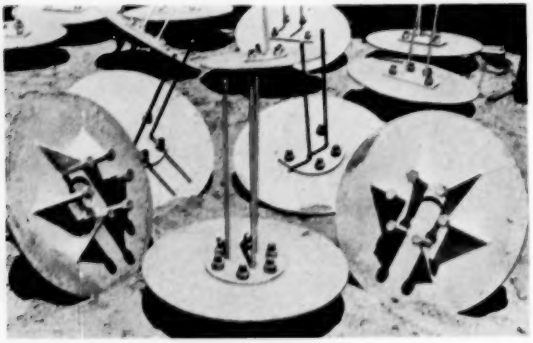

Fig. 6—Pile caps and anchors prior to installation

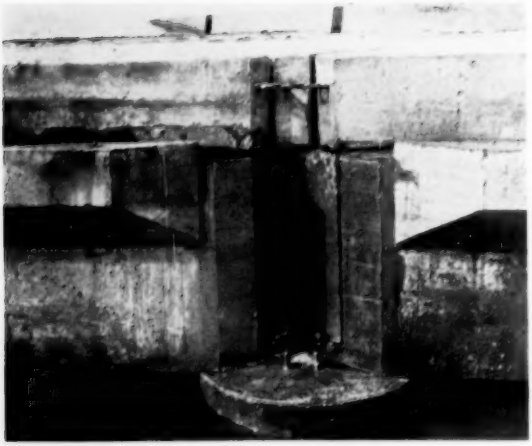

Fig. 7—Sections of girders and slabs on top of a typical pile cap

Fig. 8 — Space provided for anchors over pile prior to grouting

Positioning of the girders was facilitated by placing pipe guides over the anchor bolts that extended above water level (Fig. 5). The holes in the ends of the girder anchor plates were large enough to receive the pipes and automatic positioning resulted as the girders were lowered.

After the girders were placed, an upper plate, with dowels welded to it, was positioned over the anchor bolts using a long spindled socket wrench to place and secure the nuts. These dowels provided anchorage for the slabs as shown later. Fig. 6 shows the pile caps and anchors prior to installation. All metal other than the internal reinforcing was heavily zinc coated.

The precast slabs were then placed. The corners of the slabs were provided with U-shaped anchor rods and hairpin anchors were dropped into the open space between the ends of the girders. This space was then filled with concrete using a tremie. The section of the girders and slabs on top of a typical pile cap are shown in Fig. 7. Fig. 8 shows a section of the deck slabs prior to the grouting of the space provided for anchors over the pile. Because of clearances provided in the drawings and care exercised in positioning the pile caps, no difficulty was encountered in placing any of the precast units.

The steel to steel bearing between the girder ends and the pile caps was chosen to provide for inequalities in bearing which might result from inaccurate pile cap leveling.

The oversize holes in the girder plates likewise provided for inaccurate pile cap locating. Since the space between the girder ends was to be filled with concrete and the slabs anchored thereto, further movement of the pile relative to the girders was deemed almost impossible under the conditions at the site. The ramp is located on the sheltered bay side and is not subject to the major effects of ocean storms. In addition, the free length of the piles was negligible, since the ramp surface closely follows the natural slope of the bottom for most of its length.

The contract price for the project was within the budget, about 8 percent below the engineering estimate of $169,000. The second low bid was approximately 7.5 percent above the estimate.

The contractor informed the author that in preparing his estimate he had figured that an average of three precast units could be set during a working day. His actual experience record shows that as many as six and eight units were placed in a day.

CREDITS

The work was done for the Department of the Navy, 11th Naval District. Captain K. A. Godwin, CEC, USN, was officer in charge of construction; Commander K. P. Coykendall, CEC, USN, resident officer in charge of construction; and Harvey Cole, project design engineer for the Navy. The contractor was Ben C. Gerwick, Inc. Plans and specifications were prepared by Wilson and Wilson, Engineers, of Los Angeles, Calif.

Title No. 51-28

A report of research sponsored by the Reinforced Concrete Research Council

Shear Strength of Reinforced Concrete Beams*

Part 3—Tests of Restrained Beams With Web Reinforcement

By R. C. ELSTNER,† K. G. MOODY,‡ I. M. VIEST,§ and E. HOGNESTAD†

SYNOPSIS

Results are presented from tests on 35 restrained beams with web reinforcement. The tests were made in three series: the first comprising 22 rectangular beams and two T-beams was made as the basic series of tests designed to investigate the effects of varying amount and inclination of web reinforcement, the second comprising eight rectangular beams was made to investigate the effect of increasing beam depth, and the third comprising three rectangular beams was made to investigate the effect of increasing the ratio of shear span to effective depth of beam.

Beams were tested with one concentrated load at each overhang and one or two concentrated loads in the span. In all beams several diagonal tension cracks formed in the regions of maximum shear. One beam failed in flexure and the remaining beams failed in shear. The magnitude of the cracking load was found to depend primarily on the dimensions of the cross section and strength of concrete. All beams were able to support substantially greater loads than the cracking loads. The final shear failure occurred by destruction of the compression zone of concrete at the support or load bearing block. The magnitude of the failure load was clearly a function of the amount and type of web reinforcement.

INTRODUCTION

Experimental studies were made on simple and restrained beams with and without web reinforcement to determine the shear strength of reinforced concrete beams. The results of the tests of simple beams and of restrained beams without web reinforcement were reported in Parts 1 and 2 of this series.[1,2] The results of the tests of 35 restrained beams with web reinforcement are reported in this paper. An analysis of the results will be presented in Part 4.

SPECIMENS, EQUIPMENT, AND TEST PROCEDURES

Test program and specimens

The tests of 35 restrained beams were made in three series as indicated in Table 1: Series I comprising 22 rectangular beams and two T-beams was made as the basic series of tests

*Received by the Institute Feb. 3, 1954. Title No. 51-28 (third of a four part series) is a part of copyrighted JOURNAL OF THE AMERICAN CONCRETE INSTITUTE, V. 26, No. 6, Feb. 1955, *Proceedings* V. 51. Separate prints are available at 50 cents each. **Discussion** considered on the basis of entire series (copies in **triplicate**) should reach the Institute not later than July 1, 1955. Address 18263 W. McNichols Road, Detroit 19, Mich.

†Members American Concrete Institute, Associate Development Engineer and Manager, Structural Development Section, respectively, Portland Cement Assn., Chicago, Ill. (formerly Research Associate and Research Associate Professor, respectively, of Theoretical and Applied Mechanics, University of Illinois).

‡Member American Concrete Institute, Research Engineer, Bridge Division of the Country Roads Board, Victoria, Australia (formerly Dominion Service Fellow of the Commonwealth Fund, Department of Theoretical and Applied Mechanics, University of Illinois).

§Member American Concrete Institute, Research Assistant Professor of Theoretical and Applied Mechanics, University of Illinois, Urbana, Ill.

TABLE 1—DETAILS OF SPECIMENS*

Beam No.	Longitudinal reinforcement†			Web reinforcement			
	Number and sizes of bars	p, percent	Type‡	Size	Horizontal spacing, in.	r, percent	Type‡
Series I							
I–10a, b	4 #9 H§	4.76	F	#3 V**	6	0.52	A
11a, b	4 #9 H	4.76	F	#4 V	6	0.95	B
12a, b	4 #9 H	4.76	F	#5 V	6	1.47	C
I–s	4 #9 S§	4.76	Q	#5 V	5	1.72	M
t	4 #9 S	4.76	Q	#5 V	4	2.14	M
I–13a, b	4 #9 H	4.76	F	#3 D**	6	0.74	A
14a, b	4 #9 H	4.76	F	#4 D	6	1.35	B
15a, b††	4 #9 H	4.76	F	#5 D	6	2.09	C
I–16a, b‡‡	4 #9 H	4.76§§	F	#5 V	6	1.47§§	C
I–u	4 #7 S	2.86	O	#3 V	6	0.52	U
v	4 #7 S	2.86	O	#3 V	4.5	0.70	U
w	4 #7 S	2.86	O	#4 V	6	0.95	L
x	4 #7 S	2.86	O	#5 V	6	1.47	M
I–y***	4 #9 S	4.76	Q	#3 V	6	0.52	U
z	4 #9 S	4.76	Q	#3 V	4.5	0.70	U
α	4 #9 S	4.76	Q	#4 V	6	0.95	L
β	4 #9 S	4.76	Q	#5 V	6	1.47	M
Series II							
II–21a, b	4 #9 H	2.72	F	#3 V	6	0.52	A
22a, b	4 #9 H	2.72	F	#4 V	6	0.95	B
23a, b	4 #9 H	2.72	F	#5 V	6	1.47	C
II–e	4 #9 S	2.72	Q	#5 V	5	1.72	I
f	4 #9 S	2.72	Q	#5 V	4	2.14	I
Series IV							
IV–m	4 #9 S	4.76	T	#3 V	6	0.52	U
n	4 #9 S	4.76	T	#4 V	6	0.95	L
o	4 #9 S	4.76	T	#5 V	6	1.47	M

*All beams were 15 ft 4 in. long reinforced with intermediate grade deformed bars. Equal amounts of longitudinal steel were placed in the bottom and in the top; web was reinforced with vertical or diagonal stirrups inclined at 45 deg. All beams were made of 3000 psi concrete except when noted otherwise. For other details see Fig. 1. Beams designated only with letters (*e.g.*, I–s) were single specimens; beams designated with arabic numerals and letters (*e.g.*, I–10a, b) were companion specimens. In the second type of designation letters a and b distinguish between companion specimens.

†Refers to bottom reinforcement; an equal amount of reinforcement was provided on the top of all beams.

‡See Table 2.

§H—Hooked bars; S—straight bars.

**V—vertical stirrups; D—45 deg inclined stirrups.

††Bottom reinforcement of I–15a consisted of two #9 bars only.

‡‡T-section.

§§Based on width of stem.

***Specimens I–y, z, α, and β were made with 5000 psi concrete mix.

designed to investigate the effects of varying the amount and inclination of web reinforcement; Series II comprising eight rectangular beams was made to investigate the effect of increasing the beam depth; and Series IV comprising three rectangular beams was made to investigate the effect of increasing the ratio of the shear span* to the effective depth of the beam. All three series of beams were designed in conjunction with the restrained beams without web reinforcement reported in Part 2 of this series.[2]

Details of individual specimens may be found in Table 1 and Fig. 1. All beams were 15 ft 4 in. long and of rectangular cross section 7 in. wide, with the exception of two beams of Series I which were T-beams with the stem 7 in. wide, and the flange 23 in. wide and 4 in. deep. Beams of Series I and IV were 15 in. deep and beams of Series II were 24 in. deep; the corresponding effective depths were 12.0 and 21.0 in. for the bottom reinforcement, and

*For the purposes of this paper the shear span is defined as the distance between a reaction and the nearest interior load point.

11.75 and 20.75 in. for the top reinforcement. All beams were reinforced with four longitudinal bars on the bottom and four identical longitudinal bars on the top, both arranged in two layers. The top two bars of the bottom longitudinal reinforcement were cut off at the support bearing blocks; all other bars were continuous throughout the beams. In some beams the longitudinal steel was provided with hooks, in others all reinforcement was straight. All beams were made of a concrete mix designed for 3000 psi, except for beams I-y, I-z, I-α, and I-β which were made of a concrete mix designed for 5000 psi. Specimens of Series I were divided into four groups. Within each group of Series I and within each of the two remaining series, the percentage of web reinforcement was the only major variable. One group of Series I was made with diagonal stirrups inclined at 45 deg; all other specimens were made with vertical stirrups.

The location and relative magnitude of loads applied to the beams (Fig. 1) were such that the maximum negative and maximum positive moments were of equal magnitude, and the maximum shear occurred in the shear span. Since all applied loads were concentrated, the maximum shear was approximately constant throughout the length of the shear span. At the supports and at the interior load points both the maximum moment and the maximum shear were present.

Materials

The concrete for all specimens was made with Type I portland cement, Wabash River torpedo sand, and Wabash River gravel. Specific gravities of the sand and gravel were 2.65 and 2.70, respectively. The fineness modulus of the sand was 3.07 and the maximum size of the gravel was 1 in. Both aggregates passed the usual ASTM tests. For concrete of the

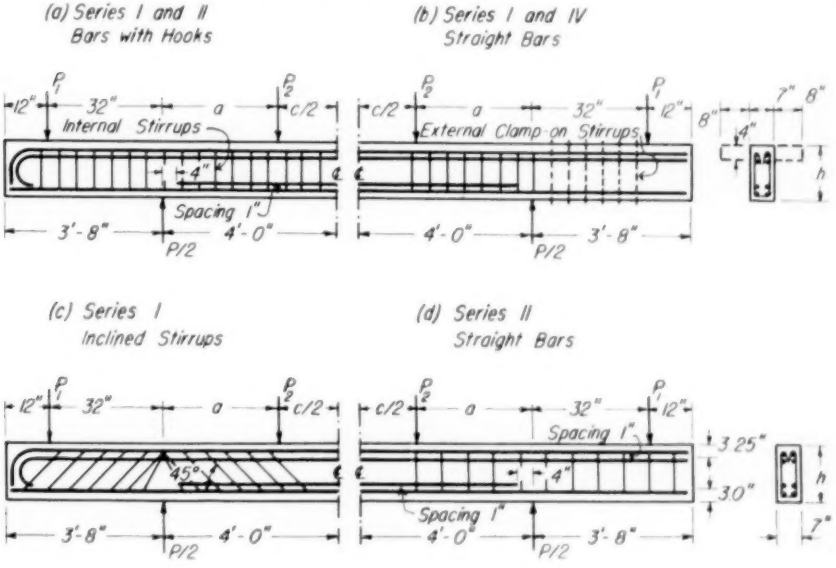

Series	c, in.	a, in.	P_1/P	P_2/P	h, in.
I	32	32	1/6	1/3	15
II	32	32	1/6	1/3	24
IV	0	48	3/14	2/7	15

Fig. 1—Details of beams

3000 psi design strength, the mix ratio of cement to sand to gravel was 1:3.67:5.21 and the cement-water ratio was 1.21; the concrete with the design strength of 5000 psi had a mix ratio of 1:2.63:3.89 and the cement-water ratio of 1.66, all ratios by weight. The average slump was approximately 3 in. The concrete strengths for the individual beams are presented with the beam test results in Table 3.

Deformed bars of intermediate grade steel meeting ASTM designation A305-50T were used for all reinforcement. Typical bars of various sizes were shown in Part 2.[2] The results of the control tests of tensile coupons are given in Table 2, in which only averages for bars of similar properties are given. Bars of the same average properties are designated in Table 2 with capital letters; the same letters in Table 1 indicate the type of bars used in any particular beam.

Fabrication of specimens

The fabrication of all beams and control cylinders was identical with that described for simple beams with web reinforcement of Series III in Part 1.[1]

Test equipment and procedures

The beams were tested in a 3,000,000-lb Southwark Emery hydraulic testing machine. In Series I and II the load was applied at four points: at the end of each overhang and at the third points in the span between the supports. In Series IV the load was applied at three points: at the end of each overhang and at midspan. Details of the testing apparatus were the same as for the restrained beams without web reinforcement.[3]

In all tests the load was applied in increments of about 10,000 lb until failure. After each increment, the machine was operated intermittently to maintain the load while cracking and creep of the specimen proceeded. After the load was stabilized, the crack pattern was noted and the following measurements were taken: strains on the tension steel near midspan and over the supports, strains on several stirrups in both shear spans, strains on the top surface of concrete near midspan, and deflections at midspan and at the load points. All tests were carried to failure. The time required for one test varied from 1 to 4 hr.

The instrumentation was the same as for restrained beams without web reinforcement.[3] Strains on the web reinforcement were measured in the same way as strains on the tension steel.

TEST RESULTS

The results of the tests are summarized in Table 3, which includes the average concrete strength f_c', the loads at the formation of the initial diagonal tension crack P_c, the failure loads P_u, and the critical steel stress at failure f_s. In addition, the table includes the nominal shearing stress v_c and ratios

TABLE 2—PHYSICAL PROPERTIES OF REINFORCEMENT

Type	Size	Number of tests	Average yield point, psi	Average ultimate strength, psi	Average elongation in 8 in., percent
A	#3	52	47,300	72,500	21.0
B	#4	51	44,000	74,000	19.8
C	#5	65	41,200	70,300	23.7
F	#9	8	45,700	74,200	26.0
I	#5	11	43,500	75,700	21.9
L	#4	14	45,800	77,000	22.7
M	#5	18	47,600	79,000	21.4
O	#7	20	42,350	73,560	24.6
Q	#9	12	43,250	71,000	26.3
T	#9	14	45,500	76,600	22.5
U	#3	16	53,840	82,100	18.8

TABLE 3—TEST RESULTS

Beam No.	Concrete strength f_c', psi*	Initial diagonal tension cracking			Failure			P_u/P_c	v_{allow}/f_c'
		P_c, kips	v_c, psi	v_c/f_c'	P_u, kips	Critical steel stress f_s,† ksi	v_u/f_c'		
Series I									
I–3a‡	2290	41	190	0.083	89	8.8	0.180	2.17	0.030
b‡	2970	49	227	0.076	101	10.1	0.158	2.06	0.030
10a	3070	40	185	0.060	163	16.6	0.246	4.08	0.064
b	2810	40	185	0.066	138	13.9	0.228	3.43	0.067
11a	3560	50	232	0.065	190	15.6	0.249	3.80	0.080
b	3180	40	185	0.058	174	18.4	0.253	4.35	0.080
12a	4000	40	185	0.046	190	19.6	0.220	4.75	0.080
b	3220	40	185	0.057	159	15.9	0.229	3.98	0.080
I–s	3470	50	232	0.067	220	19.8	0.294	4.40	0.080
t	3700	40	185	0.050	240	22.6	0.300	6.00	0.080
I–13a	3460	50	232	0.067	185	—	0.248	3.70	0.073
b	2860	40	185	0.065	170	—	0.276	4.25	0.082
14a	3510	50	232	0.066	250	—	0.330	5.00	0.107
b	3600	60	278	0.049	240	—	0.309	4.00	0.105
15a§	3330	70	324	0.098	245	—	0.341	3.50	0.129
b	3710	60	278	0.075	304	—	0.379	5.06	0.129
I–16a**	3610	60	278	0.077	271	26.5	0.348	4.52	0.080
b**	3240	60	278	0.086	282	27.9	0.403	4.70	0.080
I–1a‡	2510	40	185	0.074	77	10.9	0.142	1.93	0.030
b‡	2800	50	232	0.083	87	13.6	0.144	1.76	0.030
I–u	3740	60	278	0.074	160	22.0	0.198	2.67	0.058
v	3580	50	232	0.065	170	32.8	0.220	3.40	0.069
w	4210	60	278	0.066	180	25.2	0.197	2.99	0.075
x	3830	50	232	0.061	217	30.6	0.262	4.35	0.080
I–9a‡	5270	68	315	0.060	130	10.4	0.114	1.91	0.030
b‡	4650	62	287	0.062	130	11.1	0.129	2.10	0.030
I–y	4790	60	278	0.058	220	20.9	0.213	3.67	0.052
z	4850	60	278	0.057	222	20.5	0.212	3.70	0.059
α	5070	70	324	0.064	260	24.3	0.238	3.71	0.068
β	5130	60	278	0.054	279	28.3	0.252	4.65	0.080
Series II									
II–18a‡	2170	75	197	0.091	220	14.0	0.269	2.94	0.030
b‡	2700	96	252	0.093	180	10.9	0.175	1.88	0.030
21a	3580	75	197	0.055	310	16.4	0.228	4.06	0.059
b	3640	85	223	0.061	283	15.1	0.204	3.33	0.059
22a	3000	75	197	0.066	300	14.0	0.262	4.00	0.080
b	2710	60	158	0.058	290	19.2	0.281	4.83	0.080
23a	3230	75	197	0.061	300	16.3	0.244	4.00	0.080
b	3160	90	235	0.074	350	21.6	0.291	3.89	0.080
II–e	3420	100	263	0.077	390	21.9	0.300	3.90	0.080
f	3330	80	210	0.063	340	17.3	0.268	4.25	0.080
Series IV									
IV–l‡	3920	68	268	0.068	81	9.0	0.082	1.20	0.030
m	2860	40	158	0.055	146	21.1	0.202	3.64	0.067
n	3710	60	238	0.064	198	27.3	0.212	3.30	0.080
o	3420	60	238	0.070	218	32.1	0.253	3.63	0.080

*Determined from tests of 6 x 12-in. control cylinders.
†Estimated from strains measured at midspan.
‡Beams without web reinforcement; for dimensions see reference 2.
§Flexural failure.
**T-beams.

of the nominal shearing stresses v_c, v_u, and v_{allow} to the concrete strength f_c'.

The concrete strengths given in Table 3 are the average values determined from the tests of all control cylinders made with any particular beam. The initial cracking loads P_c were determined from the load-stirrup strain curves. The failure loads were measured by the testing machine. The critical stresses were obtained from steel strains measured at midspan and over the supports.* They represent average quantities which, if multiplied by the total area of the tension reinforcement, give the tension forces in the steel at the sections at which failure occurred. Since the determination of f_s involved strains measured at sections other than the critical, f_s is an approximate value which can be used only as a guide. The values of the nominal shearing stresses v_c and v_u were computed from the equation $v = 8V/7bd$, in which V is the maximum shear corresponding to the appropriate value of load P (V is equal to P_2 in Fig. 1), and b and d are width and effective depth, respectively, of the beam. Allowable shearing stress v_{allow} was computed in accordance with ACI 318-51.[3]

In addition to beams listed in Table 1, Table 3 includes beams I–3a, b, I–1a, b, I–9a, b, II–18a, b, and IV–1 without web reinforcement. Except for the web reinforcement, they were identical with other beams listed in the same groups. Descriptions of the beams without web reinforcement were reported previously.[2]

The shear spans of a few representative specimens after failure, and a few load-deflection curves and load-stirrup strain curves are shown in Fig. 2 through 9.

Behavior prior to formation of diagonal cracks

At low loads the behavior of restrained beams with web reinforcement was the same as that of restrained beams without web reinforcement.[2] The stirrups had no influence on the behavior since they carried either practically no stresses (vertical stirrups, Fig. 6) or only very small stresses (inclined stirrups, Fig. 8).

Initial diagonal tension cracking

At some load the strains in the stirrups began to increase rapidly, and at a load 15 to 40 percent higher one or more inclined cracks were observed. These cracks were similar to those defined in Parts 1 and 2[1,2] as diagonal tension cracks but were shorter and more difficult to detect visually. It is believed that these cracks began to form at that load at which the strains in the stirrups began to increase rapidly; however, the stirrups prevented the cracks from opening to a width susceptible to visual observations until the loads increased as indicated above. Thus for beams with web reinforcement the loads corresponding to the first sharp breaks in the load-stirrup strain curves are called the initial diagonal tension cracking loads.

The initial cracking loads are listed in Table 3, in which the specimens are divided into the same groups as in Table 1. The major variable in these

*Critical strains were determined in the same way as for restrained beams without web reinforcement.[2]

tests, the percentage of the web reinforcement, was the only variable within each group. It can be seen that cracking loads are approximately constant within each group, including the beams without web reinforcement. Thus it may be concluded that the web reinforcement has no significant effect on the magnitude of the cracking load.

In addition to the percentage of web reinforcement, the tests included inclination of the web reinforcement, percentage of the longitudinal reinforcement, length of the shear span, strength of the concrete and depth of the beam as minor variables. Of these, the first three had no significant effect on the cracking load but increases in strength of concrete, and depth of beams resulted in higher cracking loads. However, on the basis of these tests alone no definite conclusions can be reached since the test data for the minor variables are limited both in number and scope.

The ratio of nominal shearing stress v_c to strength of concrete f_c' may be compared with the corresponding allowable value v_{allow}/f_c' listed in Table 3. For most beams with web reinforcement v_c/f_c' is smaller than v_{allow}/f_c'; in other words, diagonal cracks began to form at loads lower than those corresponding to the allowable nominal shearing stress. Ordinarily, the occurrence of diagonal tension cracks at working loads is not objectionable in beams with web reinforcement, since in such beams diagonal cracks are narrow and well distributed. However, diagonal cracking could become objectionable if the arrangement of longitudinal reinforcement permitted failure at or slightly above the cracking load. Such failures, termed failures by separation, were observed in beams without web reinforcement;[2] no parallel tests were made on beams with web reinforcement, however.

Behavior after formation of diagonal cracks

All restrained beams with web reinforcement were able to sustain large increases of load beyond that causing the formation of initial diagonal tension cracks. After the cracking load had been exceeded, numerous very fine, closely spaced parallel cracks formed progressively in both shear spans. At loads approaching the ultimate two major cracks opened wide, spanning between the support and load bearing blocks but leaving zones of intact concrete around the blocks. The formation of the two major cracks indi-

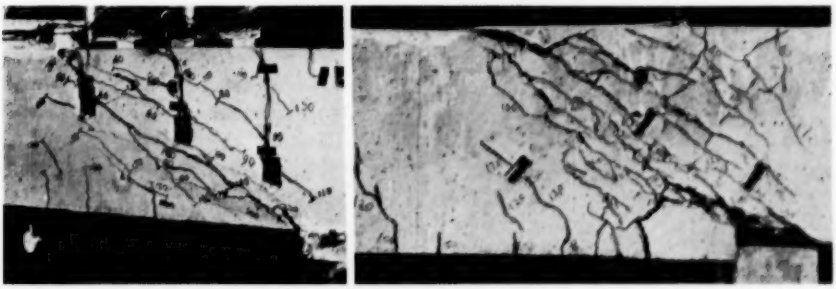

Fig. 2—Typical beams of Series I after failure. (left) Beam I-1—vertical stirrups. (right) Beam I-13a—inclined stirrups

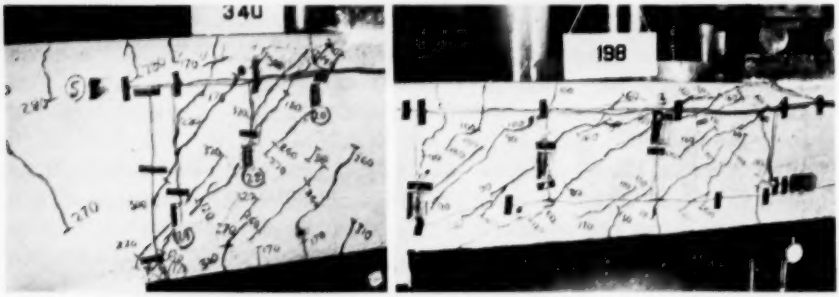

Fig. 3—Typical beams of Series II and IV after failure. (left) Beam II-f. (right) Beam IV-n

cates that full redistribution of internal stresses had taken place before failure.* The failure occurred at the maximum load by destruction of the compression zone of concrete at either the support or load bearing block. The final crack pattern is illustrated in Fig. 2 and 3, depicting the shear spans of several representative specimens after failure.

Two other phenomena were observed at loads approaching failure: extensive spalling of concrete covering the stirrups, and longitudinal splitting of the beam along two vertical planes over the bars (Fig. 4). The test results indicated, however, that neither the mode of failure nor the magnitude of the ultimate load were influenced significantly by these phenomena.

Strains measured in the tension reinforcement near midspan and over the supports were always smaller than the yield point strain, and strains measured on the top beam surface at midspan were considerably smaller than those usually associated with failure by crushing of the concrete. Thus the beams failed before their flexural capacities were reached. The only exceptions were beams I-x and I-15a. In beam I-x a small amount of yielding was observed immediately prior to failure; it is believed, however, that the yielding was not extensive enough to have any significant effect on the test results. Beam I-15a had only two bars as the bottom reinforcement and failed in flexure by yielding at midspan.

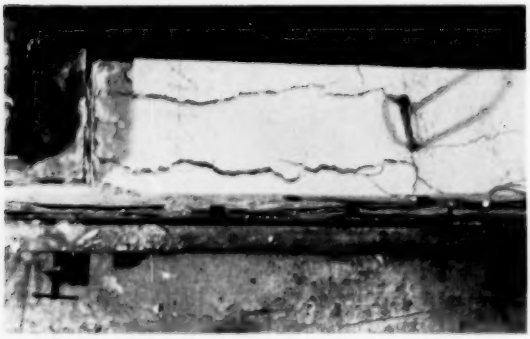

Fig. 4—Top view of beam I-14b showing splitting above longitudinal bars

*For a discussion of this phenomenon the reader is referred to Part 2 of this series.[3]

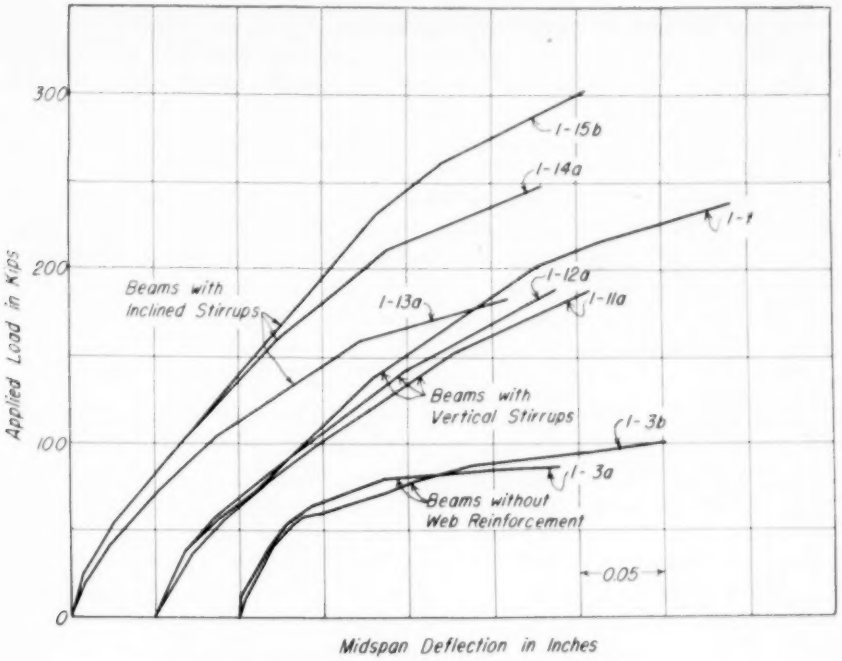

Fig. 5—Load-deflection curves for beams of Series I

Typical load-midspan deflection curves are shown in Fig. 5 for comparable beams with inclined stirrups, with vertical stirrups, and without stirrups.* The curves, terminated at the failure load, show that the failure loads were greatest for beams with inclined stirrups and smallest for beams without stirrups. The greater failure loads in beams with stirrups were reached at deflections exceeding by less than 50 percent the corresponding deflections of beams without stirrups. However, the beams with stirrups exhibited considerable ductility after the maximum load was passed.

Failure loads

When the maximum load was reached, the compression zone of concrete was destroyed adjacent to either the support or load bearing block, and the load decreased. Although this decrease of load was usually small, it was permanent; thus the maximum load is called the failure load.

Failure loads for all beams are listed in Table 3. They increase with increasing percentage of web reinforcement, concrete strength, and beam depth; they are higher for beams with inclined stirrups than for beams with vertical stirrups; but they do not seem to be affected by the percentage of the longitudinal reinforcement or by the length of the shear span. The effect of the percentage of web reinforcement is noticeable in all groups of specimens.

*For the description of beams without stirrups see Part 2 of this series.[7]

Table 3 includes ratios of ultimate load to cracking load, P_u/P_c, which vary from 2.67 to 6.00. Similar ratios for beams without web reinforcement varied from 1.0 to 3.14.[2] Since the cracking load P_c is not affected significantly by the presence of web reinforcement, the increase in P_u/P_c shows clearly that the web reinforcement increases substantially the shear strength of reinforced concrete beams.

The values v_u/f_c', also listed in Table 3, are substantially higher than the allowable values v_{allow}/f_c'. Although for all beams with web reinforcement v_u/v_{allow} exceeds 2.5, it is smaller than the corresponding ratio for beams without web reinforcement; the only exception are the beams of Series IV for which the v_u/v_{allow} values are approximately the same regardless of the presence or absence of the stirrups.

Action of stirrups

Information regarding the action of web reinforcement was obtained from measurements made by electric resistance strain gages attached to each stirrup in the regions of maximum shear near the points of intersection with major diagonal tension cracks. Since only one gage was attached to each stirrup, no data were obtained on the distribution of strain along individual stirrups; however, it is believed that the recorded stirrup strains were very close to the maximum values.

Typical load-maximum stirrup strain curves and stirrup strain distribution curves for beams with vertical stirrups are shown in Fig. 6 and 7, respectively. As has been pointed out, the stirrups remained practically unstressed until diagonal tension cracking occurred; afterward the stirrup strains increased rapidly. The strains were always largest in the stirrups located near the middle of the shear span and decreased toward the support and load points. In the majority of beams, one or more stirrups yielded before the maximum load was reached, but in only a few beams was yielding observed in all stirrups crossing the diagonal crack. In beams I-12a, I-12b, I-s, I-t, and IV-o, with

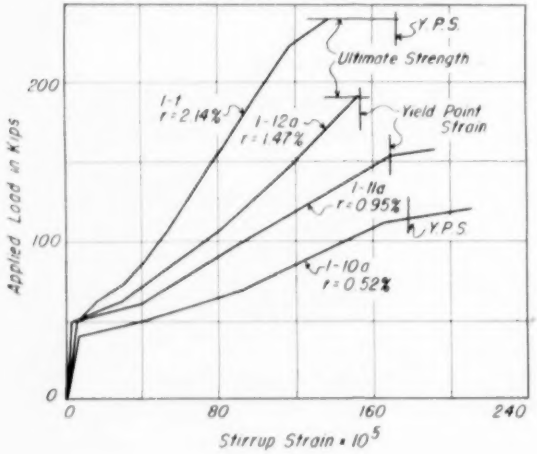

Fig. 6—Maximum stirrup strains for beams with vertical stirrups

large percentages of web reinforcement, no yielding of stirrups could be detected.

Typical load-maximum stirrup strain curves for beams with stirrups inclined at 45 deg are shown in Fig. 8. Inclined stirrups were stressed from the inception of loading since their inclination was identical with that of the principal stress at the mid-depth of the beam. Stresses ranging approximately from 1000 to 6000 psi were observed immediately before diagonal

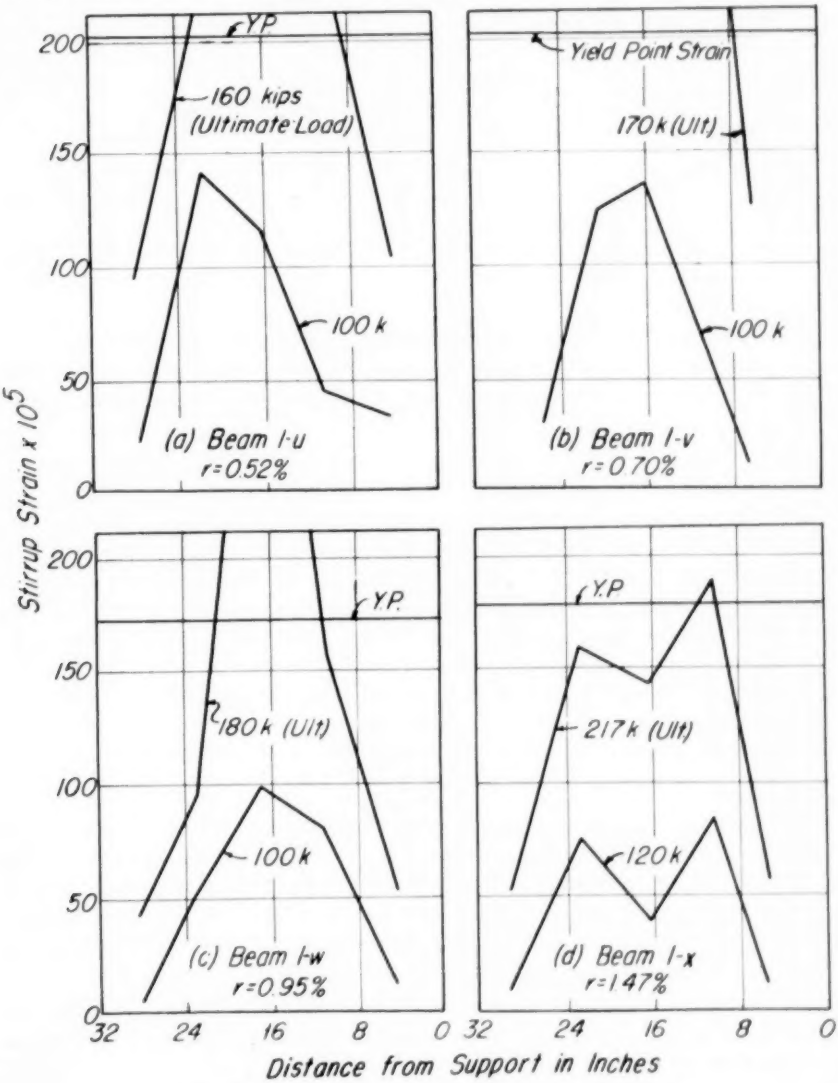

Fig. 7—Distribution of stirrup strains along shear span

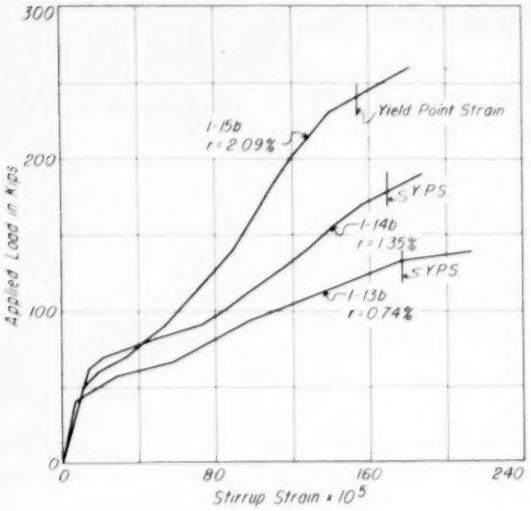

Fig. 8—Maximum stirrup strains for beams with inclined stirrups

cracking. At higher loads, strains increased rapidly and exceeded the yield point value before maximum load was reached.* The increase in load beyond that at which all inclined stirrups were yielding ranged approximately from 6 to 17 percent.

It was observed in these tests that the stirrups delayed the full development of diagonal tension cracks. In beams without stirrups only one or two diagonal tension cracks formed; these cracks then penetrated into the compression zones of concrete and thus precipitated the failure which occurred by destruction of one of these zones. In beams with stirrups, however, numerous short diagonal cracks formed since the stirrups distributed the cracks; more load was required for the cracks to develop and to penetrate into the compression zones, and thus to cause crushing of the concrete. Inclined stirrups were more effective in distributing diagonal cracks than were vertical stirrups; accordingly, more load was required for failure of beams with diagonal stirrups than for failure of beams with vertical stirrups.

Tests of T-beams

The tests of restrained beams with web reinforcement included two T-beams with vertical stirrups (I-16a and I-16b) which differed from the remaining beams of Series I only in that a flange was added as shown in Fig. 1. The amount and arrangement of longitudinal and web reinforcement was identical with that in rectangular beams I-12a and I-12b. The concrete strengths for the two pairs of beams were also similar.

Load-midspan deflection curves for the four beams are shown in Fig. 9a. It can be seen that the added flange stiffened the T-beams considerably from the inception of loading up to a load of about 80 percent of the ultimate.

*The only exception was beam I-15a which failed in flexure.

At this load, the curves became parallel, thus indicating that at high loads the stiffness of the T-beams was approximately equal to that of the rectangular beams.

The cracking loads for T-beams I-16a and I-16b were 60 kips, whereas cracking loads for the comparable rectangular beams I-12a and I-12b were 40 kips. This is in agreement with the stiffening effect of the flange indicated by the load-deflection curves. As in the rectangular beams, strains in the vertical stirrups of the T-beams were very small until cracking occurred, as illustrated in Fig. 9b.

The initial diagonal tension cracks formed in the stem of the T; as the load increased further, diagonal tension cracking developed in a manner

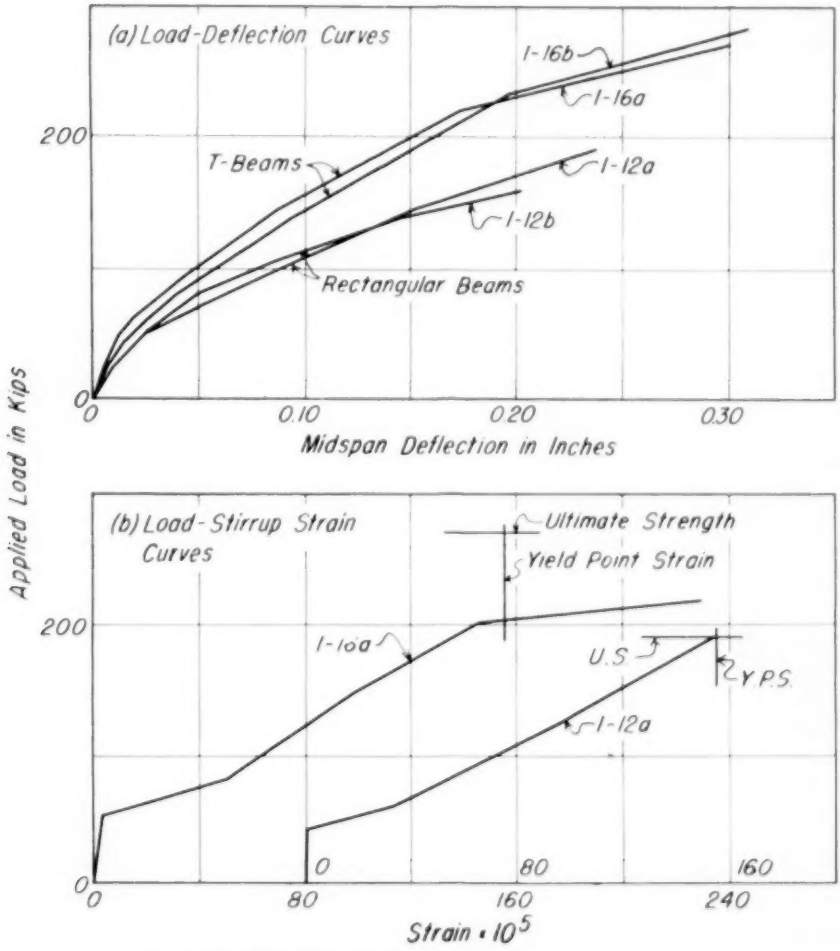

Fig. 9—Load-deflection and load-stirrup strain curves for T-beams

similar to that observed in rectangular beams with vertical stirrups. At low loads the cracks were restricted to the stem of the T-section. At approximately one-half of the ultimate load the diagonal tension cracks reached the lower face of the beams adjacent to the support bearing blocks, and a major diagonal tension crack could be distinguished. At a higher load a second major diagonal tension crack appeared in the stem of the beam above the first major crack, and minor cracking was noticed at the junction of the flange and the stem. At failure, crushing occurred in the vicinity of the support bearing block, and the upper diagonal crack extended through the flange and reached the upper surface of the beam near the interior load bearing block. The concrete covering the stirrups was cracked extensively at this stage and spalling was observed. It is believed that the beams failed when the concrete near the support bearing block was crushed but it is not clear whether this occurred before or after the upper diagonal tension crack spread through the flange. Ultimate loads attained by the T-beams I-16a (271 kips) and I-16b (292 kips) were considerably higher than those for the comparable rectangular beams I-12a (190 kips) and I-12b (159 kips).

At equal loads, the strains measured in the stirrups of the T-beams were approximately equal to those measured in the stirrups of the comparable rectangular beams as can be seen from Fig. 9b. However, the higher ultimate loads obtained in the T-beams led to yielding of several stirrups, whereas in beams I-12a and I-12b the stirrups remained elastic throughout the tests. It is believed that yielding of the stirrups may have resulted in a decrease of the degree of interaction between the flange and stem of the T-section.

CONCLUDING REMARKS

Thirty-three rectangular restrained beams with web reinforcement were tested with one concentrated load at each overhang and one or two concentrated loads in the span. In all beams several diagonal tension cracks formed in the regions of maximum shear. One beam failed in flexure and the remaining beams failed in shear. Prior to the formation of the diagonal tension cracks the behavior of all beams was the same as that of beams failing in flexure, and the stirrups were practically unstressed. Beyond the load causing the formation of the initial diagonal tension cracks the stresses in the stirrups increased rapidly.

The magnitude of the cracking load depended primarily on the dimensions of the cross section and on the strength of concrete. It was practically independent of the web reinforcement.

In all beams a considerable increase of load was possible beyond the cracking load. The final failure occurred at the section of maximum moment in the region of maximum shear; the compression zone of concrete was destroyed at this critical section. The magnitude of the ultimate load depended clearly on the amount and type of web reinforcement. It increased with increasing amount of web reinforcement and was higher for beams with diagonal stirrups than for comparable beams with vertical stirrups.

Two T-beams with vertical stirrups were also tested. These tests indicated that T-beams possess higher shear strength than rectangular beams of the same depth, concrete strength, and area of reinforcement, and of a width equal to the width of the stem of the T-beams.

Analytical expressions for predicting the shear strength of rectangular restrained beams with web reinforcement developed on the basis of these tests will be reported in Part 4. No attempt was made to develop analytical expressions for the shear strengths of T-beams, since the tests included only two such beams.

ACKNOWLEDGMENTS

The tests reported in this paper were carried out at the University of Illinois as a cooperative investigation conducted by the University of Illinois Engineering Experiment Station under the sponsorship of the Reinforced Concrete Research Council of the Engineering Foundation and the Bureau of Public Roads of the U. S. Department of Commerce. This paper is based on the doctoral dissertation of K. G. Moody.[4]

REFERENCES

1. Moody, K. G., Viest, I. M., Elstner, R. C., and Hognestad, E., "Shear Strength of Reinforced Concrete Beams. Part 1—Tests of Simple Beams," ACI JOURNAL, Dec. 1954, *Proc.* V. 51, pp. 317-332.

2. Moody, K. G., Viest, I. M., Elstner, R. C., and Hognestad, E., "Shear Strength of Reinforced Concrete Beams. Part 2—Tests of Restrained Beams Without Web Reinforcement," ACI JOURNAL, Jan. 1955, *Proc.* V. 51, pp. 417-436.

3. "Building Code Requirements for Reinforced Concrete (ACI 318-51)," ACI JOURNAL, Apr. 1951, *Proc.* V. 47, pp. 589-652.

4. Moody, K. G., "An Investigation of Reinforced Concrete Beams Failing in Shear," PhD Thesis, Department of Theoretical and Applied Mechanics, University of Illinois, June, 1953.

Magnetite Iron Ore Concrete for Nuclear Shielding*

By J. O. HENRIE†

SYNOPSIS

Discusses crushing and handling of the magnetite iron ore, which was used as the aggregate for a dense shielding concrete, and the physical properties and costs of magnetite ore concrete are compared to those of other concretes. The mix used had a compressive strength of 4000 psi in 10 days. The methods used in fabricating shielding block are described. Recommendations for producing a low cost, relatively high density shielding concrete are made. The shielding block used (9 x 9 x 18 in. nominal) had a density of 3.7 g per sq cm or 230 lb per cu ft and cost $163.50 per cu yd. The dimensions of the block were quite uniform, having a standard deviation of approximately 0.015 in.

INTRODUCTION

The need arose for an inexpensive biololgical shield in 1951 for a low power research reactor being designed at the Atomic Energy Research Department of North American Aviation, Inc. A dense concrete was selected, and many sources of dense aggregate, such as scrap iron, lead ores, barite ore, and different iron ores, were investigated. The existing literature was reviewed, but none gave sufficient detailed information to aid significantly in the economical selection of the aggregate to be used.

The aggregate material selected on an economical basis was magnetite iron ore. The magnetite, as represented by two samples, had a density of 4.95 g per cu cm and was 68 percent iron. It was estimated that a satisfactory concrete having a density of 4.0 g per cu cm or 250 lb per cu ft could be made using the ore as aggregate. Approximately 300 lb of colemanite (30 percent B_2O_3) per cu yd of concrete ($\frac{1}{2}$ percent boron by weight) were to be added to increase the effectiveness of the concrete as a neutron shield. Tests were made on a limited amount of concrete of this quality and indicated that it had good structural and shielding qualities.

A need for dense concrete arose more recently in connection with the construction of hot cells for radiochemical work. Magnetite iron ore concrete was selected as the shielding aggregate because of the economy indicated by the previous cost estimates and experience.

It was estimated that in using such concrete instead of regular concrete as a gamma-ray shield, the wall thickness could be reduced approximately

*Received by the Institute June 2, 1954. Title No. 51-29 is a part of copyrighted JOURNAL OF THE AMERICAN CONCRETE INSTITUTE, V. 26, No. 6, Feb. 1955, *Proceedings* V. 51. Separate prints are available at 50 cents each. **Discussion** (copies in **triplicate**) should reach the Institute not later than June 1, 1955. Address 18263 W. McNichols Rd., Detroit 19, Mich.

†Nuclear Engineering and Manufacturing, North American Aviation, Inc., Downey, Calif.

40 percent and still provide the same shielding qualities. Although ordinary concrete in place was estimated to cost only half as much per cubic yard as the dense concrete ($85 per cu yd compared to $170 per cu yd), the latter proved more economical for the following reasons. (1) Dense shielding windows to give the same included viewing angle through the shield walls were less expensive. (2) The area in the building taken up by the hot cell was less. (3) Manipulators and other remote equipment extending through the more dense shielding walls were slightly less expensive and more effective.

This paper describes the development of a magnetite concrete which proved very satisfactory in the hot cell construction. Conclusions and recommendations directed toward inexpensive shields are also included.

MAGNETITE IRON ORE

The magnetite iron ore used in the test cylinders in Table 1 all came from the same source, but in two different shipments. The first had a density slightly above 4.6 g per cu cm and was used in the first 16 cylinders. These tests provided necessary experience and data for writing a crushing specification. The second shipment of ore was a 65-ton carload. It had an average density of 4.58 g per cu cm and contained 65 percent iron. (The veins containing the 4.95 g per cu cm ore were not being mined at that time.)

ORE CRUSHING

The carload of ore was shipped directly to a rock milling company which had been selected to crush the ore. The ore came in minus 9-in. sizes and was crushed into two well-graded sizes, coarse and fine. Since the shield was to be made of 9 x 9 x 18-in. nominal concrete block, the coarse aggregate was limited to ¾-in. maximum size. The aggregate size gradation specified to the crushing vendor, and that actually obtained, are shown in Fig. 1.

Inspection, by sieve analysis, of the ore as it was being crushed resulted in a product which, after the jaw crusher and two sets of rolls had been properly adjusted, continually met the crushing specification. The ore was placed in 100-lb paper bags for ease in storing and handling.

CONCRETE MIX

The specified concrete mix was determined from the test cylinders of different mixes. Density of each cylinder and workability of the mix were the important factors in determining the mix to be used. Table 1 shows the results of the test cylinders. They were all water-cured, and air-dried for a day or two prior to testing.

The cylinders containing 1½- or 2-in. maximum size aggregate were more dense than those limited to a ¾-in. aggregate. This concrete had to be very carefully placed in the small cylindrical forms to avoid pockets. It would be difficult to place in forms for small block, but would be ideal for heavy monolithic shielding walls. Cylinders 17 to 22 were made from the

ore crushed to the specifications of Fig. 1. Cylinders 21 and 22 were made by the concrete block vendor from the mix used to fabricate the shielding block. One quart of calcium chloride solution per pack of cement (1 lb $CaCl_2$ per 94 lb cement) was added to decrease the setting time and allow the molds to be filled twice each day. No air-entraining agent or other additive was included in the mix.

CONCRETE SHIELDING BLOCK

The vendor selected to fabricate the block proposed a method of fabrication in which one standard form would be used and a very stiff mix tamped

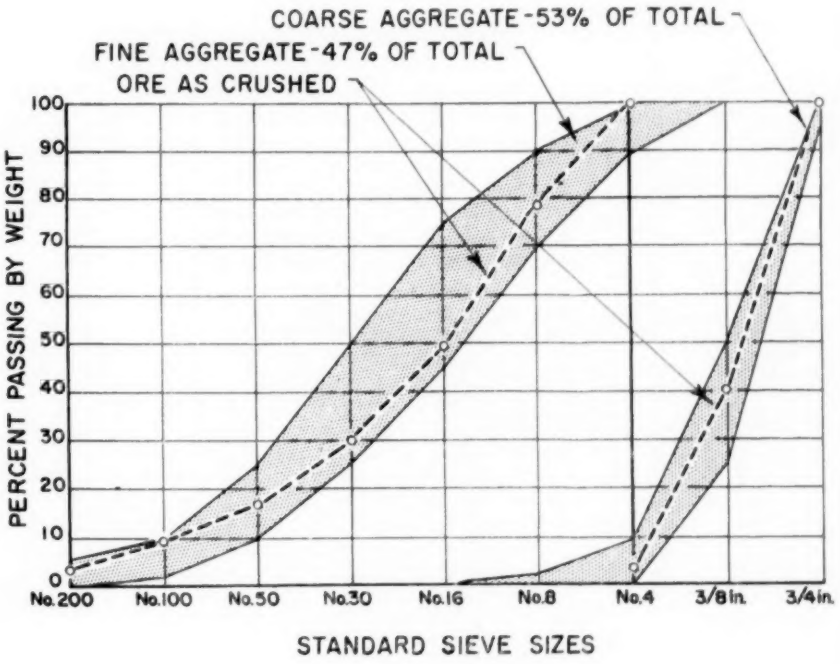

	Percent passing by weight									
Sieve size	1 in.	¾ in.	⅜ in.	No. 4	No. 8	No. 16	No. 30	No. 50	No. 100	No. 200
Specification										
Coarse	100	95-100	25-50	0-10	0-3					
Fine			100	90-100	70-90	45-75	25-50	10-25	2-10	0-5
As crushed										
Coarse		100	41	3						
Fine				100	78	49	30	17	9	3

Fig. 1—Magnetite aggregate size gradation

TABLE 1—MAGNETITE IRON ORE CONCRETE TEST CYLINDERS

Cylinder No.	Height, in.	Diameter, in.	Weight, lb	Density, lb per cu ft	Aggregate size		Per cubic yard (design)				Compressive stress, psi	Age, days	Observations—consistency and mix
									Aggregate				
					Coarse	Fine*	Water, gal	Cement, sacks	Coarse, lb	Fine, lb			
1	8.15	4.22	14.9	226	¾ in. on No. 4	V. coarse	39.5	6.5	2740	2420	930†	7	No rodding—honeycombing—harsh mix
2	8.25	4.22	15.4	230	¾ in. on No. 4	V. coarse	40.1	6.6	2780	2465	2440	28	Rodded—honeycombing—harsh mix
3	8.20	4.22	15.8	238	2 in. on No. 4	V. coarse	34.7	5.6	3510	2095	1010†	7	Rodded—honeycombing—harsh mix
5	8.00	4.22	14.6	225	¾ in. on No. 4	Fine	46.7	6.4	2650	2430	3160	28	No rodding—mix too fine
6	8.10	4.22	15.0	228	¾ in. on No. 4	Fine	47.3	6.5	2690	2465	1340†	7	Rodded—mix too fine
7	8.20	4.22	15.7	236	2 in. on No. 4	Fine	35.9	5.0	3695	1915	2150	13	Rodded—mix too fine
8	8.00	4.22	15.3	236	¾ in. on No. 4	Fine	42.5	5.9	3200	2265	1220†	7	Rodded—good mix
9	8.75	4.22	16.2	243	2 in. on No. 4	Fine	33.0	4.6	4110	1800	1290†	7	Rodded—not enough fine aggregate
11	8.15	4.22	15.1	228	¾ in. on No. 4	Fine	41.3	5.7	3095	2185	4100	28	Rodded—good mix
13	8.10	4.22	15.0	228	¾ in. on No. 4	Medium	39.8	6.5	2730	2480	1450†	7	Vibrated—mix flows well
14	8.10	4.22	15.9	242	1½ in. on No. 4	Medium	34.7	5.4	3715	2030	2800	28	Vibrated—mixed well
15	8.20	4.22	15.2	228	¾ in. on No. 4	Medium	46.7	6.2	2630	2545	1610†	7	Vibrated—mix stiff—8½ percent of the fine aggregate is −200 size.
16	6.30	4.22	11.6	227	¾ in. on No. 4	Medium	46.7	6.2	2630	2545	4940	28	
17	11.94	5.88	40.8	219	¾ in. on No. 4	Coarse	38.4	6.3	2745	2280	2410	7	Rodded—good workable mix
18	11.80	5.88	40.0	218	¾ in. on No. 4	Coarse	38.4	6.3	2570	2425	2220	7	Vibrated—good workable mix
19	11.88	5.88	40.3	216	¾ in. on No. 4	Coarse	38.4	6.3	2745	2280	3060	80	Rodded—good workable mix
20	11.88	5.88	41.3	224	¾ in. on No. 4	Coarse	38.4	6.3	2745	2280	3750	80	Vibrated—good workable mix
21	11.88	5.88	42.0	225	¾ in. on No. 4	Coarse	39.0	6.4	2730	2480	3950	10	Rodded—made by Art Concrete Products
22	11.88	5.88	42.0	225	¾ in. on No. 4	Coarse	39.0	6.4	2730	2480	4380	10	Rodded—made by Art Concrete Products

*Coarse sand—fineness modulus 2.9–3.2; Medium sand—fineness modulus 2.6–2.9; Fine sand—fineness modulus 2.2–2.6. Very coarse sand—the fine aggregate adhered to the walls of the mixer leaving a very coarse mix.

†Plaster of paris caps failed. All other 4-in. diameter cylinders were capped with sulfur and sand. The 6-in. cylinders were capped with a ½-in. Celotex pad on each end.

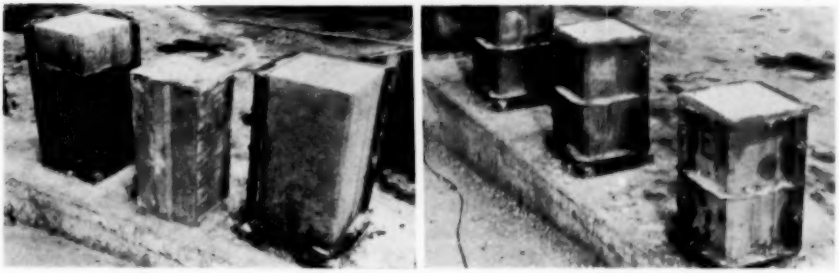

Fig. 2 (right)—Shielding block in cast iron forms. (left)—Block being stripped from forms

into it with an air hammer. The form could then be stripped immediately and the next block fabricated. Tests of this method were made using a cylindrical form. The iron ore aggregate as crushed was found to be too angular and coarse for this method of forming. Bridging between the particles occurred and resulted in a lower density than had been obtained using a more plastic mix.

The vendor then had ten cast iron split forms made. A fairly stiff concrete mix was placed in the forms and internally vibrated. The internal vibrator was slowly removed as the form was filled so that it left no large voids. This

Fig. 3—View of hot cell showing the stacking arrangement of block

method of placing resulted in a concrete density of 3.7 g per cu cm and up to 3.8 g per cu cm in some of the more dense block. The block weighed between 191 and 198 lb each and had an average weight of 194 lb. The same mix placed in the waxed cardboard test cylinders (No. 21 and 22) by rodding had a density of 3.6. Fig. 2 shows the concrete block and the cast iron forms.

The hot cell walls were made 27 in. thick. The 9 in. wide block were placed without mortar and stepped such that no crack between blocks extended more than one-third the thickness of the wall. A view of the completed hot cell is shown with the door open in Fig. 3. Note the stacking arrangement of the block on the left. Most of the block were made with a mortise and tenon to give an interlocking effect which would make the wall more rigid and also add slightly to its shielding effectiveness. Where special block were required to fit next to a beam or window, they were made by adapting the cast iron forms with appropriately sized wood blocks. Special short block were made by blocking with a steel plate and adjustable rods as shown in Fig. 2. Tubes and lines passing through the walls were cast into specially formed 27 in. wide block.

Fifty standard size block were selected at random and accurately measured. The widths ranged from $9\frac{1}{64}$ to $9\frac{3}{32}$ in.; 68 percent of them were between $9\frac{3}{64}$ and $9\frac{1}{16}$ in.; the average width was 9.056 in. The height of the block ranged from $9\frac{1}{64}$ to $9\frac{1}{16}$ in.; 78 percent of them were between $9\frac{1}{32}$ and $9\frac{3}{64}$ in.; the average height was 9.040 in. The lengths of the block were between $17\frac{15}{16}$ and 18 in.

COSTS AND COMPARISON WITH OTHER CONCRETES

The actual cost of the magnetite iron ore block was found to be less than had been estimated. The cost of the standard block is shown below:

Expense item	Cost, dollars per ton
Iron ore—F. O. B. Iron Springs, Utah	11.00
Shipping to Los Angeles	5.67
Crushing and bagging	13.00
Total ore unit cost	29.67

Cost per cu yd of concrete

Expense item	Cost, dollars per cu yd
Ore—2.60 tons × $29.67 per ton	77.20
Block fabrication including cement	86.30
Total for fabricated block	163.50

In comparing magnetite concrete costs with other concretes, the cost of forms and placing is not included. This is because such costs are highly variable and depend on the particular conditions of the job. Table 2 gives a comparison of some of the better dense concretes and regular concrete.

TABLE 2—COMPARATIVE CONCRETE COSTS—MATERIALS ONLY

	Ore*		Concrete		
	Density, g per cu cm	Cost, dollars per ton	Density, lb per cu ft	Cost,† dollars per cu yd	Cost, dollars per ton
1. Steel punchings‡	7.8	90			
Dispersed iron aggregate§	7.8	120	340	420	91
2. Ferrophosphorous§	6.5	80	290	290	74
3. Steel punchings‡	7.8	90			
Limonite	3.3	25	270	225	62
4. Magnetite	4.95	32	245	100	30
5. Magnetite	4.58	30	230	90	29
6. Barytes	4.10	30	215	85	29
7. Regular	2.70	1.50	145	10	5

*Carload lot—crushed and graded—¾-in. maximum size—in Los Angeles.
†Materials only—cement—$1.25 per bag—aggregates as listed.
‡Coarse aggregate.
§Fine aggregate.

The size of the coarse aggregate for each of the concretes is limited to ¾ in. to put them on a comparable density basis. The estimated ore costs are intended to include crushing, grading, and freight to Los Angeles. Fig. 4 shows the unit cost of the different concrete mixes as a function of concrete density.

PHYSICAL PROPERTIES

The magnetite concrete appears to have good structural characteristics. Its compressive strength compares well to that of regular concrete having the same cement content. It is difficult to cut even with a diamond saw. However, using a carbaloy tipped drill which actually breaks or chips pieces out of the concrete, holes can be easily drilled into it.

The thermal conductivity of the concrete has been experimentally determined and compared with ordinary concrete. Cylinders 6 in. in diameter and

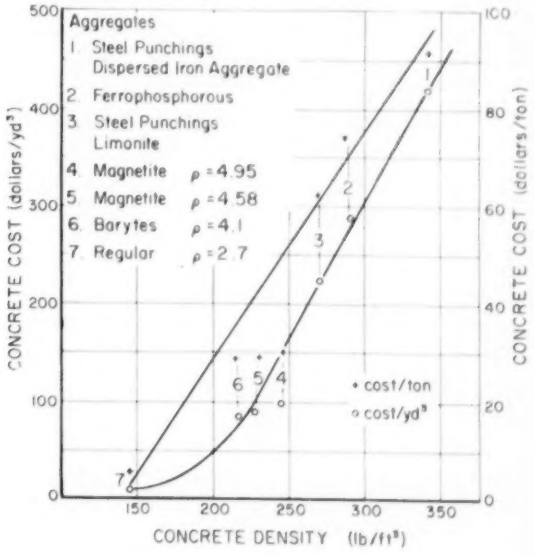

Fig. 4—Concrete cost versus density for materials only

24 in. long, each having a heating element along its centerline and thermocouples located radially out from the center, were used for the conductivity measurements. Although experiments are still in progress and the data have not been fully analyzed, the following statements can be made. (1) The thermal conductivities of the magnetite iron ore concrete and ordinary concrete are essentially the same. (2) The thermal conductivity at 95 F dropped from 1.2 to 0.85 Btu per hr per sq ft per deg F per in. after the average temperature of the cylinders had been cycled between 90 F and 250 F three times in a three-week period.

The effects of nuclear irradiation and high temperatures on the concrete have not been fully determined.

SHIELDING PROPERTIES

The gamma-ray shielding properties of the magnetite concrete have been computed empirically from its chemical composition. Adjustments have been made to account for buildup due to Compton scattering. The curves of Fig. 5 show the reduction in gamma ray intensities versus the magnetite iron ore concrete thickness for various gamma-ray energies. The curves are calculated for broad beam conditions, no correction being made for inverse square attenuation. The data agrees closely with published data for magnetite concrete.[1]

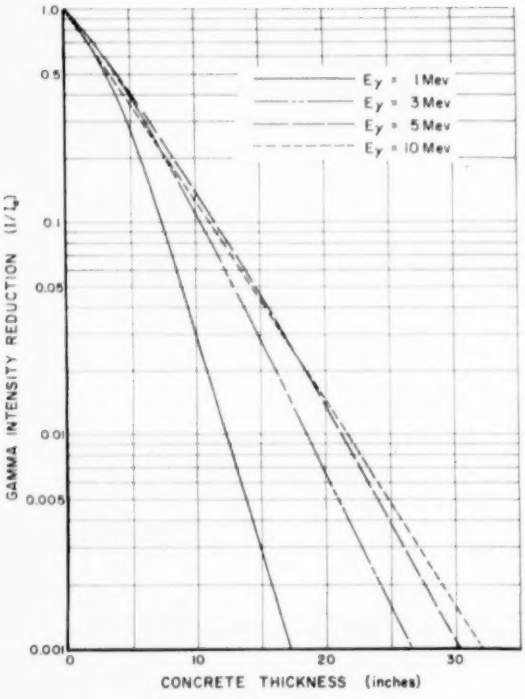

Fig. 5—Attenuation of gamma rays (broad beam) of various energies in magnetite iron ore concrete having a density of 230 lb per cu ft

Experiments carried on in the vertical thermal column of the "water boiler" type research reactor at North American Aviation, Inc., indicate that the thickness of the magnetite concrete required to reduce the fast neutron intensity by a factor of 10, one "tenth value layer," is 7.6 in. The tenth value layer for ordinary concrete was similarly determined to be 9 in.

If a neutron shield is required, it seems advisable to add boron in some form to the concrete mix. This would not only stop the thermal neutrons almost immediately, but the boron would preferentially capture the neutrons as they were thermalized and emit most of the binding energy in the form of alpha particles rather than as hard gamma rays which are produced when thermal neutrons are captured by iron atoms. Alpha particles would be captured immediately in the concrete, whereas some of the gamma rays, being harder to stop, would penetrate the shield. Therefore, boron would be added to capture the thermalized neutrons and thereby decrease the number of secondary gamma rays getting through the shield.

Since boron increases the setting time of portland cement concrete, care must be taken in selecting the form of the boron-containing material to be added. If colemanite is added, the particles below say a No. 30 sieve size should be screened or washed out to decrease the colemanite surface area in contact with the mixing water. This in effect decreases its solubility. The addition of calcium chloride offsets to some extent the effect of the boron.

CONCLUSIONS AND RECOMMENDATIONS

Concretes of various types are often used for shielding personnel and equipment from gamma rays, x-rays, and neutrons. Concrete has the advantages that it can easily be cast into various shapes at a relatively low cost, and it has good structural properties. Since regular concrete has a relatively low density and accompanying relatively poor shielding qualities, the trend has been to develop a high-density concrete having good shielding and structural properties. Increasing the density has increased the cost of the concrete, especially above 3.5 or 4 g per cu cm.

In attempting to produce a relatively low cost high-density concrete in a particular area, one should investigate the density and cost of suitable concrete materials in that area. Estimated crushing, grading, handling, and shipping costs should also be added to the aggregate cost. With this information the density of the concrete and cost of materials per cubic yard can be determined. By plotting the unit cost of materials versus the density of the concrete, as in Fig. 4, the most economical shielding concrete for the area can probably be determined.

After the aggregate has been selected, a more detailed engineering study should be made to reduce crushing and handling costs and increase the concrete density.

The aggregate could be crushed and graded into 8 or 10 different sizes then reblended in proper proportions to result in the optimum concrete density. However, for most materials suitable for concrete aggregates,

crushing and separating them into two or three well-graded sizes and blending them together in the proportion which results in the most dense workable mix will require less time, result in a near maximum concrete density, and cost much less.

For fabricating concrete shielding block, a recommended maximum size aggregate to be used is ¾ or 1 in. This is to reduce the size and number of voids which might occur, especially at the surfaces of the block. For extra large block or heavy shielding walls, a 2- or 4-in., or possibly larger, maximum size aggregate could be used and would result in a concrete having a higher density and requiring less cement per unit volume.

Since the aggregate particles are very sharp and angular and also because of their high density, the mix does not flow as well as a regular concrete mix having the same aggregate size distribution and cement and water content. For maximum density and minimum shrinkage, the mix should be kept as stiff as is practicable. An internal vibrator will cause the mix to flow well and help eliminate voids.

Because of the high density of the concrete, the regular batch size for a mixer load will generally have to be decreased to avoid overloading the mixer. This is especially true when large capacity mixers are used.

For large shielding-concrete jobs, where obstructions in the forms are excessive the prepacked method of placing will probably result in a shield having a higher and more uniform density than would be obtained by regular placing methods.[2]

The methods used in casting the concrete shielding block seem to have been very satisfactory. Tolerances were held to within 1/32 of an in., when necessary, without a significant increase in cost.

REFERENCES

1. Callan, E. J., "Concrete for Radiation Shielding," ACI JOURNAL, Sept. 1953, *Proc.* V. 50, pp. 17-14.

2. Narrow, Lewis, "Barytes: Handle with Care!" *Engineering News-Record*, V. 152, No. 19, May 13, 1954, pp. 36-37, 40.

Title No. 51-30

Flat Slab Solved by Model Analysis*

By GERALD BOWEN and R. W. SHAFFER†

SYNOPSIS

A practical model analysis procedure for determining elastic moments, shears, torsions, and deflections in any plate structure under transverse loads is presented. This method, known as "photo reflective stress analysis" or the "Presan method," is described in some detail. A specific analysis and reinforcing steel design of a continuous square bay flat plate supported by columns of finite diameter is presented and compared to mathematical analysis of the same structure using ACI Building Code moment coefficient (M_o) and standard elastic analysis and design procedures.

INTRODUCTION

In the field of structural engineering, use of models as a design tool has become increasingly prevalent in the past 25 years. Experimental stress analysis of structures is an extremely important tool, not only for research and development work but also as the basis of the design of specific structures.

Obviously, model analysis methods find their main applications in those structures where accurate mathematical analyses are either impossible or are exceedingly tedious and complex. One such structural problem is that involving two-way or biaxial bending as found in floors or roofs of flat slab buildings. Although the total moment in fully continuous, square, or rectangular bays may be found readily, determination of the actual distribution of these moments within the individual bays is a difficult mathematical problem. In structures where the bays are trapezoidal or triangular, or slab configuration is not constant in thickness, an accurate mathematical analysis of the stress pattern becomes so involved that it is impractical.

In effecting the solution of a flat slab with irregular column arrangement for Parklabrea Towers, Los Angeles, the method of model analysis known as "photo reflective stress analysis," or the "Presan method," was developed by Bowen, Rule and Bowen, designing structural engineers, in consultation with Prof. R. R. Martel of California Institute of Technology. This paper demonstrates the application of this method to a relatively simple flat plate problem, and shows its application as a design tool.

*Presented at the ACI 50th annual convention, Denver, Colo., Feb. 24, 1954. Title No. 51-30 is a part of copyrighted JOURNAL OF THE AMERICAN CONCRETE INSTITUTE, V. 26, No. 6, Feb. 1955, *Proceedings* V. 51. Separate prints are available at 50 cents each. **Discussion** (copies in **triplicate**) should reach the Institute not later than June 1, 1955. Address 18263 W. McNichols Rd., Detroit 19, Mich.

†Members American Concrete Institute, President and Vice-President, respectively, Presan Corp., Los Angeles, Calif.

DESCRIPTION OF FLAT SLABS

The term "flat slab" as used herein denotes a structural member which transmits vertical loads directly to columns, walls, or other major supporting members without the use of intermediate supporting beams. Special types of flat slabs include flat plates which are slabs of uniform thickness throughout; haunched slabs which have increased slab thickness adjacent to column; or joisted slabs which consist of a series of relatively small joists at a uniform size and spacing, placed perpendicular to each other and supporting a thin membrane. Haunched slabs may have either a sudden change of thickness at the edge of the haunch or the thickness may vary gradually from slab thickness to a maximum haunch thickness at the column. All of the column or wall supports may have column or wall capitals as required.

DESIGN PROBLEMS

Moment, shears, and deflections, used to determine the proper slab thickness and degree of reinforcement, are functions of the size and spacing of supporting members, configuration of the slab, superimposed loads on the slab, and other structural features such as holes in the slab for stair wells and ducts, or the location of spandrel or other framing beams. Superimposed loads may be subject to extreme variation, both in magnitude and in placement. Dead load may not be uniformly distributed if the slab is haunched. Live loads may be uniformly distributed or concentrated; alternate bays may be loaded to produce "skip loading" moments, and shears or lateral loads may produce bending in the slab if part or all of the lateral resistance is in columns.

The method of construction may also impose special loads. For example, two separate loading conditions are found in lift-slabs where contiguous, cantilever spans are later connected to act as continuous spans under live load.

To complete the final design of a slab, values of maximum moment, shear, and deflection and distribution of moment must be evaluated and located. These values determine the required size, length, and spacing of tension reinforcement (conventional bars or prestress units), the thickness of slab as determined from deflections and from compressive and diagonal tension stresses in concrete, and the size and placement of shear reinforcement if required.

Values of elastic deformations are required if cambering of the slab is a feature of the design or for other reasons.

Supporting structural elements must be designed to carry vertical slab loads and, in some cases, unbalanced slab moments. Vertical loads to columns, walls, and spandrel or special framing beams are defined by those within the area bounded by zero shear lines. Loading conditions and conditions of continuity determine the unbalanced moments delivered to spandrel beams, columns, or walls.

BASIC THEORY

Bending moments, torsional moments, shears, and deflections may be defined as functions of the curvature of the neutral surface of the slab in two mutually perpendicular directions. Letting these directions be defined as x and y, the following equations* hold true for any structure under transverse load acting as a plate:

$$M_x = FI\,(k_x + \mu\, k_y) \text{ and } M_y = FI\,(k_y + \mu\, k_x) \quad (1)$$

$$M_{ty} = FI\,(1 - \mu)\,\frac{\partial\,(\Sigma\; k_x\;\Delta x)}{\partial y} \quad (2)$$

$$Q_x = \frac{\partial\, M_{ty}}{\partial x} + \frac{\partial\, M_x}{\partial x} \text{ and } Q_y = -\frac{\partial\, M_{ty}}{\partial_y} - \frac{\partial\, M_y}{\partial_y} \quad (3)$$

if the slab is of constant thickness, Eq. (3) becomes

$$Q_x = FI\,\frac{\partial\,(k_x + k_y)}{\partial x} \quad (3a)$$

$$\delta = \Sigma\,\Sigma\, k_x\, \overline{dx}^2 \quad (4)$$

Eq. (1), (2), and (3) depend on the basic assumptions that the slab is homogeneous, that Hooke's law remains valid throughout all ranges of existing stresses, that the thickness of the slab is small relative to the spans between supporting members, and that deflections of the slab are small relative to the thickness of the slab. Eq. (4) is independent of these assumptions, being based on geometry only.

Nomenclature

b = reference to building when used as subscript
D = flexural rigidity = FI
E = modulus of elasticity
F = flexural constant = $E/(1 - \mu^2)$
I = moment of inertia of unit slab width = $t^3/12$
k_x = curvature of neutral surface of slab in assumed x direction
M_x = bending moment of unit slab width in assumed x direction
M_{tx} = torsional moment of unit slab width in assumed x direction
M_p = principal moment of unit slab width
m = reference to model when used as subscript
Q_x = shear in unit slab width in assumed x direction
t = thickness of slab
x and y = assumed, mutually perpendicular directions
δ = deflection of neutral surface of slab
μ = Poisson's ratio

THE PRESAN METHOD

The Presan method of biaxial stress determination consists of the following procedures:

a. Construction of a model of the basic structure in accordance with the laws of similitude

b. Loading of the model with scale loads of known magnitude to represent loading conditions of the basic structure

c. Recording of curvatures of the slab in its loaded condition

d. Graphical manipulation of curvature values to obtain moments, shears, and deflections of the basic structure

e. Presentation of final data in a convenient, usable form for design of the structure

*Timoshenko, S., *Theory of Plates and Shells*, McGraw-Hill Book Co., Inc., New York, N. Y., 1940.

Laws of similitude between the model and prototype dictate that the model material be homogeneous and follow Hooke's law throughout the ranges of stresses imparted to the model, that Poisson's ratio be the same for the model material and the prototype material, that the model be a scale replica of the prototype, and that model loads be to a known scale of the loads on the basic structure.

In addition to satisfying these laws of similitude, from a practical standpoint, the model material must also be readily available in wide ranges of thickness, must have one surface plane to within a minimum curvature of 300 in., and must have this surface capable of being made reflective. It must be easily machined with standard machine tools and have a relatively low modulus of elasticity so that readable curvatures may be obtained with small loads that are easy to apply, maintain, and regulate.

After a thorough investigation into the availability of model materials, Lucite was selected. Lucite has an average modulus of elasticity of 370,000 psi and an average Poisson's ratio of 0.38. Concrete has a Poisson's ratio of 0.18 in the usual ranges of mixes and strengths and the results of this nonconformance will be discussed later in the paper.

ANALYSIS BY PRESAN METHOD WITH NUMERICAL EXAMPLE

For purposes of numerical illustration, an analysis was made of one bay of an infinitely continuous slab, supported by columns at 20-ft centers. The column diameter was assumed as $15\frac{1}{2}$ in. and the slab thickness was set at $6\frac{3}{4}$ in. Ultimate stress at 28 days is assumed as 3750 psi. The structure was designed to support its dead load and an additional 50 lb per sq ft live load. Building dimensions and building loads are shown in Fig. 1.

Prior to construction of the model, a model drawing is prepared which dimensions the model and shows any special loading conditions which may be necessary. In the case of the example it would be obviously impossible to model an infinite continuum, so the effect of continuity was approximated closely by modeling an adjacent line of bays on each side of the bay to be analyzed and reproducing continuity beyond these bays by means of an edge-loaded cantilever. The cantilever edge represented the zero moment line of an interior bay and the edge load reproduced the shear along these lines. This loading strip as well as other model dimensions is shown on the model drawing in Fig. 1.

A pattern was then made, using any convenient material, to the dimensions of the model drawing. From the pattern, the model was reproduced from one solid piece of Lucite through the use of the profile duplicator, a machine developed specially for this purpose. Machining of the Lucite model is done with high-speed routers and drills so that the Lucite is not heated excessively during machining and so that the properties of the material are not changed locally because of "burning." Accuracy of model construction with this method is to within $\pm$ 0.001 in.

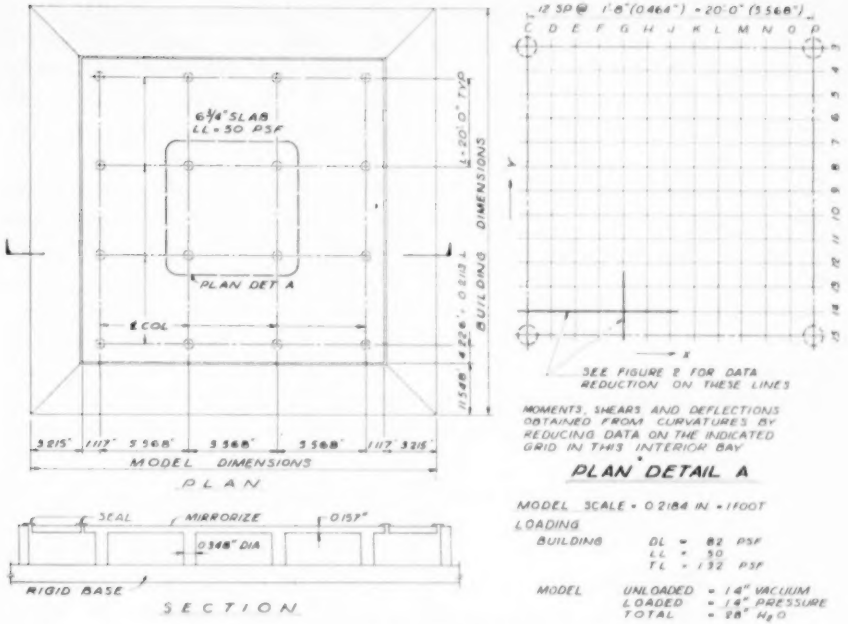

Fig. 1—Building and model details

After construction of the model the top surface was made reflective by depositing on it, under vacuum, an extremely thin coating of aluminum. The model was then mounted on a rigid base which is arranged for the application of model loads using compressed air or vacuum.

For design purposes, the usual slab loading can be expressed as a uniformly distributed load. This loading is applied to the model directly by applying compressed air or vacuum pressure to the under side of the model slab. In the event that differential uniform loads are desired on different areas of the same slab, plastic bags are fabricated to fit the contours of the under side of the slab and compressed air is applied to the bags at required pressures. Concentrated loads are applied by use of graduated weights, scaled to conform to the scale of the uniform dead or live loads.

Lateral loads can also be applied parallel to the surface of the slab to simulate seismic or wind loads if qualitative or quantitative distribution of moments into the slab system is required.

In its final position, ready for loading, the surface of the model is in a vertical plane and it is so placed in relation to a camera that it reflects onto the camera negative a grid of parallel lines. The camera negative, grid, and model surface are in parallel planes at known distances from each other.

If the reflective surface of the model were an optically perfect plane, the reflected grid of lines would be perfectly parallel in the unloaded condition

of the model. The reflective surface of the model is never perfectly plane, however, so prior to each photograph of the model in a loaded condition, a photograph is made in the unloaded condition. The unloaded condition is usually photographed as a vacuum (equivalent to 14 in. water in the example) while the loaded condition is photographed as an equal pressure (equivalent to 14 in. water in the example).

Loads applied to the model produce curvature in the reflective surface. These curvatures distort the reflected grid of lines, making them appear at decreased spacing when the slab curves convex to the lens and at increased spacing when the curvature of the slab is concave to the lens.

The model is rotated in its plane 90 deg and the unloaded and loaded grid of lines are photographed as before, using the same loads. If principal moments are to be obtained as part of the design data, the model is rotated in its plane to a position half way between the two previous positions and the unloaded and loaded reflected grid of lines are again photographed using the same model loads.

Optical equations, not herein presented, demonstrate that:

$$k = C\left(1 - \frac{J}{K}\right) \qquad (5)$$

where k = curvature of the surface, J = grid spacing for zero curvature, and K = observed grid spacing of curved surface. C = a constant which depends on the distance between reflective surface and the camera lens.

The problem of accurately and economically determining k from the photographed grid spacings was solved by designing a "data reduction machine" which magnifies the spacing between grid lines, measures the grid space K, and plots the curvature k to a determined scale. This machine produces a series of bar graphs along desired straight lines on the model, the ordinate of which represents the curvature of the model and the abscissa, the linear distance on the model. These diagrams are curvature diagrams, defining curvature in one direction.

In the example, curvature diagrams were prepared on lines C through P and 3 through 15 as shown on plan detail A of Fig. 1, and the unloaded (vacuum) and loaded (pressure) curvature diagrams, manually smoothed to form a smooth curvature curve, are shown in Fig. 2. As shown in Fig. 2, the diagram for loaded condition is superimposed on the diagram for unloaded condition with ordinates plotted to the same datum.

From these curvature diagrams, obtained in two perpendicular directions, with another curvature diagram obtained at 45 deg between, bending moments, shears, torsional moments, principal moments, tangents to the elastic surface, and deflections of the elastic surface were obtained.

Equations evaluating moment, torsional moment, and shear are all functions of $F = E/(1 - \mu^2)$. The physical characteristics of Lucite as measured by the modulus of elasticity and by Poisson's ratio may vary from sample to sample because of variations of age, temperature, and humidity. Therefore,

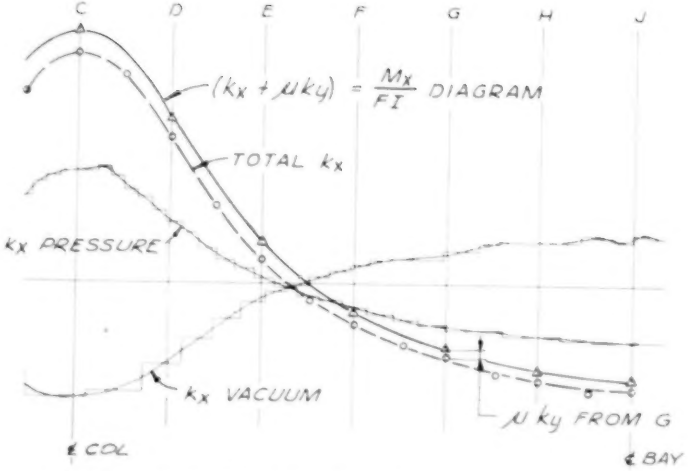

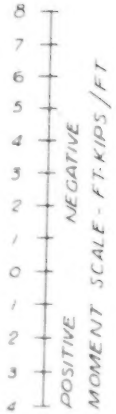

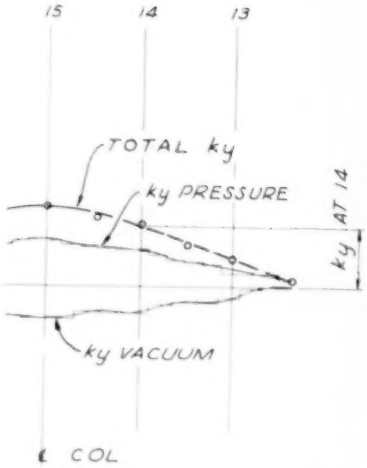

CURVATURE DIAGRAM - X DIRECTION ON LINE 14

PARTIAL Y CURVATURE DIAGRAM ON LINE 6

DIAGRAM SCALES $M_x = FI(k_x + \mu k_y) = \frac{q_b}{q_m} R^2 FI C h_t$

q_b = 132 PSF q_m = 28 IN WATER = 145.6 PSF
R = 12/0.2784 = 43.1 IN PER IN
F = 486700 PSI (FROM CIRCULAR PLATE TEST)
I = $0.157^3/12$ = 0.0003164 IN^4 PER IN
C = 0.00863 $1/IN^2$ (OPTICAL & MACHINE CONSTANT)

$\therefore M_x = 2237\, h_t$ OR 1 IN HT = 2.237 FT-KIPS PER FT

Fig. 2—Curvature diagrams

the value of F, the flexural constant, is determined from each sample of model material by testing another portion of the sample as a circular flat plate with clamped edges, the solution for which is known. The value of F for this example was 476,800 psi.

Bending moments

Bending moments in one direction are obtained in the following manner. The net curvature diagrams are constructed by algebraically deducting the unloaded ordinate from the corresponding loaded ordinate on each diagram. This compensates for any initial curvature in the model. To the net curvature diagram in the assumed x direction, Poisson's ratio correction $\mu\ k_y$ is added to the corresponding k_x ordinate. The value of Poisson's ratio for concrete (0.18) is used for this operation.

If the moment of inertia were constant throughout the length of the diagram, this corrected curvature diagram would be the M/F diagram and the vertical scale could be computed, giving values of M_x directly. However, the thickness of the slab may vary, either because of haunches, spandrels or intermediate framing beams, or because of slight variations in model construction. To compensate for this variation, the final thickness of each model as fabricated is measured at close intervals throughout the model and the ordinates to the net curvature diagrams, corrected for Poisson's ratio, are further corrected for variations in slab thickness by multiplying the height of the $(k_x + \mu\ k_y)$ diagram by t^3, producing bending moment diagrams to a selected scale.

In the example, the model thickness did not vary by more than 0.001 in. from the correct value so no thickness correction was required. Consequently, the net curvature diagram, corrected for Poisson's ratio, is the final M_x

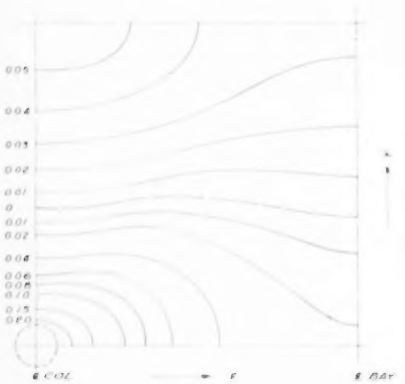

Fig. 3a—Contours of equal values of C
$M_y = CwL^2$

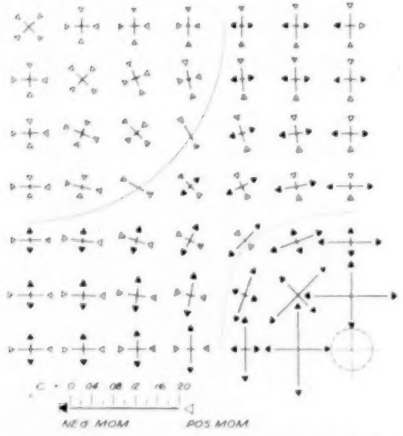

Fig. 3b—Principal moments and trajectories
$M_p = CwL^2$

Column diameter to span = 1:15.5
Slab thickness to span = 1:36

diagram and this diagram, for line 14, is shown in Fig. 2. The similitude equations are also shown in Fig. 2 and the scale of the moment diagram is calculated thereon.

Bending moments in the y direction were evaluated on lettered lines as shown on plan detail A, Fig. 1. These moments were nondimensionalized to be functions of a constant C, where $M_y = CwL^2$, and contours of equal values of C are presented in Fig. 3a.

Corrected net curvature diagrams in the x, y, and xy directions were combined, using Mohr's circle, to produce the value and direction of principal moments. These principal moments were nondimensionalized as were the M_y moments and the values of C in $M_p = CwL^2$ are presented as vectors in Fig. 3b. Determination of the value and direction of principal moments is seldom of practical importance in the design of biaxial bending systems. However, Mohr's circle may be applied in determining the bending moments in any direction and thus has some application in determining stresses and the degree of necessary reinforcement in slabs reinforced in other than the conventional biaxial method (*e.g.*, radial-circumferential patterns).

Torsional moments

Values of torsional moment in the x and y directions were obtained from the Mohr's circle studies previously mentioned and were nondimensionalized as functions of β_T where $-M_{tx} = M_{ty} = \beta_T wL^2$. Contours of equal values of β_T are presented in Fig. 4a. Values of maximum torsional moment are not of great practical importance except in certain special conditions of structural

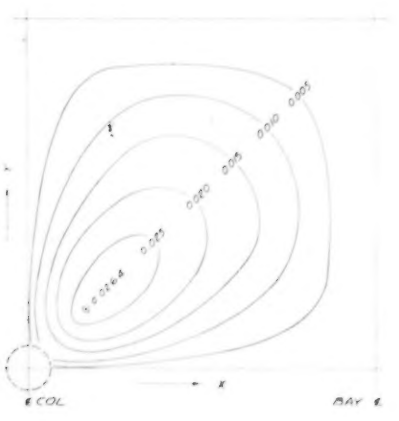

Fig. 4a—Torsional moment contours of equal values of β_T

$$-M_{tx} = M_{ty} = \beta_T wL^2$$

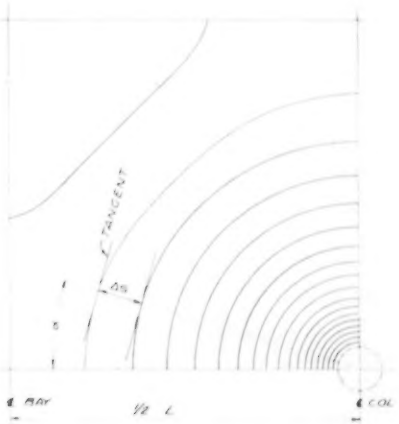

Fig. 4b—Shear contours of equal total curvature

$$V_a = 0.4239\, w \frac{L}{\Delta s} \text{ lb per ft}$$

L and Δs in same units

Column diameter to span = 1:15.5
Slab thickness to span = 1:36

configuration where they may lead to greater stresses than those produced by direct bending and shear.

Shear

Distribution of shear within a bay is determined directly from curvature diagrams by finite differences in accordance with Eq. (3) or (3a). For slabs with varying thicknesses this operation is fairly complex and the final results are best expressed as contours of equal shears in pounds per unit width of slab. However, as indicated by Eq. (3a), the shear in a given direction in a slab of uniform thickness is a function of the change of total curvature $(k_x + k_y)$ with respect to the change in distance in the given direction. Fig. 4b presents contours of equal total curvatures and defines the shear at an angle α as an inverse function of the distance between adjacent contours. The distance ΔS shown in Fig. 4b is the shortest distance which can be drawn between the indicated, adjacent contours and thus defines the maximum shear and its direction at that location. The shear in any direction may be obtained by scaling the distance between the adjacent contours in the direction desired and substituting that value in the equation $V = 0.4239\ w\ (L/\Delta S)$. In the investigated bay, maximum shearing stress is 140 psi which requires shear reinforcement. This reinforcement is not included as a part of the paper.

It should be emphasized that all functions of bending moment, torsional moment, and shear, as heretofore discussed, are directional and the desired direction of the function must be determined before the value of the function can be evaluated.

Deflection

The elastic deflections of the slab are functions of the second summation of the curvature diagrams in any one direction. This process of taking the second summation of scaled values of the curvature diagrams does not yield results commensurately accurate with values of moments and shears but values within 10 percent of the correct value can be consistently obtained with careful operations. The maximum deflection as calculated for the example was within 2.53 percent of the theoretically correct value as obtained by solving the series function for maximum deflection. Contours on the elastic surface of the example are shown in Fig. 5 as contours of equal α in the expression $\delta = \alpha\ (wL^4/Et^3)$.

Total moment

The total moment in a bay, defined as the numerical sum of the maximum total positive moment along the bay centerline and the maximum total negative moment along the column centerline, for a uniformly loaded, square bay is given by the expression $M = 0.125\ wL^3 \left(1 - \frac{8r}{\pi L} + \frac{8r^3}{3L^3}\right)$ where r is the effective radius of the column or column capital. For normal ranges of the ratio of $2r$ to L, this expression for moment agrees closely with the expression $M = 0.125\ wL^3 \left(1 - \frac{2C}{3L}\right)^2$ where $C = 2r$. For loads and di-

Fig. 5—Elastic surface contours of equal α

$$\delta = \frac{wL^4}{Et^3}\alpha \text{ in.}$$

mensions used in the example, the total moment evaluated from the first expression is 121.5 ft-kips and from the second expression it is 121.22 ft-kips. The total moment evaluated by the Presan method for the given example is 122.90 ft-kips, or 1.15 percent above the correct, statical moment. A total moment of 121.5 ft-kips is used throughout the rest of the example in evaluating the amount and distribution of reinforcement in the bay.

Expression of results

The expression of results of studies determining principal moments, torsional moments, shears, and deflections as shown for the example in this paper are satisfactory and workable, although, for a specific analysis of the slab structure the results would not be nondimensionalized. However, bending moments in the directions in which reinforcing is contemplated must be expressed in such a way as to facilitate both the determination of quantities of reinforcement and the required length of bars.

Bending moment can be presented as contours of equal bending in any desired direction. From these contours the total moment in any given width of slab can be computed and the total amount of reinforcement to resist this total moment determined. If both long and short bars are to be used in a given width of slab, the point at which the long bars will no longer resist the existing bending moment can be determined and short bars started so that they are developed in bond at that point.

Since contours must be plotted, placement of reinforcement is simplified if ordinates to moment diagrams are divided by $f_s\,jd$ to produce A_s diagrams. From these diagrams, contours of equal A_s can be plotted directly. These contours for the example, would be similar in form to the contours of equal values of C as shown in Fig. 3a. Partial contours of equal A_s are shown in Fig. 7. From contours of equal A_s, the total amount of reinforcing in any given width of slab can be determined directly and, if long and short bars are used in the same band, the point at which the short bars are no longer necessary can be directly determined from the contours.

As previously defined, ordinates to moment diagrams represent the values of bending moment parallel to the direction of the diagram. If a series of parallel moment diagrams are cut with a plane normal to the direction of the diagrams, the intercept of diagrams on the plane defines the moment profile. Thus, ordinates to the moment profile represent values of bending moment perpendicular to the direction of the profile. Moment profiles of maximum positive moment at the bay centerline and maximum moment at the column centerline are shown in Fig. 6. These profiles show, in addition to the magnitude of moments, the true distribution of moments across the bay.

Agreement with theory

The fact that Poisson's ratio is 0.18 for concrete and 0.38 for the model material leads to the only general disagreement between the Presan method of analysis and the known, theoretical solutions. Poisson's ratio enters calculations for moment in the determination of the flexural rigidity $EI/(1 - \mu^2)$, and in the curvature correction applied to curvatures at 90 deg to the direction of considered bending. The procedure used in making a Presan analysis is to use $\mu = 0.18$ in correcting curvatures and to determine the flexural constant of the model material experimentally, based on μ of the material. This procedure gives correct results of moment, torsional moment, and shear in all cases where the expression of these functions is a continuous, parabolic series.

At cantilever edges, at edges adjacent to large openings in the slab, and in cases where the load is not uniformly distributed, this procedure gives incorrect results, the percent of error for M_x being greatest when k_x is small and k_y is large so that the μk_y correction is significant. This occurs, however, in areas of low bending moment so that errors introduced are not particularly significant. The usual Presan procedure in these cases is to graphically construct smooth, parabolic curves from support lines to edge conditions of zero moment as representing the corrected curvature diagrams.

Since it is not always possible to make a true scale reproduction of the prototype and still have the surface of the model a plane so that it may be made reflective, it is sometimes necessary to model columns, walls, and spandrel or other framing beams to an equivalent stiffness on the bottom of the slab. Equivalent stiffness in axial deformation or flexural deformation is not a function of Poisson's ratio and therefore there is no direct error introduced. However, when spandrel or framing beams offer torsional restraint, there are small errors introduced which are well within the limits of conventional design procedure.

Comparison of Presan total moment with ACI M_o

As previously outlined, the Presan total moment and the statical moment for the example equals $0.125\ wL^3 \left(1 - \frac{2C}{3L}\right)^2 = 121.5$ ft-kips. Total moment M_o as defined by the ACI Building Code (ACI 318-51) equals $0.09\ wL^3$

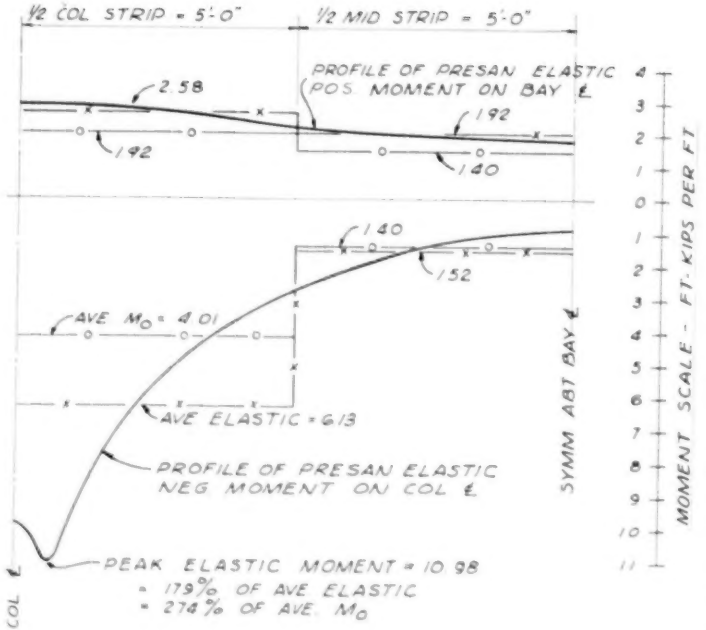
½ COL STRIP = 5'-0"
½ MID STRIP = 5'-0"
PROFILE OF PRESAN ELASTIC POS. MOMENT ON BAY ℄
2.58
1.92
1.92
1.40
1.40
1.52
AVE M_o = 4.01
AVE ELASTIC = 6.13
PROFILE OF PRESAN ELASTIC NEG. MOMENT ON COL ℄
PEAK ELASTIC MOMENT = 10.98
= 179% OF AVE ELASTIC
= 274% OF AVE. M_o
COL ℄
SYMM ABT BAY ℄
MOMENT SCALE - FT-KIPS PER FT
4 3 2 1 0 1 2 3 4 5 6 7 8 9 10 11

Fig. 6a—Distribution of moment. Presan elastic versus M_o

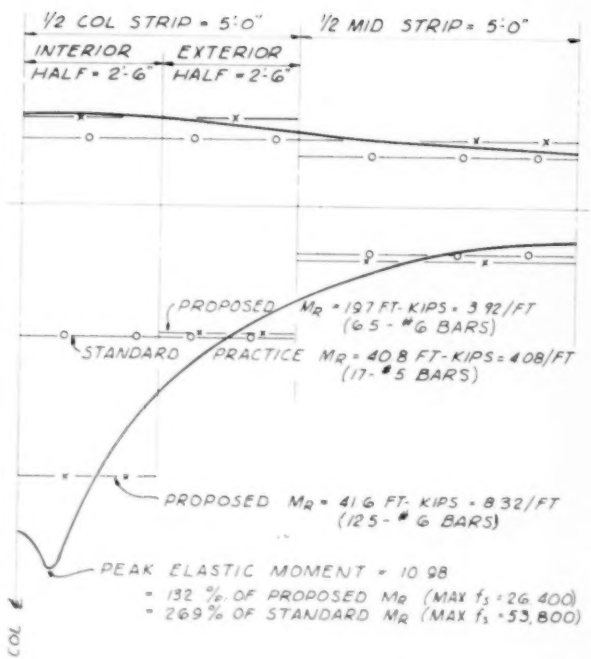
½ COL STRIP = 5'-0"
½ MID STRIP = 5'-0"
INTERIOR HALF = 2'-6"
EXTERIOR HALF = 2'-6"
PROPOSED M_R = 197 FT-KIPS = 3.92/FT (6.5 - #6 BARS)
STANDARD PRACTICE M_R = 40.8 FT-KIPS = 4.08/FT (17 - #5 BARS)
PROPOSED M_R = 41.6 FT-KIPS = 8.32/FT (12.5 - #6 BARS)
PEAK ELASTIC MOMENT = 10.98
= 132 % OF PROPOSED M_R (MAX f_s = 26,400)
= 269 % OF STANDARD M_R (MAX f_s = 53,800)
COL ℄

Fig. 6b—Resisting moment of supplied steel

$\left(1 - \frac{2C}{3L}\right)^2$, which equals 87.3 ft-kips or a total moment which is 28.1 percent less than the true statical value.

Not only is the value of the ACI total moment low, but there are appreciable differences between the percentages of this total moment distributed to locations of maximum negative and positive moment in column and middle strips as determined from a Presan analysis when compared with standard ACI coefficients. These differences vary with structural conditions such as unbalanced spans or haunches. In fact, for certain configurations or support conditions, the zero moment contour closes around the columns, thus producing positive moment rather than the listed negative ACI coefficient for middle strip at column centerline.

Table 1 lists, and Fig. 6a compares, these coefficients for the example. It will be observed that for the square bay of the example the maximum variation between coefficients is between 46 percent for ACI column strip negative and 50 percent for the Presan analysis at the same point, or a variation of 8.9 percent. Introducing further the discrepancy in total moment, the average negative ACI column strip moment is 34.0 percent lower than the average negative Presan column strip moment. The peak elastic negative moment is 274 percent of the average negative ACI column strip moment.

Table 1 compares Presan moment coefficients, moments, and required steel areas with those based on the ACI total moment using ACI moment coefficients, and also with those based on the correct total statical moment using ACI moment coefficients slightly modified by standard practice in placing bars. The variation between distribution of the Presan total moments and the ACI total moment of M_o is shown graphically in Fig. 6a.

Placement of reinforcing steel

To complete the example, the investigated bay was reinforced to resist the bending moments as determined from the Presan analysis and this placement was compared with a completed conventional design using the same total moment with bars placed in accordance with standard practice. Bar sizes and lengths thus determined are listed in Table 1 and the resisting moments of both systems of reinforcement are shown graphically in Fig. 6b.

To compensate, insofar as is practical, for the condition where the negative moments near the edge of the column are very high, three lengths of bars were used in the Presan design to resist the negative column strip moment. The long and intermediate bars were spaced evenly in the full column strip while the short bars were concentrated adjacent to the column where more reinforcement was necessary. The effect of such concentration of bars is shown in the relatively low amount of overstress at the peak elastic moment compared to conventional design.

To reinforce the investigated bay for flexure only by the Presan design requires 2.73 lb of steel per sq ft while reinforcement following standard

TABLE 1—COMPARISON OF MOMENT COEFFICIENTS, MOMENTS, AND REQUIRED STEEL

	Presan method Total moment = 121.5 ft-kips					ACI M_o = 87.3 ft-kips			ACI standard practice Total moment = 121.5 ft-kips				
Location	Moment, ft-kips	Percent total moment	Total steel area, sq in.	Bar selection	Cumulative steel area, A_s per ft	Percent total moment	Moment, ft-kips	Total steel area, sq. in	Percent total moment	Moment, ft-kips	Total steel area, sq in.	Bar selection	Cumulative steel area, A_s per ft
Column strip													
Negative	61.3	50.1	8.12	6—#6 x 12 ft 3 in. 7—#6 x 7 ft 6 in. 6—#6 x 5 ft 4 in.*	0.264 0.572	46	40.1	5.19	45.9	55.7	7.37	9—#6 x 12 ft 9 in. 9—#4† 9—#4†	0.396 0.576
Positive	25.8	21.2	3.26	9—#4 x 14 ft 3 in. 8—#4 x 9 ft 6 in.	0.18	22	19.2	2.43	22.8	28.5	3.6	9—#4 x 24 ft 9 in. 9—#4 x 24 ft 9 in.	0.18
Middle strip													
Negative	15.2	12.5	1.92	10—#3 x 12 ft 3 in. 8—#3 x 8 ft 0 in.	0.11	16	14.0	1.77	15.65	19.0	2.4	6—#4‡ 6—#4‡	0.12
Positive	19.2	15.8	2.43	7—#4 x 14 ft 9 in.	0.14	16	14.0	1.77	15.65	19.0	2.4	6—#4 x 21 ft 6 in.	0.12

*Place bars in interior half (5 ft 0 in.) of column strip.
†Bent up from column strip positive.
‡Bent up from middle strip positive.

practice requires 3.19 lb of steel per sq ft, or 17 percent more. Since total moment in the bay is the same for both methods, most of the indicated 17 percent saving is in the fact that in the Presan design, short bars are carried only the normal distance (12 bar diameters) past the point where they are no longer required to resist bending while standard practice carries some bars a considerable distance past their required length, although other bars are of insufficient length. Fig. 7 shows the bar layout for both the Presan and the standard practice design. The excess and insufficient lengths mentioned above are indicated where they exist.

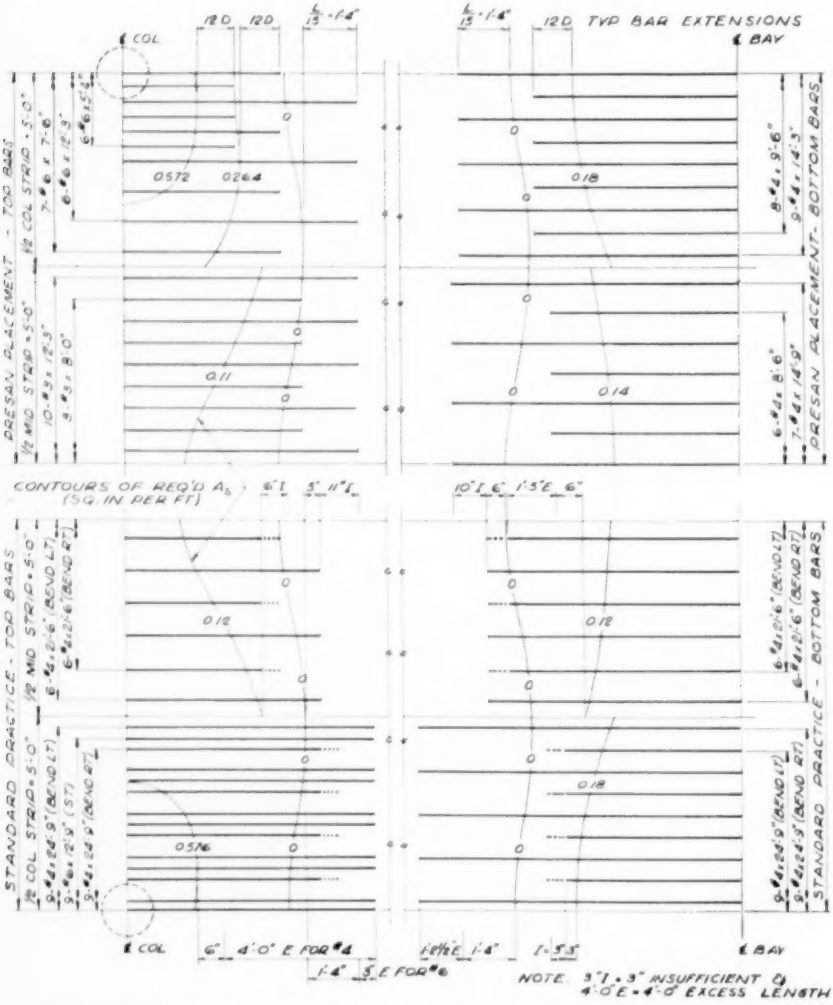

Fig. 7—Presan placement versus standard practice. Both based on total moment = 121.5 ft-kips

It should be emphasized that the square bay used as an example results in the closest correlation between code and elastic distribution coefficients of total moment. It also illustrates the least divergence between placement and required length of reinforcement. The direct application of ACI moment coefficients and standard practice to some forms of flat slabs which fall within the limits set by the ACI Building Code may result in a totally inadequate design.

CONCLUSIONS

General

The use of flat slab floor and roof systems is increasing constantly as engineers discover the advantages of the system and design and construction procedures are improved. Given adequate tools with which to design, engineers will find that flat slab floor and roof systems compete successfully in most cases with wood and steel construction, particularly when insurance costs are considered. This makes it imperative that code provisions for flat slab design be kept in line with all current advancements.

Proposed revision to ACI Building Code, Chapter 10

1. The correct total statical moment in a uniformly loaded bay, with a coefficient of 0.125, should be used in Eq. (18), Section 1002, and Eq. (19), Section 1003, of the ACI Building Code.

2. The distribution factors given in Table 1004(a) for interior flat slab panel without drop panel should be revised in accordance with distributions listed in Table 1 of this paper under "Presan method—percent total moment." The remaining percentages in Section 1004 should be confirmed or revised by similar analyses.

3. Additional restrictions should be placed on the use of Section 1003 in flat slab design, such as maximum ratio of live to dead load.

4. A provision for concentration of two-thirds of column strip negative steel in the central one-half of the strip would improve the structural capacity of the slab, as shown in Fig. 6, and reduce the effects of plastic flow. Plastic flow and shrinkage effects would also be reduced by providing compressive steel in the area near the column where allowable K values are exceeded. In this example, using $f_c' = 3750$ psi, the maximum allowable K value of 298 will be exceeded inside the contour $C = 0.153$, and the maximum compressive concrete stress is 2250 psi, or 60 percent f_c', without this compressive reinforcing.

5. Sections 1002 and 1003 should be expanded to provide specific limitation on extensions of bent or straight bars to satisfy zero moment or intermediate contours, as shown in Fig. 7.

6. Use of Section 1002 should be limited to square and rectangular bays, and attention called to the fact that the distributions called for in Section 1004 for slabs with drop panels are valid only for one given relative stiffness of drop panel to center slab.

7. Requirements for slab thickness should be revised to include provision for restraint of supports and design load.

ACKNOWLEDGMENT

The authors would like to give credit for editing the manuscript to R. E. Franklin, senior engineer, Presan Corp. He added materially to the expansion of the paper.

Fly Ash–Sulfur Mixture for Capping Concrete Test Cylinders*

By HUBERT F. McDONELL†

SYNOPSIS

Various materials used in capping concrete cylinders were investigated to develop, if possible, a mixture that was economical and would produce caps that within 2 hr would not flow or fracture when the specimen was tested. A fly ash–sulfur mixture combined in the proper proportions and melted and used at the recommended temperatures produced caps that met all of the requirements.

INTRODUCTION

Capping the Florida State Road Department's concrete cylinders in preparation for testing has always constituted a major problem since they average from 50 to 100 per day.

For a number of years the department used a 50–50 mixture of Type I portland cement and molding plaster as the concrete cylinder capping material. This combination produced caps that were unsatisfactory unless they were allowed to harden at least 24 hr before testing. Considerable trouble was experienced due to the caps chipping during handling, and in disintegrating when subjected to the sprays in the moist room for periods of 24 hr or longer.

High early strength cement, Type III, was later substituted in place of the Type I cement, which improved the quality of the caps somewhat, particularly at earlier ages. This combination produced satisfactory caps provided they were allowed to harden overnight. This could be arranged for cylinders arriving in the laboratory several days prior to the date they were due to be tested, but proved to be unsatisfactory for the cylinders arriving the day they were due to be tested.

The use of high early strength cement in postwar concrete construction created a condition that required further investigation of capping mixtures since the number of cylinders being received the day they were due to be tested had more than doubled from that of previous years.

It was imperative that a change be made in the capping materials previously used; therefore, a commercial product composed of sulfur and fire clay was tried. This material produced excellent caps but was too expensive to

*Received by the Institute Aug. 2, 1954. Title No. 51-31 is a part of copyrighted JOURNAL OF THE AMERICAN CONCRETE INSTITUTE, V. 26, No. 6, Feb. 1955, *Proceedings*, V. 51. Separate prints are available at 35 cents each. **Discussion** (copies in **triplicate**) should reach the Institute not later than June 1, 1955. Address 18263 W. McNichols Road, Detroit 19, Mich.

†Member American Concrete Institute, Assistant Engineer of Tests, State Road Department of Florida, Gainesville, Fla.

use in capping all of the cylinders, so its use was limited to the cylinders arriving the day they were to be tested. Therefore, an investigation was begun in an attempt to develop a capping mixture that was both satisfactory and economical.

INVESTIGATIONS OF VARIOUS MIXTURES

The first investigations were made with mixtures of commercial grade sulfur (100 percent passing the 325-mesh sieve) and various materials including cement, fine sand, rock screenings, and fuller's earth. None of these mixtures were satisfactory since there was distortion and cracking in all of the caps. Practically all means of developing a satisfactory mixture had been exhausted when fly ash was included and with amazing success. By varying the proportions it was established that one part of fly ash to six parts of sulfur by weight produced a cap that was satisfactory in every respect. Further investigation indicated that crude unscreened sulfur melted and handled better than the refined sulfur. The cost of this mixture was found to be approximately one-half the cost of the commercial mixture.

No attempt has been made to reclaim the capping material after the cylinders are tested, except in an experimental stage which did not prove successful.

PREPARATION OF FLY ASH–SULFUR MIXTURE

It was found that a large electric roaster (24 qt) was ideal for preparing the mixture. It is melted at 450 to 500 F after which the temperature is reduced to 200 F until the mixture reaches a fluid state comparable to lightweight motor oil, when it is ready to be used. The 200 F temperature should be maintained throughout the period it is being used for capping cylinders.

Fig. 1—Electric roaster, hood with blower, and capping molds

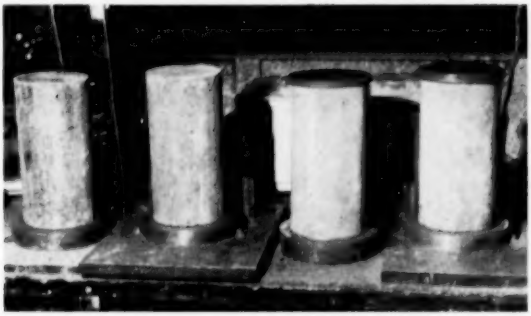

Fig. 2—Concrete cylinders in capping molds

It is imperative that the mixture be melted beneath a small hood with blower attached (Fig. 1), so that all of the fumes will be removed.

60 TO 75 CYLINDERS CAPPED PER HOUR

One man can cap 60 to 75 concrete cylinders (6 x 12 in.) per hour when using four molds. Since the material hardens within a few seconds after it is poured into the molds, the capping operation is continuous. A ladle that holds just the right amount is used in pouring the mixture into the mold. The cylinder is immediately placed in the mold since the material hardens so rapidly that it can be removed in 30 sec.

An average charge will furnish enough material to cap both ends of from 50 to 60 cylinders, with an average of ¾ lb per cylinder.

The molds (Fig. 2) are made from circular steel plates 8 in. in diameter and 1¼ in. thick. They are machined to a depth of ⅝ in., the bottom being 6¼ in. in diameter and sides tapered so that the diameter across the top is

Fig. 3—Capping concrete cylinders and pavement cores

6¾ in. These measurements may indicate that the molds are larger and deeper than necessary. However, based on past experience, it has been found that some concrete cylinders cast in the field tend to have rough and irregular ends. In these cases an excessive amount of capping material is required so that the capped surfaces are approximately at right angles to the axis of the specimen. Each mold has two pieces of ⅜ x 2½-in. steel guides 8½ in. high and spaced 5 in. apart (see Fig. 1). The guides are welded to the molds to insure the cylinders being capped in a position that complies with the specifications.

TEST RESULTS

Test results obtained on the fly ash–sulfur mixture at various ages, when combined in the proportions of one part fly ash to six parts of sulfur by weight are given below. Compressive strength of 2 x 2-in. cubes at the ages of 1, 2, and 5 hr were:

Total load at 1 hr	Total load at 2 hr	Total load at 5 hr
18615	20400	20810
19455	21080	20180
19470	20260	21550
Avg—19180	Avg—20580	Avg—20847
4795 psi	5145 psi	5212 psi

Test results indicate that the compressive strength obtained at the age of 2 hr meets the American Assn. of State Highway Officials' requirements for capping material for concrete cylinders.

CONCLUSION

The Division of Tests has been using this mixture for capping all of the department's concrete cylinders, concrete pavement cores, and brick for more than 2 years (Fig. 3). In no case has any of the caps failed, even though a large number of the cylinders represented prestressed concrete which tested as high as 7500 psi. This mixture has produced such excellent results that the fly ash and crude sulfur are now purchased in lots of 1 ton each.

Current Reviews*

of Significant Contributions in Foreign and Domestic Publications

Bridges

Analysis of continuous bridge girders with floating supports (in Croatian)

SVET JANKOVIC, *Nase Graderinarstvo* (Yugoslavia), V. 8, No. 7, 1954, pp. 181-190
Reviewed by J. J. POLIVKA

Other methods and previous publications in this field are reviewed, especially those by W. Ritter, L. Vianello, K. Müller-Breslau, Engesser, Winkler, and M. Ritter. Author's simplified method is presented. Five-moment equations with introduced coefficients of subsidence are solved. These equations are reduced to Clapeyron's three-moment equations when the coefficients of subsidence are zero. Equations for great number of spans are developed and simplifications for smaller number of equal spans are discussed. Tables calculated for greater number of spans simplify the analysis.

Several prestressed concrete bridges in south Germany (Verschiedene Spannbetonbrucken in Suddeutschland)

FRITZ LEONHARDT, *Proceedings*, Deutscher Beton-Verein, Wiesbaden, V. 50, 1953, pp. 80-101
Reviewed by PAUL ROGERS

All of these bridges have used Dr. Leonhardt's well-known system of movable semi-circular anchor blocks.

The bridge at Rosenstein is of 225-ft span, 80 ft wide, and is of box girder construction. Unlike previous Leonhardt bridges, this one has four separate anchor blocks at each end, and prestressing was carried out both longitudinally and transversely. Furthermore, the bridge acts as a rigid frame, which was achieved through the medium of diagonal prestressed anchor members hidden in the abutments. The bridge carries two streetcar tracks, plus a four lane highway and sidewalks, and the box girders contain pipes and conduits for utilities.

The railroad bridge at Kochendorf has five spans of 42 ft maximum, and is also of box girder construction. The prestressing cable follows the maximum moment diagram, and special provisions are made above supports to counteract the increased compression stresses which are due to load reactions, plus a vertical component of the cable stress.

The bridge at Donautal is a continuous five-span highway bridge with a maximum span of 230 ft, built with open spandrels, and using four adjacent anchor blocks which are prestressed simultaneously.

Research on highway bridge floors

N. M. NEWMARK and C. P. SIESS, *Proceedings*, Highway Research Board, V. 33, 1954, pp. 30-53
AUTHORS' SUMMARY

Reviews the research on highway bridge floors carried out at the University of Illinois, 1936 to 1954. Object of this research has been to determine the behavior of reinforced concrete slabs subjected to vehicle wheel loads and to investigate the effects of the many variables encountered in different types of bridge-floor construction. The methods used have included a combination

*A part of copyrighted JOURNAL OF THE AMERICAN CONCRETE INSTITUTE, V. 26, No. 6, Feb. 1955, *Proceedings* V. 51. Address 18263 W. McNichols Rd., Detroit 19, Mich. Where the English title only is given in a review, the book or article reviewed is in English. If it is followed by a foreign title the work reviewed is in that language. In those cases where the foreign title cannot conveniently be set in type or is not available, the language of the original article is indicated in parenthesis following the English title. Copies of articles or books reviewed are **not** available through ACI. Available addresses of publishers are listed in the June "Current Reviews" each year. In most cases ACI can furnish addresses of publications added later.

of mathematical analyses as well as extensive tests on scale-model bridges and on full-size elements of bridges.

Two types of bridges have been studied: the simple-span solid-slab bridge with integral curbs and the I-beam bridge. Tests have been made on both right and skew bridges of both types, and on both simple-span and continuous I-beam bridges. Extensive analytical and experimental studies of composite action in I-beam bridges have also been made. In addition to these studies of actual bridge types, there have been several analytical and experimental investigations of fundamental problems involved in the behavior of slabs subjected to concentrated loads.

The paper includes brief descriptions of each phase of the investigation with references to the several publications in which the research methods and results have been reported in more detail.

Construction

Flat buildings erected with portal crane

JAN F. REYMERT, *World Construction*, V. 6, No. 6, Nov.-Dec. 1953, pp. 19-21

Describes how the use of a portal crane has helped reduce costs and arduous manual labor in housing construction in Sweden. The crane described has an opening between legs of 47 ft and a lifting height of 40 ft from rails to hook which enables it to straddle the standard flat building. It has been in operation since 1948 and has brought about many changes in the methods used in the construction of flats. Among these changes is the replacement of standard inside walls with walls of precast concrete lifted into place by the crane. More recently brickwork has been replaced with walls precast of lightweight concrete.

Twin 90-in. concrete pipelines divert storm runoff for Paducah, Ky.

E. E. BOLLS, JR., *Civil Engineering*, V. 24, No. 6, June 1954, pp. 64-66

Storm sewer project included approximately 16,000 ft of reinforced concrete pipe varying in diameter from 60 to 90 in. Length of double 90-in. line was 2709 ft. Construction details are given.

Lift slab construction saves Clemson time and money

WILLIAM G. LYLES, *Consulting Engineer*, V. 4, No. 3, Sept. 1954, pp. 38-42

Reviewed by ARON L. MIRSKY

Design and construction of new dormitory at Clemson Agricultural College is described.

Reinforced concrete water tower for the Central Building Research Institute, Roorkee

O. P. JAIN, *Indian Concrete Journal* (Bombay), V. 28, No. 9, Sept. 1954, pp. 370-374

Discusses design of the base slab of the tank, the supporting tower, and its foundations for 25,000-gal. reinforced concrete water tank.

The folded plate—a lighter, stronger concrete roof

MILO S. KETCHUM, *Consulting Engineer*, V. 4, No. 1, July 1954, pp. 51-53, 72

Reviewed by ARON L. MIRSKY

Two types of roof contours were used in a building for a Denver equipment firm: Z-shaped (to permit clerestory lighting to be used) for the office area, and V-shaped for the shop and display area. Spans were 75 ft with 22 ft overhangs at each end, for the Z-type; and 80 x 18 ft (valley to ridge) for the V-type; latter also carried two 15-ton cranes in each bay. Design procedure was that of George Winter and Minglung Pei ("Hipped Plate Construction," ACI JOURNAL, Jan. 1947, *Proc.* V. 43, pp. 505-532). Construction was by movable forms; placing problems were overcome by proportioning concrete mixes of the proper consistency. Author speculates on an intriguing possibility: folded-plate roofs combined with tilt-up walls to form a complete shell with walls continuous with the roof.

Assembly-line technique results in low-cost concrete construction at Forrestal Village

WILLIAM R. LORMAN and CARL K. WIEHLE, *Civil Engineering*, V. 23, No. 11, Nov. 1953, pp. 58-62

Demonstrates adaptability of concrete to large-scale housing. Excellent description of construction details. Foundations, ground floors, and entrance platforms were cast in place. Wall panels and second-story floor and roof slabs were precast. Exterior walls were sandwich panels with cellular glass as the insulation material. As a result of mass production and assembly-line erection technique, construction costs were approximately 88 per sq ft.

African Gold Coast harbor project

World Construction, V. 7, No. 2, Mar.-Apr. 1954, pp. 19-20

Describes extensions to the Gold Coast harbor of Takoradi. The main wharf extension, a 1400-ft continuation of the deep-water quay wall was built of precast concrete block weighing about 15 tons. The block were laid in horizontal courses, bonded and keyed with concrete joggles.

Printing works for the Bank of England

Concrete and Constructional Engineering (London), V. 49, No. 11, Nov. 1954, pp. 337-342

Prestressed precast members and arch construction are utilized in two-building printing plant. Main hall has double arch ribs with north-light shells spanning between them. The two ribs comprising each arch are 3 ft 6 in. apart to accommodate various services. Arches were precast in sections and prestressed in place. Shells were cast in place with movable formwork. Balanced cantilever construction was used in general printing hall, the roof of which is 94 ft wide. It consists of four free-standing bays, each comprising four cantilever beams (prestressed) between which there are north-light shell roofs. Shells were precast and then prestressed in place. Multiple-story sections of buildings and retaining wall also utilized precast elements in combination with in situ concrete. Formwork and erection and prestressing techniques were notable throughout project.

An articulated groyne

Concrete and Constructional Engineering (London), V. 49, No. 10, Oct. 1954, pp. 323-325

A flexible concrete groin or jetty was built of two parallel rows of 15-ton concrete blocks, which are free to settle independently of one another, but held together below beach level by a flexible linkwork of bull-head rails.

Mixer for making aerated concrete

The Engineer (London), V. 198, No. 5141, Aug. 6, 1954, p. 209

Reviewed by Aron L. Mirsky

Advantages claimed for aerated cement mortar used for grouting include increased resistance to frost and chemical attack, and reduced cost due to the bulking effect. British mixers, of 4- or 8-cu ft capacity, use two sets of blades mounted on a common shaft inside a vertical drum of 29-in. diameter. Aeration is achieved by the addition of a detergent to the mix. A pump mounted on the same chassis delivers grout at pressures up to 100 psi.

Spanish east coast harbors (Les ports de la cote Est de l'Espagne)

J. Costet, *Annales des Ponts et Chaussees* (Paris), V. 124, No. 1, Jan.-Feb. 1954, pp. 1-25

Future fishing center of the Port of Dieppe (Le futur centre de maree du Port de Dieppe)

M. Desbazeille, *Annales des Ponts et Chaussees* (Paris), V. 124, No. 1, Jan.-Feb. 1954, pp. 69-91

Reviewed by Aron L. Mirsky

First paper is an interesting account of recent construction at the ports of Malaga, Alicante, and Valencia, describing briefly the new piers, sheds, silos, the modern roads and railways, and other facilities. [An abstract of this article, in English, was published in *Civil Engineering and Public Works Review* (London), Mar. 1954, p. 254.]

In similar vein, albeit less concerned with structural aspects, is the second paper, which discusses the facilities already constructed, and those which should be constructed to place Dieppe on a par with Continental fishing ports. Economic considerations are stressed.

Junior high with every unit expandable

Architectural Forum, V. 101, No. 4, Oct. 1954, pp. 122-125

This school building, utilizing prestressed and precast concrete, is designed to be easily expandable. Framing of classroom unit was prestressed concrete to main-floor level, precast post and lintel above. Auditorium framing used precast columns. Some walls and spandrels consisted of precast sandwich panels. Floors used reinforced concrete joists or precast channel slabs. Roof of classroom unit was prestressed concrete panels.

Largest structure to date built by lift-slab method

Edward K. Bryant, *Civil Engineering*, V. 23, No. 9, Sept. 1953, pp. 52-54

Construction of three-story, 1500-man barracks at U. S. Naval Amphibious Base, Norfolk, Va., utilized lift-slab method. The building is shaped like two E's back to back. Over-all frontage is 477 ft; over-all depth, 302 ft 8 in.; and each wing is 47 ft 4 in. wide.

Dams

Structural behavior of concrete gravity dams

G. Gunn and W. G. Morison, *Ontario Hydro Research News*, Hydro-Electric Power Commission of Ontario, V. 6, No. 2, Apr.-June 1954, pp. 1-8, 19

AUTHORS' SUMMARY

Results of this extensive instrumentation program have provided a reliable check on many theoretical assumptions and have yielded field data which will assist the design of similar structures in the future. Large thermal cracks do not exist in the interior of the mass concrete studied despite the placement of large monoliths. Apparently the effect of the slow decline in temperature and the resulting increase in stress are offset by concrete creep and autogenous growth; it is evident that the tensile strength of the concrete is not exceeded. Uplift pressures are low and have remained constant during the past three or four years. No high or serious stresses were observed at any of the measuring stations; the measured strains, deflections, and joint and shear movements indicate that the structures are behaving as a homogenous mass on a rigid foundation and have the structural properties of good quality concrete.

Sarda hydroelectric power station—VI

Baleshwar Nath, *Indian Concrete Journal* (Bombay), V. 28, No. 9, Sept. 1954, pp. 361-367

Concluding article in series, with previous articles in July and September 1950, April 1951, May 1952, and July 1953 issues of *Indian Concrete Journal*. Describes construction of spiral roofs, cable galleries, control room, outdoor substation, and intake gate structure.

Reservoirs and water power plants. V. 1—Dams (Stauanlagen und Wasserkraftwerke)

Heinrich Press, W. Ernst & Sohn, Berlin, 1953, 212 pp.

Reviewed by J. J. Polivka

Of special interest are chapters on concrete dams: (1) gravity dams (general design and use, structural analysis, details); (2) arch dams (general design and use, their limitations, allowable stresses, various methods of design as one- and two-plane method, shell type method, method of cylindrical shell, experimental stress analysis); (3) shell and dome type dams; (4) dams with piers; and (5) multiple arch dams. Other chapters deal with reconstruction and repair of dams, increase of their height, underground dams, methods of construction, and maintenance. Special attention is given to recent developments in concrete dams, their economy and safety (as *e.g.*, originated by Bureau of Reclamation, Lars Jorgenesen, Ambursen, Dischinger, Komendant, Press).

Design

Folded plate theory and analysis (Faltwerke)

Joachim Born, Verlag Konrad Wittwer, Stuttgart, 1954, 204 pp., 21 DM

A complete treatment of the analysis and design for "folded plate" or hipped plate construction. The approach is logical with a minimum of theory and higher mathematics and a generous use of pictures, sketches, and diagrams. Each theoretical derivation is followed immediately by numerical examples of its application. The material includes simple hipped plate, complex (more than two plates meeting at a joint), symmetrical and unsymmetrical loads, and uniform and concentrated loads. Hipped plate analysis is applied not only to roofs (gable end and hip end, north-light, butterfly, pyramidal, etc.) but also to bunker silo storage structures, stairways, and horizontal balcony slabs. A bibliography of selected papers from 1920-1954 is included. Some of the few known test results on such structures are discussed. It should be valuable for study to advanced students and to practicing engineers for design. Reinforced concrete designers should appreciate this structural form, particularly since it represents nearly as efficient a use of concrete as thin shells without recourse to curved forms.

Design of reinforced concrete beams with light tensile reinforcement from the modulus of rupture (Le calcul a la rupture par flexion des poutres en beton arme' a faible pourcentage d'armature tendue)

R. Chambaud, *Annales de l'Institut Technique du Batiment et des Travaux Publics* (Paris), No. 78, June 1954

Reviewed by Phillip L. Melville

The elastoplastic theory was used to design lightly reinforced beams at the modulus of rupture. To explain higher actual bending moment at failure the author shows that the appearance of the stage of strain hardening of the steel beyond the ductile

stage allows a steel stress that exceeds the yield point. The bond of steel to concrete is an important factor in this problem. It is concluded that the beams followed the law of elastoplasticity. To support the conclusion, 150 tests are analyzed. Twenty-four references are addended.

Strength of plain, reinforced, and prestressed concrete under the action of combined stresses, with particular reference to the combined bending and torsion of rectangular sections

HENRY J. COWAN, *Magazine of Concrete Research* (London), No. 14, Dec. 1953, pp. 75-86
AUTHOR'S SUMMARY

A theory for the strength of concrete and reinforced concrete under the action of combined stresses is advanced which combines Rankine's maximum principal stress criterion and Coulomb's internal friction criterion. Equations for the strength of plain, reinforced, and prestressed concrete in combined bending and torsion are then derived. The distinct difference between primary bending and primary torsion fracture is explained by the dual character of the criterion of failure. It also accounts for the increase in the torsional strength of a reinforced concrete section resulting from the addition of bending. Prestressing delays the formation of tension cracks until the compression due to the initial prestress has been offset, and it therefore effects a great improvement in the torsional strength of concrete.

Doubly-reinforced beams: a quick method of design

J. S. SAVONA, *Concrete and Constructional Engineering* (London), V. 49, No. 11, Nov. 1954, pp. 333-336

A table and graph are presented as a quick method of designing or checking stresses in doubly-reinforced beams. Examples illustrate prodecure.

Model tests of concrete structures (Ensayos estaticos mediante modelos de estructuras de hormigon)

HERMANN BEER, *Publication* No. 1, Academy of Exact Sciences and of Technology, Tucuman National University, Argentina, 1950, 55 pp.
Reviewed by J. J. POLIVKA

Reviews previous methods and results of model testing and discusses the advantage and disadvantage of photoelasticity. The model material used by the author and Prof. E. Tschech was similar to that employed by the Bureau of Reclamation: a composition of gypsum, diatomaceous earth, and water. After a series of tests a 1:0.5:1.2 (measure by weight) mix was chosen. This material had a modulus of elasticity varying from 2100 to 4200 ksi (according to the amount of binder and borax); permissible stresses were 140 psi in compression and 40 to 55 psi in tension; specific weight was 0.9 (56 lb per cu ft). A special chapter deals with the relationship between dimensions, stresses, and deflections of the model compared with those of the structure. Tests are described for several arch dams built in Austria. Preparatory tests are also described and illustrated (*e.g.*, triangular cantilever under triangular loading corresponding to hydraulic pressure of a gravity dam). In the second part of the book, tests and complete stress analysis of an arch dam are described; the results are compared with theoretical analysis (by Tölke, Ritter, Bousinesq, Vogt) and previous model tests (Bureau of Reclamation, Oberti).

Influence lines for continuous beams. Unit ordinates tabulated

E. MARKLAND, *Engineering* (London), V. 178, No. 4621, Aug. 20, 1954, pp. 242-243
Reviewed by ARON L. MURSKY

Labor of calculating rotations over supports of multispan continuous beams is considerably reduced by applying unit angular distortion at an intermediate support and using slope-deflection equations to obtain relations between rotations, thus reducing number of simultaneous equations to be solved to two. A table of unit influence line ordinates is given to reduce the labor of calculating ordinates.

Load distribution on the piles of a pile grid (Die Lastverteilung auf die Pfaehle eines Pfahlrostes)

E. JACOBY, *Der Bauingenieur* (Berlin), V. 29, No. 2, Feb. 1954, pp. 47-50
Reviewed by ARON L. MURSKY

Analysis of load distribution by methods of elastic deformations. Two cases are considered: (1) continuous groups, as under retaining walls, and (2) isolated groups, as under crane footings. Method is claimed to be applicable to groups containing piles with assorted batters. Discussion, by E. Krey and the author, appears in *Der Bauingenieur*, July 1954, p. 272.

Materials

Possible uses of aluminous cement with other cements in sundry surroundings (Possibilites d' emploi du ciment fondu avec d' autres ciments au sein de diverses ambiances)

M. DURIEZ, *Annales de l'Institut Technique du Batiment et des Travaux Publics* (Paris), No. 75-76, Apr.-Mar. 1954

Reviewed by PHILLIP L. MELVILLE

Aluminous cement made by burning bauxite and lime has special properties: very high early strength, high resistance to acid waters, will set at below freezing temperatures, good refractory, low resistance to bases especially free lime and alkalies. It consists essentially of anhydrous monocalcic aluminate. Research indicates that no chemical reaction will take place between concretes with aluminous and portland cements. Bases from portland cement will affect and weaken aluminous cement concrete only when they are porous. Speed in setting of the aluminous cement may be controlled by adding variable amounts of slag cement.

Materials of construction

M. O. WITHEY and G. W. WASHA, 9th Ed., John Wiley & Sons, Inc., New York, N. Y., 1954, 850 pp., $9

The book has been brought up to date, including much new material. As a background, it covers sources and manufacturing. A brief treatment of engineering mechanics introduces a section on testing and testing equipment. Aggregate, cement, and concrete properties and tests receive a thorough treatment. Designers and specification writers will benefit by this section which includes extensive test data on properties and conditions capable of supplying answers to many nonroutine questions and problems. This book will be a definite asset to the reference library of practicing engineers and concrete contractors.

Variations in quality of cement

L. BOYD MERCER, *Commonwealth Engineer* (Melbourne), V. 41, No. 1, Aug. 1953, pp. 20-24

While cements produced today satisfy specification requirements, there exists a lack of uniformity from manufacturer to manufacturer and time to time. The suggestion is made that greater consideration be given to testing cement in concrete and that the cement industry establish "target" strengths much the same as used for proportioning concrete. The alternative is mentioned of placing a maximum limit, as well as a minimum, for cement testing to reduce the variation in the various cement groups.

Concrete proportions (Composition des betons)

R. VALETTE, *Revue des Materiaux de Construction* (Paris), No. 463, Apr. 1954, pp. 87-98; No. 464, May 1954, pp. 127-136

Reviewed by PHILLIP L. MELVILLE

It is bluntly stated that the only basis for concrete mix design is Feret's law for a voidless concrete with a minimum water content for a given amount of cement. The voids in the wet aggregates shall be less than 56 percent of the volume of the cement paste. To obtain optimum conditions a minimum of sand is required and a gap-gradation must be used. Recent studies by Pasquet, Lezy, Joisel, Manche, and Martin are reviewed to show that their methods are only right when they agree with the authors and use gap-gradation as an application of Feret's law. The resulting efficiency in the use of the cement, increased workability, and durability are discussed. Examples are given with detailed description of the working methods to be employed in proportioning so that only a trial batch is needed as verification of this "foolproof" method. The author does not emphasize the painstaking care with which the aggregates are selected and controlled nor the economy of the mix. He appears to challenge anyone to improve on his method of concrete mix design.

Entrained air benefits lightweight-aggregate concrete

FRANCIS J. MARDULIER, *Civil Engineering*, V. 24, No. 1, Jan. 1954, pp. 56-59

The properties of lightweight aggregate which produce harsh concrete also make it difficult to entrain air in the concrete. The type of air-entraining agent used to best advantage is usually different than that used in regular concrete, and often must be designed for the specific type of aggregate. Mixing sequence also differs between lightweight concrete with and without air entrainment. Range of air contents for various types and classes of lightweight concretes is given, as well as properties of such concrete.

Decorative and protective coatings for concrete (in Dutch)

A. L. Klaasen, *Cement* (Amsterdam), No. 15-16, 1954, pp. 260-261

Reviewed by John W. T. Van Erp

In the last 25 years tremendous progress has been made in the development of coatings for specific purposes, which can be classified according to the following main groups: (1) decorative treatment; (2) light protection against deterioration by occasional contact with aggressive vapors and liquids; and (3) heavy protection against deterioration by continuous contact with aggressive substances as in silos, containers, and industrial structures. The various coatings analyzed and classified approximately in the above categories are: plaster (1), silicates and mineral base paints (1, 2), cement (1, 2), paints (emulsions or oil base, 1, 2), lacquers (rubber, polyvinylbase, etc., 1, 2, 3), silicones (2), and bituminous coatings (2, 3).

Producing lightweight aggregate from slate

Walter B. Lenhart, *Rock Products*, V. 57, No. 3, Mar. 1954, pp. 92-98

Two-kiln plant for producing expanded lightweight aggregate is mechanized throughout for high efficiency and economy. Excavation, crushing and screening, and calcining operations are described.

Air-entrained concrete

Harrison F. Gonnerman, *Consulting Engineer*, V. 4, No. 4, Oct. 1954, pp. 52-61

Reviewed by Aron L. Mirsky

Subtitled "A Look at the Record," article presents both a brief historical summary and an even briefer survey of current practice.

Experimental comparison between Lossier cement and Swedish standard cement in cement mortar (in Swedish)

Gunar Lindh, *Meddelanden* (Bulletin) No. 31, Swedish Cement and Concrete Research Institute at the Royal Institute of Technology, Stockholm, 1954, 40 pp.

Author's Summary

In tests made on specimens of cement paste and cement mortar, special attention was given to those factors which were considered to be decisive in estimating the suitability of the concrete for use in underground concrete tanks for storage of hydrocarbons, particularly gasoline. Accordingly, the tests dealt with the following characteristics of the cement: swelling or dilatation, particularly under the action of alternate curing in water and in air; resistance to frost action; strength, which was examined with due regard to the conditions resulting from prevention of dilatation; and the water-absorbing capacity.

The report concludes with a recommendation relating to the proposed use of Lossier cement in expanding concrete for the underground tanks. So far as the properties of Lossier cement are known at the present time, it cannot be regarded as advisable to utilize this cement in concrete for the construction of underground tanks. If Lossier cement should be used for structures of this type or for similar structures, then it is suggested that the water-cement ratio should be low and that the water-curing period should be long, from 2 to 4 weeks.

Pozzolanic cements from blast furnace slag

R. C. Lied, J. H. Handwerk, and T. N. McVay, *Rock Products*, V. 56, No. 12, Dec. 1953, pp. 130, 136

Quenched blast furnace slag was investigated to determine whether differences in crystal-to-glass ratio in slags had an effect on the pozzolanic activity of cements. Time of set and tensile strength tests were used to evaluate the pozzolanic activity. Data are given on microscopic examinations, tensile strength tests, and time of set tests. The greater the amount of glass, the greater the tensile strength of the cement. Slags containing the most glass also had the fastest time of set, showing that the glass content markedly affects pozzolanic activity.

Aggregate grading and the design of concrete mixes

D. A. Stewart, *Reinforced Concrete Review* (London), V. 3, No. 4, 1954, pp. 187-195 (including discussion)

Single-sized aggregates are recommended to produce more uniform concrete. This gap-grading allows a tight mechanical interlock to develop in the coarse aggregate which permits form removal as soon as the concrete has been placed. Segregation in transit is less likely to occur because the ratio of size of coarse to fine particles is relatively large. Gap-grading produces high-quality concrete more cheaply than continuous grading. The separate bins and individual weighing operations for each size of stone necessary to obtain a low standard deviation are major reasons for this cost difference.

Pavements

Rigid pavement investigation model studies of pavement joints

Ohio River Division Laboratories, Corps of Engineers, U. S. Army, Mariemont, Ohio, June 1954
HIGHWAY RESEARCH ABSTRACTS Oct. 1954

Presents results of a laboratory study of keyed construction joints, using small-scale models, and sets forth criteria from which the most advantageous dimensions for a keyed joint can be determined. It summarizes results obtained from some 300 model specimens, and describes the equipment and techniques employed. Criteria are presented for the determination of the key dimensions as a function of the slab thickness.

It is recommended that the following criteria be adopted for determining key dimensions for keyed construction joints: (1) vertical depth of key, 0.2 of slab thickness; (2) horizontal depth of key, 0.1 of slab thickness; and (3) slope of bevel key, 4 on 1.

Stresses in subgrade under rigid pavement

GERALD PICKETT and DANIEL K. Y. AI, *Proceedings*, Highway Research Board, V. 33, 1954, pp. 121-129
AUTHORS' SUMMARY

Simplified expressions for the theoretical stresses in the subgrade under a pavement are obtained. The simplification results from the substitution of an arbitrary combination of two solutions based upon plate theory for the usual rigorous solution of a two-layered system. The range of application of the substitute solution is greatly extended by arbitrary choice in each component solution of the factor which expresses the effect of the Poisson's ratios of pavement and subgrade on the radius of relative stiffness.

Use of simplified expressions is facilitated by the inclusion of tables from which the stresses for given conditions may be obtained by interpolation.

Concrete roads: research and constructional experience

British Constructional Engineer (London), V. 4, No. 4, Mar. 1954, pp. 21, 23-25

A review of some of the problems in concrete pavement construction and progress toward their solution. Topics include slab design, joint spacing and design, riding quality, surface texture, and quality control.

New, heavier runways built for U. S. bombers

Construction Equipment, Apr. 1954, p. 16
ARBA TECHNICAL INFORMATION DIGEST May 1954

A project for the U. S. Air Force at Carswell Base, Fort Worth, Texas, includes the building of a 3300 ft long, 16–18 in. thick, 300 ft wide, reinforced concrete runway. Another contract calls for the strengthening of an existing apron. Specifications require that the 6 to 10 in. concrete slab be overlain with 10 to 15 in. of new concrete to provide a minimum thickness of 20 in. The old pavement was first tested with a 50-ton pneumatic-tired roller. Broken concrete was replaced and AP-5 asphalt was pumped under the weak areas.

Joint-sealing maintenance operations

C. W. MCCAUGHEY, *Proceedings*, Highway Research Board, V. 33, 1954, pp. 355-359

Describes use of cold-applied, ready-mixed rubber sealer in concrete pavement joints.

Concrete pavement 9 in. thick supported by 4 ft of selected material

CONRAD H. LANG, *Civil Engineering*, V. 23, No. 11, Nov. 1953, pp. 44-46

Description of design and construction of pavement on New York State Thruway.

New technique for repairing spalled joints

Public Works, Nov. 1954, p. 68
ARBA TECHNICAL INFORMATION DIGEST Dec. 1954

Spalling of contraction joints on a recently built concrete expressway was caused by faulty installation of joint assemblies and improper edging of joints. These joints were repaired by removing the spalled portions, thoroughly cleaning the area to be patched, and filling with a concrete patching mixture.

A concrete saw was used to make a vertical cut 1½ to 2 in. deep about 6 in. back of the contraction joint and extending the length of the damaged section. After removing 1½ to 3 in. of broken concrete, the area was cleaned and grouted. A joint cap was inserted over the contraction plate and the patching mixture proportioned 1:5, 40 percent coarse pea gravel and 60 percent sand was placed and vigorously tamped to insure positive contact with the slab being patched. After finishing and edging and an interval allowed for setting, the joint cap was removed and the joints filled with joint filler.

Precast concrete

Precast construction in a multiple-story school

Concrete and Constructional Engineering (London), V. 49, No. 10, Oct. 1954, pp. 307-314

A school covering about 54,000 sq ft is being used as a prototype for the "Intergrid" system of construction. This system was designed for buildings of up to four stories. It is comprised of light prestressed frames and precast panels to form the floors and outer walls, all of which conform to a 3 ft 4 in. module. Details are given on columns, column heads, beams, floor and roof slabs, walls, and method of construction.

Precast concrete slabs for industrial floors

P. F. Van der Meulen Bosma, *Rock Products*, V. 56, No. 12, Dec. 1953, pp. 182-183

Describes production and use of several types of precast floor and pavement slabs in The Netherlands.

Prestressed concrete

Calculation of deflections and bending moments at the supports of prestressed beams

E. W. Bennett, *Concrete and Constructional Engineering* (London), V. 48, No. 11, Nov. 1953, pp. 343-348

A table of formulas is presented for common profiles of cables in beams of uniform cross section to simplify (a) calculation of the initial deflection of a beam due to the prestressing force, and (b) evaluation of the secondary moments caused by the prestressing of a statically indeterminate structure.

Examples are presented of the use of the table for both of these cases. An example is also given of the use of the formulas in designing indeterminate prestressed structures.

Manufacture of prestressed concrete pipes

J. Hasker, *Constructional Review* (Sydney), V. 26, No. 7, Nov. 1953, pp. 16-22

Describes two methods of manufacturing prestressed concrete pressure pipe: (1) wire winding of a preformed shell and (2) internal pressure stressing. In the case of the wire-winding method, a discussion of the theory and the results of pressure tests are included.

For the wire winding process a formed shell, longitudinally prestressed at casting, is wound with high-tensile wire under a predetermined tension. The exposed steel is then covered with a coating of cement mortar.

Internal pressure stressing is accomplished by placing an expandable sheet metal core inside the pipe before the concrete has set, surrounding it with solidly packed sand, and applying internal pressure and heat to the core. The pipe can be removed from the mold in 24 hr. A recent development of a special colloidal solution, which forms a film between itself and the concrete, has eliminated the sand and the core.

Design of longitudinal cables in circumferentially wound prestressed concrete tanks

A. R. Curtis and H. J. Cowan, *Magazine of Concrete Research* (London), No. 15, Mar. 1954, pp. 123-126

Authors' Summary

During the circumferential prestressing of a cylindrical tank, longitudinal bending stresses are set up; if cracks are to be avoided, the tensile stresses must be eliminated by a longitudinal prestress. The paper develops a theory by which the magnitude of this longitudinal prestress may be determined. It is assumed that the thickness of the wall is small compared with the diameter of the cylinder, and that the concrete behaves elastically.

New type of prestressed pile

Concrete and Constructional Engineering (London), V. 49, No. 3, Mar. 1954, pp. 113-115

Describes a precast prestressed concrete pile which consists of hollow units 1 ft 4 in. square and 5 ft long. (See also "Current Reviews," ACI Journal, Dec. 1954, *Proc.* V. 51, p. 392.) The hollow section gives this pile a section modulus double that of a solid pile of comparable weight. The short, standard sections make it unnecessary to have stockpiles of different length piles. Provision is made for lengthening the pile in place.

Prestressed deck proves cheapest for new Hoboken pier

Theodore O. Blaschke and David A. Hopkins, *Civil Engineering*, V. 24, No. 2, Feb. 1954, pp. 50-53

The prestressed concrete deck, 700 x 328 ft, consists of two major elements: pretensioned precast stringers and post-tensioned pile-cap bents. Details are also presented on other aspects of the pier.

Building at London Airport. Prestressed precast frames and beams

Concrete and Constructional Engineering (London), V. 49, No. 1, Jan. 1954, pp. 14-17

Generally the main building consists of prestressed concrete members simply supported on two columns. The cafeteria and dining room are spanned by 14 precast frames 12 ft on center with a span of 48 ft center-to-center of columns.

The frames are prestressed by high-tensile alloy steel bars which were post-tensioned. All components were precast on the site. Each frame consisted of footings, columns, and main beams in halves. The sequence of operations in erecting the frames is given.

Two unusual prestressed-concrete buildings: Printing works for Bank of England

Engineering (London), V. 178, No. 4623, Sept. 3, 1954, pp. 315-317; *The Engineer* (London), V. 198, No. 5145, Sept. 3, 1954, pp. 334-336

Reviewed by Aron L. Mirsky

Main production hall consists of 22 identical 36-ft bays of prestressed arched beams and concrete north-light (sawtooth-type) shell roofs. Arched beams are constructed in pairs, with 3.5-ft gaps to provide space for services; beams are asymmetrical, with 125 ft clear span and 35 ft maximum clear rise, and were precast in segments. The general printing hall uses a balanced-cantilever roof of 94-ft span, supported by a central row of twin columns 10.5 ft apart; roof is also of north-light shell construction. The ends of the cantilevers were loaded temporarily during prestressing operations to prevent overstressing the concrete at the top of the beams in compression.

Layout of these interesting and unusual structures was based primarily on production processes; emphasis was on repetition of construction elements.

Prestressed "cow palace" for Los Angeles

Charles J. Pankow, Jr., *Concrete*, V. 61, No. 12, Dec. 1953, pp. 3-4

Describes construction of 80,000-sq ft agricultural exhibit building in Los Angeles. Basic framing system is comprised of prestressed concrete girders and purlins, supported by cast-in-place exterior columns and precast interior columns. Typical bay spacing is 36 x 50 ft. The 18-ft high perimeter wall is precast concrete panels and the nearly flat roof is a 3-in. monolithic slab.

Prestressed concrete (Il cemento armato precompresso)

Giuseppi Rinaldi, Vitali e Ghianda, Genoa, Italy, 1954, 104 pp., 2000 lire

Magazine of Concrete Research Sept. 1954

The book is divided into four parts, the first of which gives a brief historical review of the technique of prestressing, followed by a description of the principal systems, particular attention being paid to the system developed by Professor Rinaldi.

The second section consists of a typical specification for a prestressed concrete structure with end-anchored cables, followed by a résumé of the practices of several European countries: Italy, Belgium, Germany, France, Switzerland, and England.

The third section consists of typical calculations for bridges of 22-m and 46-m span, and drawings of several of the prestressed bridges in the vicinity of Bologna.

The last section gives the results of tests carried out on a prestressed beam of 26-m span built up of precast units.

Properties of concrete

Permeability of concrete (Betongens vattentathet)

Per Nycander, *Meddelande* 113, Statens Provningsanstalt, Stockholm, 1954, 22 pp.

Discusses effect of various factors on permeability of concrete, including grading and particle shape of aggregate, air entrainment, conditions of moist curing, and water absorption during curing. After water pressure is applied to concrete, factors discussed include dissolved air content in the water and dependence of leakage on water pressure.

Determination of nonevaporable water in hardened portland cement paste

L. E. Copeland and J. C. Hayes, *ASTM Bulletin*, No. 194, Dec. 1953, pp. 70-74

Authors' Summary

A revised method for determining the nonevaporable water of hardened portland cement pastes consists in drying samples in an evacuated space which is connected to a moisture trap held at − 79 C. The new method is simpler to use than the old since the partial pressure of water vapor is controlled more easily. Less time is usually required for the drying process and the precision of the measurement is slightly greater.

Dynamic testing of materials

L. J. Mitchell, *Proceedings*, Highway Research Board, V. 33, 1954, pp. 242-258

Author's Summary

Describes dynamic tests of both sonic velocity and resonant frequency types. Sonic velocity tests were made to evaluate the effect of both air-filled and water-filled cracks on transmittal of signals through concrete. Another series of investigations consisted of sonic-velocity measurements on masses of sand, gravel, combinations of sand or gravel with water, and freshly mixed concrete.

Resonant-frequency dynamic tests were compared to sonic velocities. Flexural and torsional resonant frequency testing on rock cores revealed unusual reactions. Some indications of heterogeneity and loose structure were evident even in apparently sound specimens. Irrational values of Poisson's ratio, which were frequently indicated by these cores, are discussed.

Pulse-velocity techniques and equipment for testing concrete

E. A. Whitehurst, *Proceedings*, Highway Research Board, V. 33, 1954, pp. 226-242

Describes several devices which have been developed for measuring pulse velocities through concrete. The devices fall into three categories: (1) pulse generated by single physical impact with no provision for visual observation of test signals, (2) pulse generated electronically and visual observation of signals, and (3) pulse generated by physical blow and visual observation of signals. A brief résumé is also presented of the interpretations which various investigators have made of pulse velocity test results.

An investigation of the erosive effect on concrete of soft water of low pH value

P. E. Halstead, *Magazine of Concrete Research* (London), V. 6, No. 17, Sept. 1954, pp. 93-98

Author's Summary

The effects of soft moorland water on concrete has been studied by tests on 4-in. concrete cubes immersed in moorland water or tap water for periods of up to 4 years. After immersion in soft water, all types of concrete lost strength and weight to an extent which increased as the immersion was prolonged. Cubes made of portland cement concrete of very high strength or high alumina cement concrete lost about one-third of their strength after 4 years' immersion. Cubes of concrete of all other types, irrespective of strength or kind of cement used, lost about half their strength after 4 years' immersion. Concrete containing entrained air behaved similarly, but concrete painted with bitumen maintained its strength while the coating was intact.

Testing the strength of concrete by the ultrasonic-pulse method

R. Jones and J. H. Wettern, *Concrete and Constructional Engineering* (London), V. 49, No. 11, Nov. 1954, pp. 343-347

Describes the use of the ultrasonic-pulse method to assess the strength of precast units used to form sections of primary and secondary beams which were to be assembled and prestressed on the site to form the beams in a school building.

Testing of concrete by an electromagnetic method—1 (L'Essai non destructif des ouvrages en beton arme)

F. Laisne and J. L. Cloquet, *La Technique Moderne-Construction* (Paris), V. 9, No. 4, Apr. 1954, pp. 119-124

Reviewed by Alexander M. Turitzin

A procedure to determine the quality of concrete and its strength by an electromagnetic method was proposed by French engineers at the Conference on Nondestructive Testing of Concrete, held in Paris in January, 1954. Called the "sonic method," it consists of measuring the speed of the propagation of an elastic wave, set up by a vibration mechanism, and the subsequent determination of the modulus of elasticity and Poisson's ratio of the concrete, both of which are functions of its density. The testing equipment includes an oscilloscope, a vibrator, an oscillator-amplifier unit, and a pickup. It is claimed that this method can be successfully used in the field, as well as in the laboratory, on specimens up to 1 m thick, with an accuracy within 1 percent. In addition to determining the quality of the concrete, it can be used to determine the location of cracks in the concrete and its aggregates, the quality of construction joints, and the bond between the concrete and reinforcement. The greatest advantage of this method lies in its nondestructive effect on specimens and the possibility of testing them under the progressive influence of adverse

chemical agents and abnormal atmospheric conditions. It can be used, also, to check concrete which has been subject to fire and frost action, or prematurely placed under a severe loading condition.

Testing of concrete by a radioactive method—2 (L'Essai non destructif des ouvrages en beton arme)

F. Laisne and J. L. Cloquet, *La Technique Moderne-Construction* (Paris), V. 9, No. 7, July 1954, pp. 263-266

Reviewed by Alexander M. Turitzin

Mr. Brocard of the Laboratoire du Batiment et des Travaux Publics is presently engaged in perfecting a method to determine the strength of concrete by measuring its resistance to the penetration of radioactive gamma rays. The extent of the penetration of radioactive rays through concrete of known thickness is a function of its density. Therefore, if a radioactive emission of a known magnitude is applied to the surface of a concrete specimen, it is possible, by means of a Geiger counter, to determine the intensity of the rays at the opposite side of the specimen. It is claimed that with this method the density may be determined with an accuracy of 1 or 2 percent and that it is possible to establish the relationship between the density and the compressive strength of concrete.

Further temperature and moisture characteristics of concrete-curing methods

Phillip L. Melville, *Proceedings*, Highway Research Board, V. 33, 1954, pp. 265-280

Author's Summary

An investigation previously reported (*Proceedings*, Highway Research Board, V. 31, 1952, p. 148; see "Current Reviews," ACI Journal, Oct. 1953, *Proc.* V. 50, p. 180) was extended to a paving project in southern Virginia to evaluate the relative ability to retain moisture and control temperature of five curing methods: (1) clear liquid-membrane seal in a single application, (2) clear liquid-membrane seal in two equal consecutive applications, (3) white-pigmented liquid-membrane seal, (4) white waterproof paper, and (5) tan waterproof paper. For the purpose of comparison, slabs without any artificial curing were included in the project.

Under the test conditions the order in which the methods proved themselves, on the average, best able to retain moisture was: (1) white waterproof paper, (2) tan waterproof paper, (3) white-pigmented liquid-membrane seal, (4) double clear-membrane seal, (5) single clear-membrane seal, and (6) no cure.

Records indicate the average order of effectiveness to maintain low and uniform temperatures to be: (1) white waterproof paper, (2) tan waterproof paper, (3) white-pigmented liquid-membrane seal, (4) clear liquid-membrane seal, (5) no cure, and (6) double clear-membrane seal.

Structural research

Testing of columns with uniformly distributed transverse loads

Paul C. Paris, *The Engineering Journal* (Montreal), V. 37, No. 8, Aug. 1954, pp. 945-949

Reviewed by Aron L. Mirsky

J. A. Van den Broek's "Formula II" ("Columns Subject to Uniformly Distributed Transverse Loads," *The Engineering Journal*, March 1941; the beam column: *Elastic Energy Theory*, Wiley, New York, 2nd edition, 1942, pp. 236 ff), which is based on the assumption that the deflected column may be presented by a sine curve, was subjected to experimental verification. Results indicate close correspondence between theoretical and experimental values; the small discrepancies noted in the range $1/r = 55$ to $1/r = 115$ are indicated by the author to be due to shortcomings of the testing equipment (which, incidentally, reviewer considers an excellent example of applied engineering) rather than of the theory.

Frost action on small footings

W. A. Trow, *Ontario Hydro Research News*, Hydro-Electric Power Commission of Ontario, V. 5, No. 3, July-Sept. 1953, pp. 11-16

Research program on control of frost heaving of small footings is described, and preventive measures proposed. To achieve resistance to frost heave, the cross section of the portion of the footing within the zone of frost penetration should be as small as possible. Below the frost zone the base of the footing can be enlarged to transmit the load safely to the soil. Curves giving bearing pressures required to prevent footing heave for rectangular, continuous, square, and circular footings assist in selection of proper footing size.